

AD-A044 481

ENERGY SYSTEMS CORP NASHUA N H
DOWNED AIRMAN POWER SOURCE (DAPS) FOR INCLUSION INTO THE RSSK-1--ETC(U)
JAN 77 R E LECOMPT, R S CHRISTIE
ESC-0289-1FR

NADC-76045-40

F/G 13/1

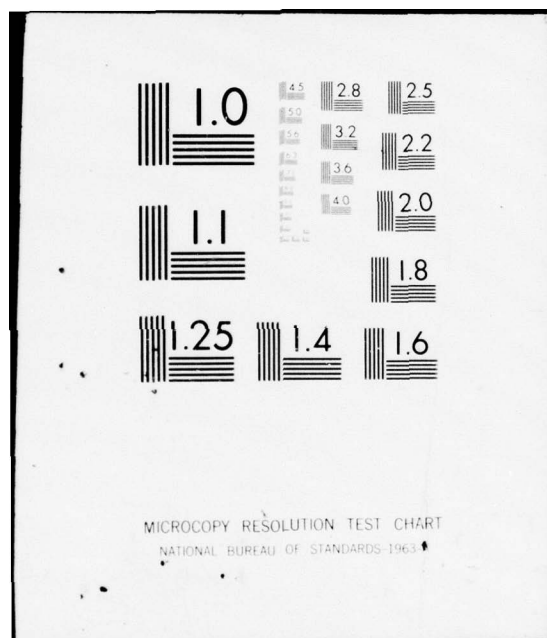
N62269-76-C-0289

NL

UNCLASSIFIED

1 OF 2
AD
A044481





ADA044481

Report No. NADC-76045-40

11
B.S.

Report No. ESC-0289-1FR

DOWNED AIRMAN POWER SOURCE (DAPS)
FOR INCLUSION INTO THE RSSK-1A AIRCRAFT
EJECTION SEAT TO BE USED BY DOWNED PILOTS
FOR ENVIRONMENTAL ANTI EXPOSURE PROTECTION

Richard E. LeCompte & Roger Christie
ENERGY SYSTEMS CORPORATION
1 Pine Street
Nashua, New Hampshire 03060

January 1977

Final Report for Period 10 April 1976 to 10 January 1977

APPROVED FOR PUBLIC RELEASE, DISTRIBUTION UNLIMITED

Prepared for
Crew Systems Department
NAVAL AIR DEVELOPMENT CENTER
Warminster, Pennsylvania 18974

DDC
RECEIVED
SEP 22 1977
C

Monitoring Agency
NAVAL AIR SYSTEMS COMMAND (AIR-340B)
Department of the Navy
Washington, D. C. 20361

AD No. —
DDC FILE COPY

SECURITY CLASSIFICATION OF THIS PAGE (When Data Entered)

19 REPORT DOCUMENTATION PAGE		READ INSTRUCTIONS BEFORE COMPLETING FORM
1. REPORT NUMBER (18) NADC-76045-40 ✓	2. GOVT ACCESSION NO.	3. RECIPIENT'S CATALOG NUMBER (1)
4. TITLE (and Subtitle) Downed Airman Power Source (DAPS) for Inclusion into the RSSK-1A Aircraft Ejection Seat to be Used by Downed Pilots for Environmental Anti Exposure Protection.		5. TYPE OF REPORT & PERIOD COVERED Final Report. 10 April 1976 thru 10 Jan 1977
7. AUTHOR(s) (10) Richard E./LeCompte & Roger Christie		6. PERFORMING ORG. REPORT NUMBER (14) ESC-0289-1FR
9. PERFORMING ORGANIZATION NAME AND ADDRESS Energy Systems Corporation 1 Pine Street Nashua, N. H. 03060		8. CONTRACT OR GRANT NUMBER(s) (15) N62269-76-C-0289
11. CONTROLLING OFFICE NAME AND ADDRESS Crew Systems Department Naval Air Development Center Warminster, Pa. 18974 Code 4043		10. PROGRAM ELEMENT, PROJECT, TASK AREA & WORK UNIT NUMBERS AIRTASK No. W-SL14-001
14. MONITORING AGENCY NAME & ADDRESS (if different from Controlling Office) Naval Air Systems Command (AIR-340B) Department of the Navy Washington, D. C. 20361		12. REPORT DATE (11) January 1977
		13. NUMBER OF PAGES 175
		15. SECURITY CLASS. (of this report) Unclassified
		15a. DECLASSIFICATION/DOWNGRADING SCHEDULE
16. DISTRIBUTION STATEMENT (of this Report) APPROVED FOR PUBLIC RELEASE: DISTRIBUTION UNLIMITED		
17. DISTRIBUTION STATEMENT (of the abstract entered in Block 20, if different from Report) DDC RECEIVED SEP 22 1977 C		
18. SUPPLEMENTARY NOTES		
19. KEY WORDS (Continue on reverse side if necessary and identify by block number) Downed Airman Power Source (DAPS), Catalytic Heater, BTU/Hr, Watts, Rigid Seat Survival Kit (RSSK), portable thermoelectric power source		
20. ABSTRACT (Continue on reverse side if necessary and identify by block number) A source of heat to extend survival time during search and rescue operations for downed airman in cold environments. The heat source is derived from the catalytic combustion of propane fuel with resultant release of chemical energy in the form of heat. The heat is picked up by a heat transfer fluid in heat exchangers, and pumped to the man via umbilicals on the DAPS to a tubulated under garment worn by the airman (continued)		

DD FORM 1 JAN 73 1473

EDITION OF 1 NOV 65 IS OBSOLETE
5 N 0102-LF-014-6601 3

UNCLASSIFIED

SECURITY CLASSIFICATION OF THIS PAGE (When Data Entered)

391675 ii

AB

SECURITY CLASSIFICATION OF THIS PAGE (When Data Entered)

where the heat is dumped. The system is a closed loop, and therefore, after dumping its heat the fluid is returned to the DAPS where it picks up additional heat. The system is capable of supplying up to 250 thermal watts to the airman at fluid temperatures of approximately 100 to 105°F. The fluid flow rate is approximately .25 to .30 gallons per minute. The system also has a 12 VDC DC-DC converter used to power an emergency flasher or transmitter.

S N 0102-014-8601

SECURITY CLASSIFICATION OF THIS PAGE (When Data Entered)

FORWARD

This report is an account of work performed under
Contract No. N62269-76-C-0289.

It has been prepared in accordance with MIL STD 847A:
Format Requirements for Scientific and Technical Reports Prepared
by or for the Department of Defense.

ACCESSION for	
NTIS	Wile Section <input checked="" type="checkbox"/>
DDC	Buff Section <input type="checkbox"/>
UNANNOUNCED	<input type="checkbox"/>
JUSTIFICATION	
BY	
DISTRIBUTION/AVAILABILITY CODES	
Dist.	SPECIAL
A	

SUMMARY

This report is a summary of work performed under Contract N62269-76-C-0289. The contract terminated with the delivery of one preproduction DAPS heater that would be stowable within the three RSSK-1A seat kits as manufactured by East/West Industries, Rocket Jet Division of American Flight Safety and Scott Aviation, Inc.

The intended use of the DAPS heater is to supply heat, (up to 250 thermal watts) to an airman should he have to bail out in extreme cold environments. The heat supplied is used to extend survival time during search and rescue operations.

The source of heat is derived from the catalytic combustion of propane gas. The heated fluid is pumped to the airman via umbilicals to a tubulated undergarment worn by the airman.

The use of this system can extend survival time for up to six hours at 32°F water and 20°F air.

ACRONYMS & SYMBOLS

NADC	-	Naval Air Development Center
CSD	-	Crew Systems Department
DAPS	-	Downed Airman Power Source
ESC	-	Energy Systems Corporation
RSSK	-	Rigid Seat Survival Kit
SCFH	-	Standard Cubic Feet Hour
q	-	heat BTU
\dot{q}	-	heat BTU/Hr
h	-	Heat transfer coefficient (BTU/Hr °F ft ²)
A	-	Surface Area (ft ²)
T	-	Temperature (°F)
ρ	-	Density (lb/ft ³)
V	-	Velocity (feet/sec.)
D	-	Diameter (ft)
μ	-	Viscosity (lb/hr. ft.)
RN	-	Reynolds number
L	-	Path Length (ft)
D _e	-	Equivalent Diameter (ft)
θ	-	Inclined angle (°)
G	-	Air Gap
L	-	Diffuser Length (ft)
T _D	-	Throat Diameter (ft)
E _L	-	Running Voltage (volts)
I _L	-	Running Current (amps)

Acronyms & Symbols Continued

E_{OC}	-	Open Circuit Voltage (volts)
R_L	-	Load Resistance (ohms)
R_i	-	Internal Resistance (ohms)
C	-	Gas Constant (propane = 105)
F	-	Pressure Ratio
C_p	-	Specific Heat (BTU/lb °F)
P	-	Power(Watts)
T_η	-	Thermal Efficiency (%)
S_η	-	System Efficiency (%)

TABLE OF CONTENTS

	<u>Page</u>
1.0 INTRODUCTION	1
1.1 <u>Contract N62269-73-C-9313</u>	1
1.2 <u>Contract N62269-74-C-0500</u>	1
1.3 <u>Contract N62269-76-C-0444</u>	1
1.4 <u>Contract N62269-76-C-0289</u>	7
2.0 TECHNICAL DISCUSSION	7
2.1 <u>Seat Kit Study</u>	7
2.2 <u>Impact on DAPS Configuration</u>	13
2.3 <u>Fuel Supply Comparison & Design</u>	13
2.3.1 Fuel Supply Design	13
2.3.2 Stress Analysis	19
2.3.3 Fuel Tank Leak Rate Test	20
2.4 <u>Combustion Chamber</u>	20
2.4.1 Purpose of Re-Design	20
2.4.2 Comparison of Two (2) Designs	22
2.4.3 Developmental Combustion Chamber Analysis and Testing	22
2.5 <u>Venturi Analysis & Tests</u>	39
2.6 <u>DC Motor Evaluation</u>	45
2.7 <u>Exhaust Gas Analysis</u>	50
3.0 DAPS DESIGN	55
3.1 RSSK 1A DAPS Requirements	55
3.1.1 General Requirements	55
3.1.2 Specific Requirements	56
3.1.2.1 System Operation	56
3.1.2.2 Design	57
3.1.2.3 Performance	57
3.1.2.3.1 Thermal	57
3.1.2.3.2 Hydraulic	58
3.1.2.3.3 Electrical	59
3.1.2.4 Storage	59
3.1.2.5 Environment	60
3.2 <u>Final DAPS Configuration</u>	60
3.2.1 Pump/Motor Assembly	60

3.2.2	Combustion Chamber Assembly	65
3.2.3	DC-DC Converter	66
3.2.4	Fuel Regulator	66
3.2.5	Fluid Manifold	66
3.2.6	Fuel Input Connector	66
3.2.7	Piezoelectric Starter	66
3.2.8	12 VDC Output Connector	69
3.3	<u>Fuel Tank</u>	69
3.3.1	Mounting Plate	69
3.3.2	Fuel Coil	69
3.3.3	Fuel Umbilical	69
3.3.4	Fuel Connector	71
3.3.5	Manifold Block	71
3.3.6	Pressure Relief Valve	71
3.4	<u>Interface of DAPS System with the Fuel Coil to the Seat Kit</u>	71
4.0	RELIABILITY AND MAINTAINABILITY	71
4.1	<u>Introduction</u>	71
4.2	<u>Reliability Program Description</u>	72
4.2.1	Reliability Program Management	72
4.2.2	Reliability Design and Evaluation	72
4.2.2.1	Design Techniques	72
4.2.2.2	Reliability Analysis	80
4.2.2.3	Problem Areas	84
4.2.2.4	Parts Reliability	94
4.2.2.5	Failure Mode, Effects and Criticality Analysis	94
4.2.2.6	Effects of Storage	96
4.2.3	Reliability Testing	96
5.0	SYSTEM FINAL TEST	108
5.1	<u>Test Set Up</u>	108
5.1.1	Thermal	108
5.1.2	Hydraulic	108
5.1.3	Electrical	110
5.2	<u>Required Calculations</u>	110
5.2.1	Thermal Efficiency	110
5.2.2	System Efficiency	112
5.2.3	Electrical Performance	112
5.3	<u>Test Results</u>	113
6.0	CONCLUSIONS	121
6.1	<u>Design & R & M Conclusions</u>	121

	<u>Page</u>
6.1.1 Seat Kit Study	121
6.1.1.1 <u>Differences in a Single Manufacturer's Seat</u> <u>Kit Due to Tolerances</u>	121
6.1.1.2 <u>Differences in a Single Manufacturer's Kit Due</u> <u>To Production Run</u>	121
6.1.2 Design Layout	122
6.1.3 Developmental Testing & System Design	122
6.1.3.1 <u>Catalytic Bed Size</u>	122
6.1.3.2 <u>Thermoelectric Module Thermal Contact</u>	123
6.1.3.3 <u>Heat Exchanger Design</u>	123
6.1.4 System Build	124
6.1.5 System Test	124
6.1.6 Reliability and Maintainability	124
 7.0 RECOMMENDATIONS	 125
7.1 <u>Design</u>	125
7.1.1 Reduced Volume of Catalyst	127
7.1.2 Optimized Heat Exchanger Design	127
7.1.3 Optimized DAPS Electrical Network	127
7.1.4 Improved Pump	128
7.1.5 Power Sharing	129
7.2 <u>Reliability and Maintainability</u>	131
7.2.1 Reliability Development Testing	131
7.2.2 Reliability Demonstration Test Support	132
 APPENDIX A Calculation of Initial Failure Rates	 134
APPENDIX B Calculation of Predicted Individual Component Failure Rates	142
APPENDIX C Thermal Requirements for Cold Water and Life Raft Exposures	152
APPENDIX D RSSK-1A DAPS Operating Instructions	156
APPENDIX E Maintenance and Repair	159

LIST OF FIGURES

<u>Figure</u>	<u>Title</u>	<u>Page</u>
1	DAPS with Cover Removed	2
2	DAPS with Fuel System in Scott 1A Seat Kit	3
3	DAPS with Fuel System in Scott 1A Seat Kit as Packaged for Delivery	4
4	Fuel Coil (N62269-75-C-0444)	5
5	0444 DAPS with Fuel-Connector in place (N62269- 75-C-0444)	6
6	RSSK-1A Scott Kit	9
7	RSSK-1A Rocket Jet Kit	10
8	RSSK-1A East/West Kit	10
9a	Comparison of Corner Void Volume (Scott & Rocket Jet)	11
9b	Comparison of Corner Void Volume (East/West)	11
10	Fuel Coil (N62269-76-C-0289)	14
11	Fuel Plate and Umbilical (N62269-75-C-0444)	15
12	Fuel Plate and Umbilical (N62269-76-C-0289)	16
13	RSSK-1A Scott Kit with Mounting Brackets	18
14	Commercial Fuel Cylinder	21
15	Exploded View of Old Combustion Chamber	23
16	Assembly View of Old Combustion Chamber	23
17	Exploded View of New Combustion Chamber	24
18	Assembly View of New Combustion Chamber	24
19	Thermocouple Location	27

<u>Figure</u>	<u>Title</u>	<u>Page</u>
20	Temp. Profile vs Fuel Pressure at Fixed Fluid Flow Rate	28
21	Temp. Profile vs Catalytic Bed Size at Fixed Fluid Flow Rate	29
22	Temp. Profile vs Fuel Pressure and Bed Location in Various Fluid Flow Rates	30
23a	7.15 Gram Catalytic Bed	33
23b	12.4 Gram Catalytic Bed	33
23c	28.5 Gram Catalytic Bed	34
24	Reynolds Number and Flow Rate vs Efficiency	35
25	Sieder Tate Graph	38
26	Diffuser Geometry Variables	40
27	Air/Fuel Ratio vs Air Gap	41
28	Schematic Diagram of Electrical Test Stand	46
29	Schematic Diagram of Hydraulic & Thermal Test Stand	47
30	Flow Rate vs Current	48
31	Flow Rate vs Power	49
32	Absorption Spectra of Carbon Monoxide (CO)	52
33	Absorption Spectra of Propane (C ₃ H ₈)	52
34	Carbon Monoxide Calibration Curve	53
35	Propane Calibration Curve	54
36	RSSK-1A DAPS with Cover	61
37	RSSK-1A DAPS with Cover Removed	62
38	RSSK-1A with Fuel Supply as Packaged for Delivery in the Scott RSSK-1A Kit	63
39	Exploded View of Combustion Chamber	64
40	Schematic of DC-DC Converter Wiring showing 4 Pin Conn.	67
41	Fuel Coil (N62269-76-C-0789)	68

<u>Figure</u>	<u>Title</u>	<u>Page</u>
42	Method of Mounting DAPS to Fuel Plate	70
43	DC-DC Converter Derating Guidelines	73
44	System Mission Profile	76
45a	Reliability Dependency Diagram-Storage Stage	77
45b	Reliability Dependency Diagram-In Flight Stage	78
45c	Reliability Dependency Diagram-Eject Stage	79
46	Fuel Tank Leakage Rate	98
47	Test Fuel Tank Leakage Rate	100
48a	Equipment Failure Record	102
48b	Failure Summary Record	103
48c	Failure Identification Report (Part A)	104
48d	Failure Identification Report (Part B)	105
48e	Failure Identification Report (Part C)	106
48f	Failure Identification Report (Part D)	107
49	Test Stand	109
50	Voltage and Flow Rate vs Time	120

LIST OF TABLES

<u>Table</u>	<u>Title</u>	<u>Page</u>
1	Temp Profile Data	31
2	Heat Exchanger Comparisons	37
3	Air Gap Data 7° Diffuser .005 Orifice	42
4	Air Gap Data 12° Diffuser .005 Orifice	43
5	Air Gap Data 20° Diffuser .005 Orifice	44
6	RSSK-1A Component Replacement Schedule	81
7	RSSK-1A Failure Rate Data	82
8	Failure Mode, Effects and Criticality Analysis	85
9	Fuel Tank Leakage Rate	97
10	Test Fuel Tank Leakage Rate	99
11	Test Results at 10 psig	114
12	Test Results at 20 psig	115
13	Test Results at 26 psig	116
14	Test Results at 26 psig in one incremental step	117
15	Exhaust Gas Concentrations	118
16	DC-DC Converter Performance	119

1.0 INTRODUCTION

The development of the Downed Airman Power Source (DAPS) for inclusion in the Rigid Seat Survival Kit - 1A (RSSK-1A) has proceeded over the last three years at Energy Systems Corporation, Nashua, New Hampshire. This effort has taken place under a series of research and development contracts from the Naval Air Development Center (NADC), Crew Systems Department (CSD).

A brief summary of these contracts and their results is provided here as background material for personnel unfamiliar with DAPS development.

1.1 Contract No. N62269-73-C-0383

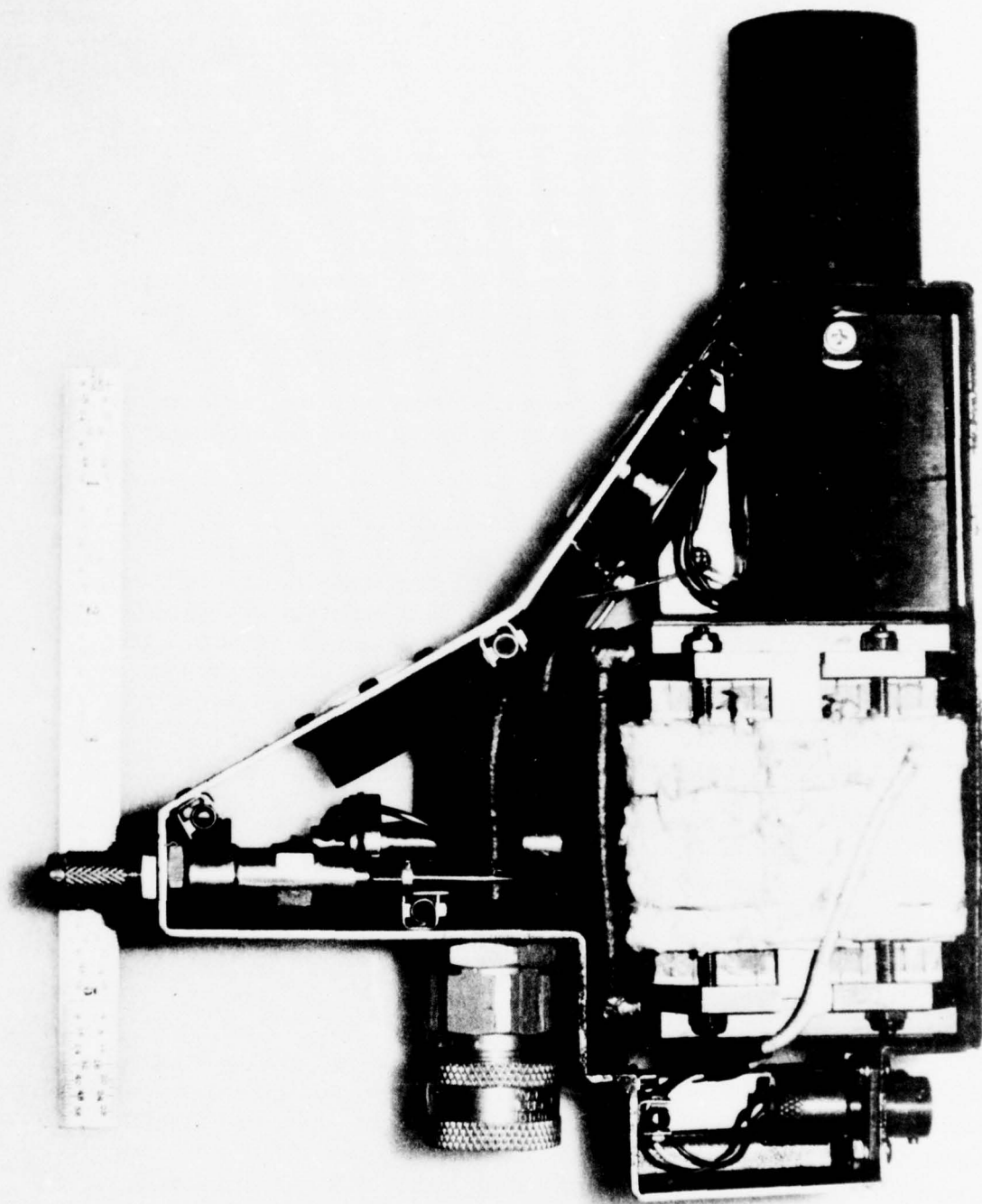
This contract consisted of a study to determine the feasibility of designing a heater system that would be compatible with the RSSK-1A and RSSK-8A seat kits. It was concluded at this time that a DAPS could be designed for either the 1A or 8A seat kits, but that the same DAPS could not be interchangeable between the two.

1.2 Contract No. N62269-74-C-0500

Based on ESC recommendations of the 0383 contract, this contract was awarded to design and fabricate actual RSSK-1A hardware. The DAPS heater unit (Figure 1) and fuel tank system (Figure 2) were designed and one system fabricated. Delivery of this unit to NADC took place in December 1974. (Fig. 3)

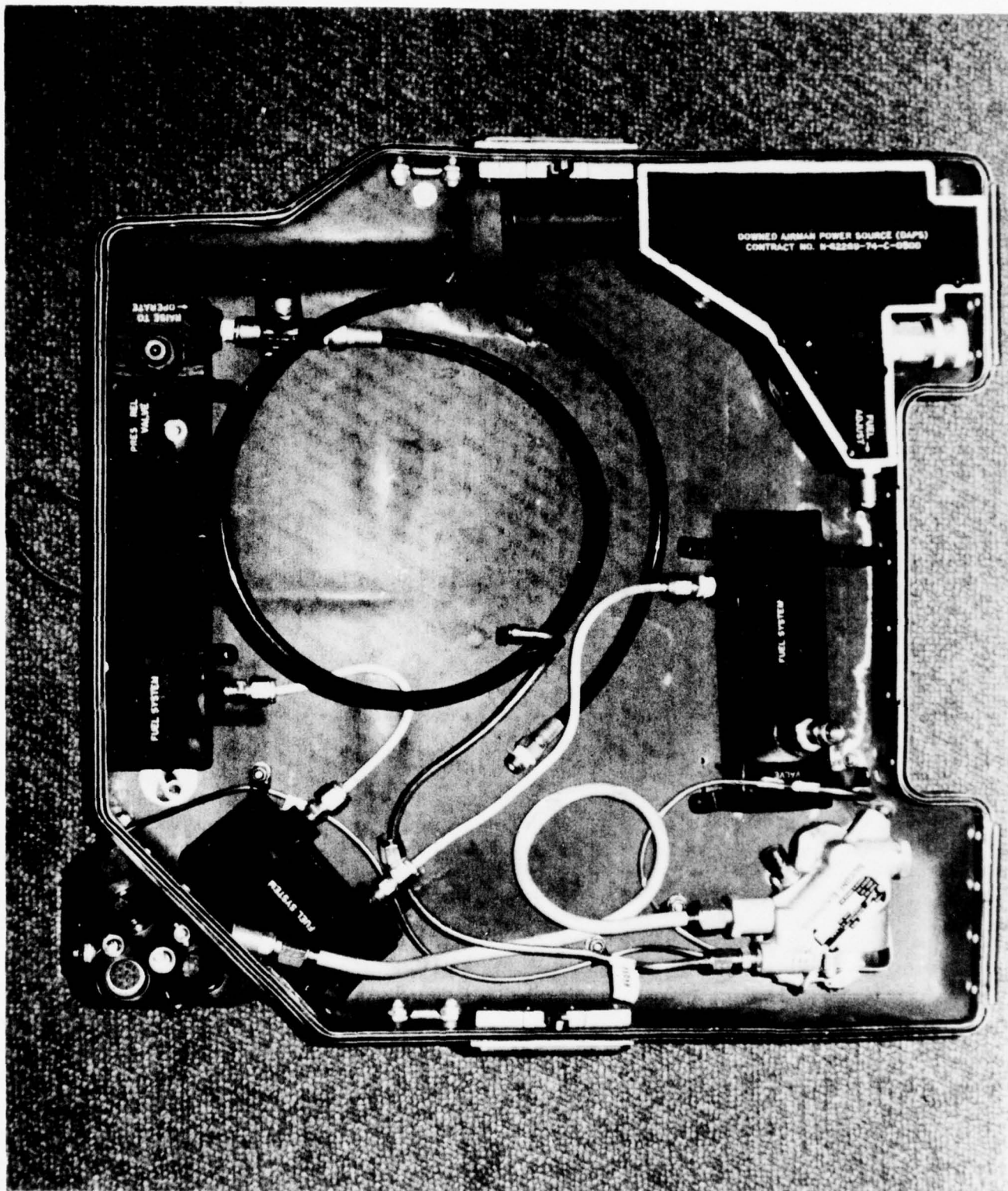
1.3 Contract No. N62269-76-C-0444

The reduction to practical hardware accomplished under the 0500 work proved to be sufficient motivation and justification on the part of NADC to proceed with the procurement of ten additional systems, slightly modified from the 0500 design. The principal change was the incorporation of a fuel coil that was more easily mounted in and removed from the seat kit (Figure 4 & 5). The previous design (Figure 2) comprised three manifolded rectangular steel tanks that required removal of the oxygen coil for mounting and also required a significant amount of rework to the seat kit in the form of mounting holes to hold the fuel subsystem in place. A secondary drawback of the design was that the fuel tank was permanently attached to the heater and had to be used in conjunction with



DAPS with Cover Removed
RSSK-1A DAPS

Contract N62269-74-C-0500

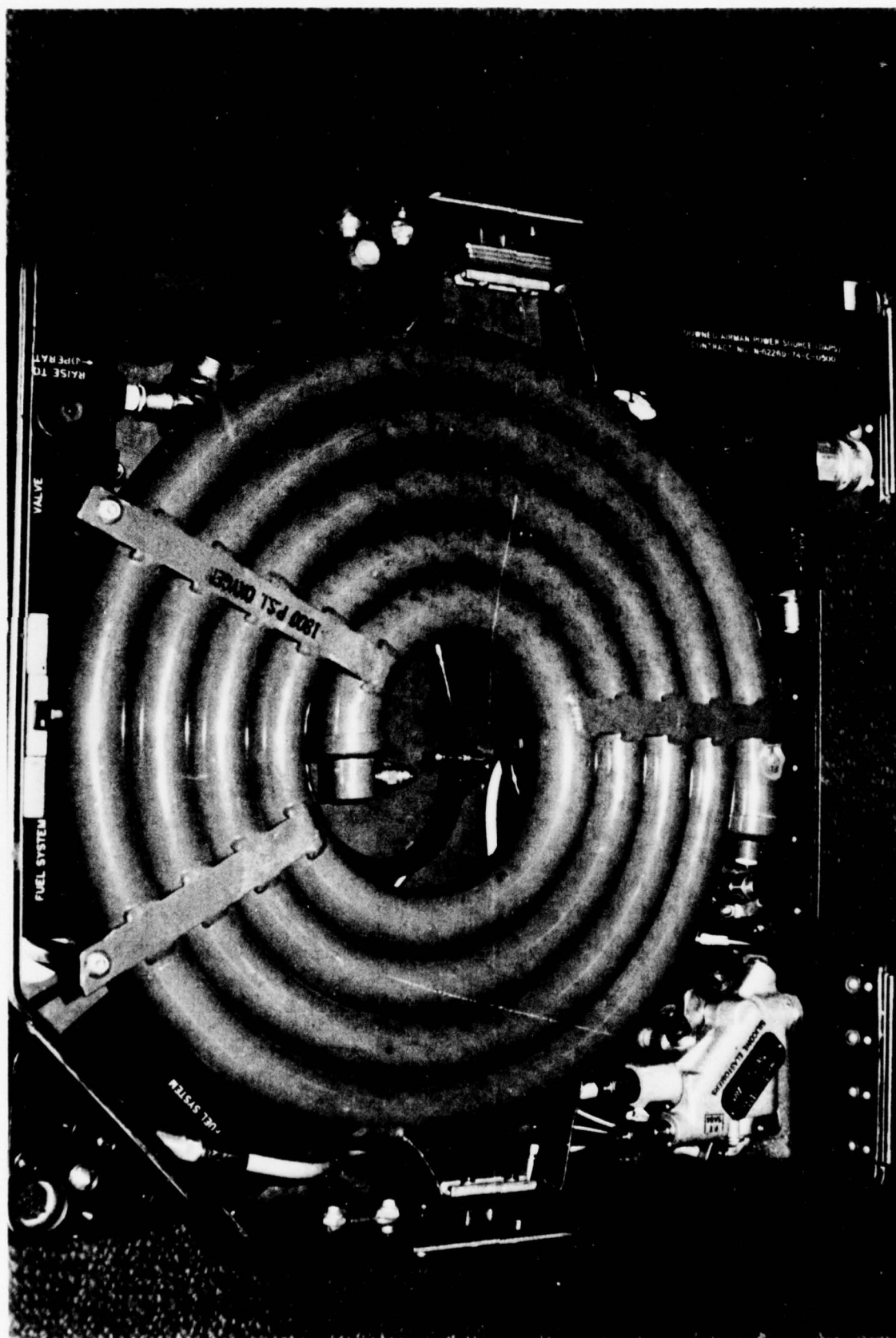


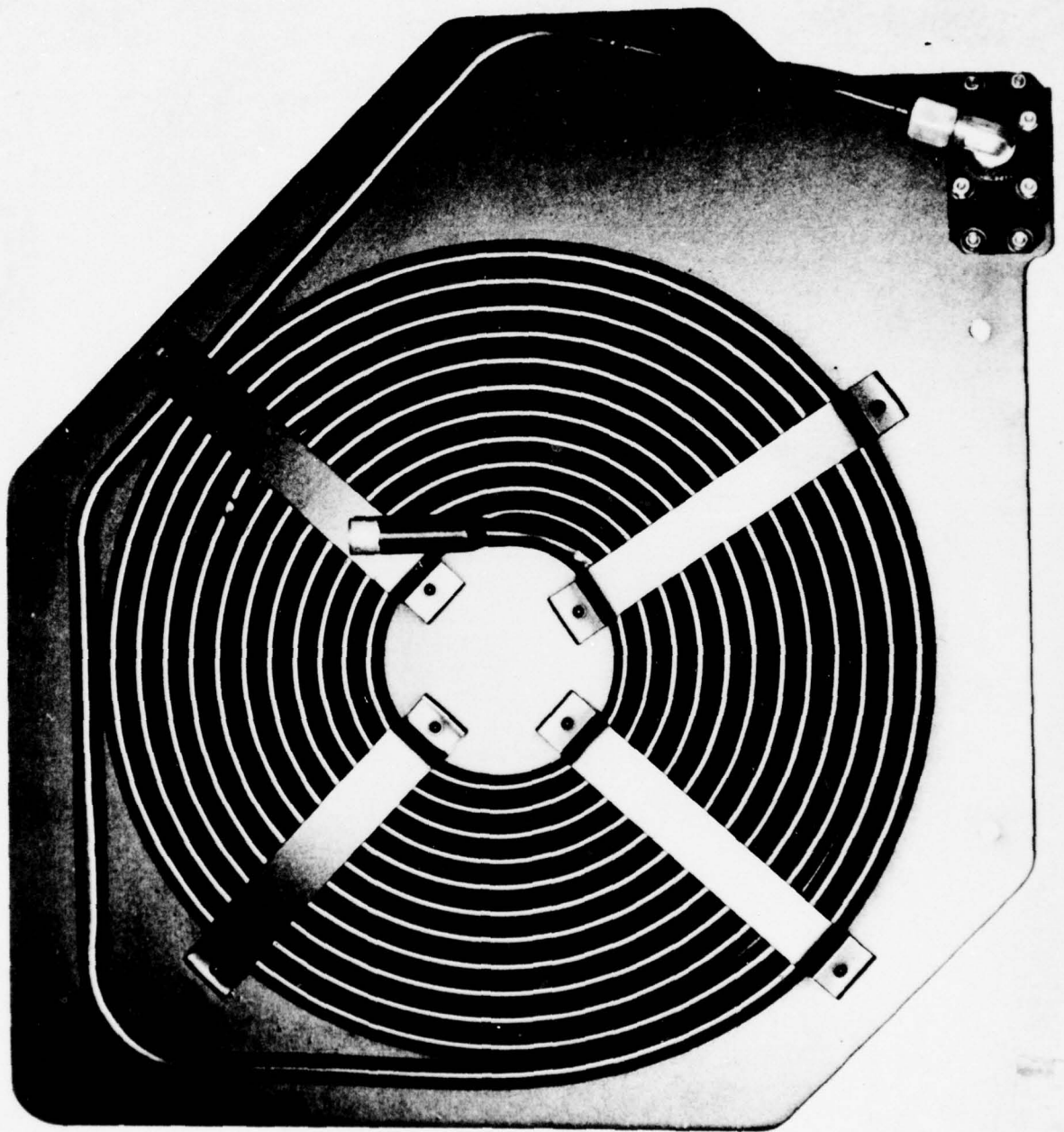
DAPS With Fuel System
Contract N62269-74-C-0500

Figure 2

DAPS With Fuel Supply
As Packaged for Delivery
Contract N62269-74-C-0500

Figure 3





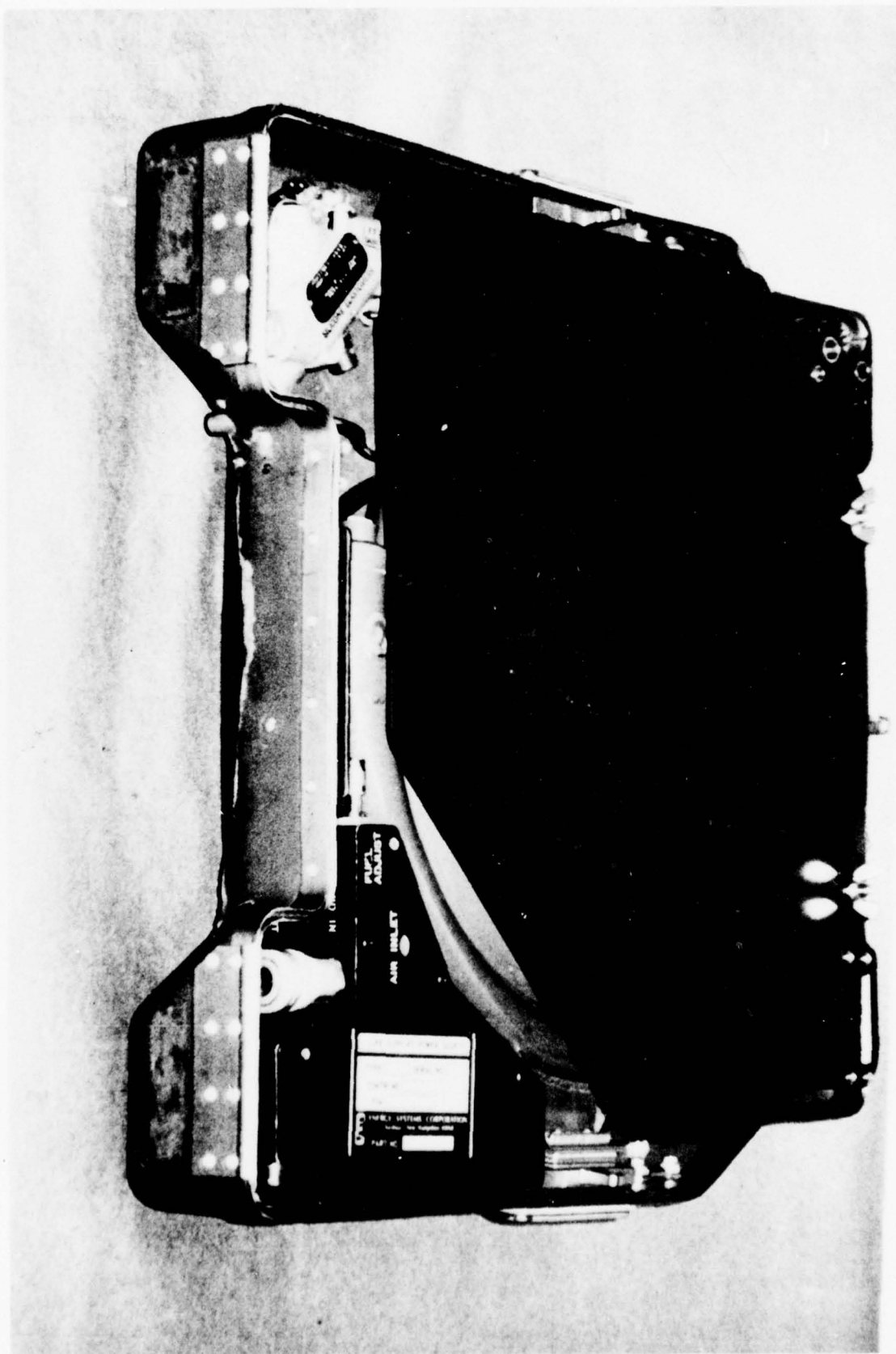
DAPS Fuel Coil

Contract N62269-75-C-0444

Figure 4

DAPS With Fuel Supply
As Packaged for Delivery
Contract N62269-76-C-0444

Figure 5



the entire seat kit because the fuel was hard mounted under the fixed oxygen supply. The new fuel system (Figure 4) significantly reduced system weight and greatly facilitated mounting and removal. This design also enabled the fuel and heater to be completely removed from the kit, and the kit to be discarded if so desired.

1.4 Contract N62269-76-C-0289

After delivery of these ten test and evaluation DAPS, it was determined that although the RSSK-1A seat kit design has only one Federal Stock Code Number the kits as manufactured by various suppliers all were not identical. The specification to which the kits are fabricated only specifies overall external dimensions and allows virtually unlimited leeway to mount internal components inside the kit assembly. This leeway in Seat Kit internal component configuration and mounting location resulted in a severe problem when it came to utilizing the DAPS as designed for the Scott Seat Kit in the kits fabricated by the other two manufacturers, i.e., Rocket Jet Co. and East/West Industries. The differences among the three kits fabricated by these vendors necessitated a single DAPS design that would be 100% interchangeable among seat kits as manufactured. The 0289 contract was awarded to design such a DAPS and to provide for fuel tank attachment with minimum impact on existing seat kit components.

The -0289 Contract resulted in the delivery of a radically altered design from that of previous units. These changes were mandated by the severe volume restriction encountered in the various kit designs requiring the utilization of only the least void volume common to all these kits.

The DAPS design problems, solutions and the rationale behind design choices, together with an in-depth report of engineering test and evaluation performed on this system are the subject of this Final Report.

2.0 TECHNICAL DISCUSSION

2.1 Seat Kit Study

The RSSK-1A seat kits used in active fleet service are fabricated by two manufacturers. These are Scott Aviation and

Rocket Jet Division of American Safety Flight Systems, Inc. A third manufacturer, East/West Industries, Inc., has submitted its model of the RSSK-1A kit for the first article inspection to Dayton T. Brown, Co., Bohemia, Long Island, New York.

Although this kit is not in actual service in the field there is a definite possibility that future procurements could be obtained from East/West Industries.

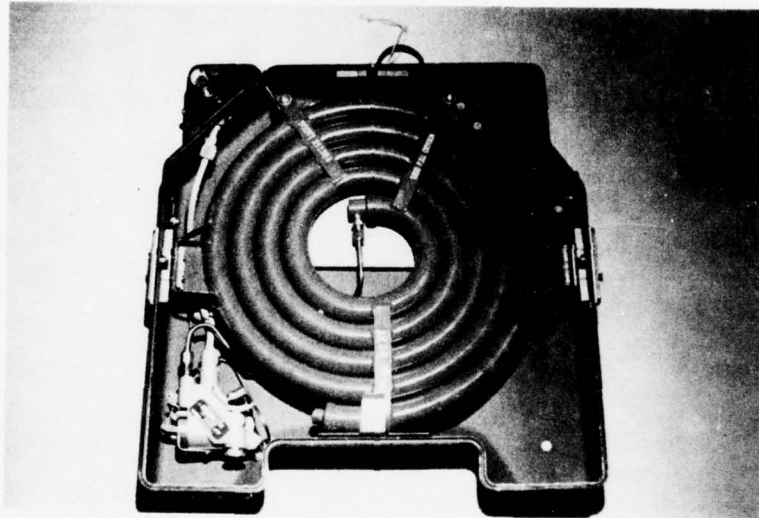
So as to fulfill the contract requirements of delivering a DAPS heater suitable for packaging in the three kits as fabricated by the three major manufacturers it was necessary to procure one of each of the representative types.

The task of procuring one each of the three representative kits proved to be a significant problem in itself. NADC had a Scott kit available as GFE for use by Energy Systems Corporation but was unable to procure either of the remaining two designs. A kit fabricated by Rocket Jet was obtained on a 60 day loan agreement from the manufacturer although no drawing package was available. With the Rocket Jet kit in-house it was possible to extensively inspect and photograph the kit for use in the design effort.

It was never possible for Energy Systems Corporation to obtain a kit manufactured by East/West Industries. Through an agreement between NADC and Dayton T. Brown it was made possible for ESC personnel to inspect and photograph the East/West design. At the time of this inspection a mock-up of the proposed DAPS design was used to check its fit. Based on this GO-NO-GO analysis it was determined that the proposed mock-up would be compatible with the RSSK-1A seat kits of all three manufacturers.

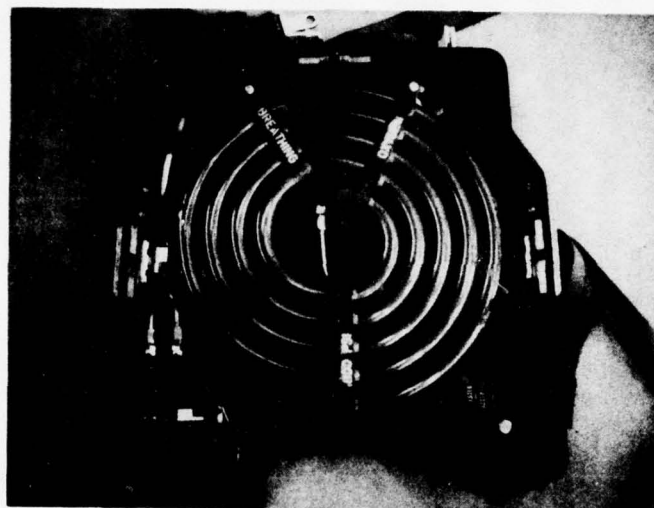
The most severe difference among the three seat kits is the method of attaching the emergency oxygen coil in the kit. These differences are more readily appreciated by inspecting the photographs of each of the kits as shown in Figures 6, 7 and 8.

The oxygen supply consists of a spiral wound coil of steel tubing to which is integrally attached the required mounting bracketry. Scott and East/West aviation mount the coil in such an orientation as to make possible the utilization of that space under the



Scott RSSK-1A Seat Kit

Figure 6



Rocket Jet RSSK-1A Seat Kit
Figure 7



East /West RSSK-8A Seat Kit
Figure 8

CORNER VOID



Figure 9a
Scott & Rocket Jet

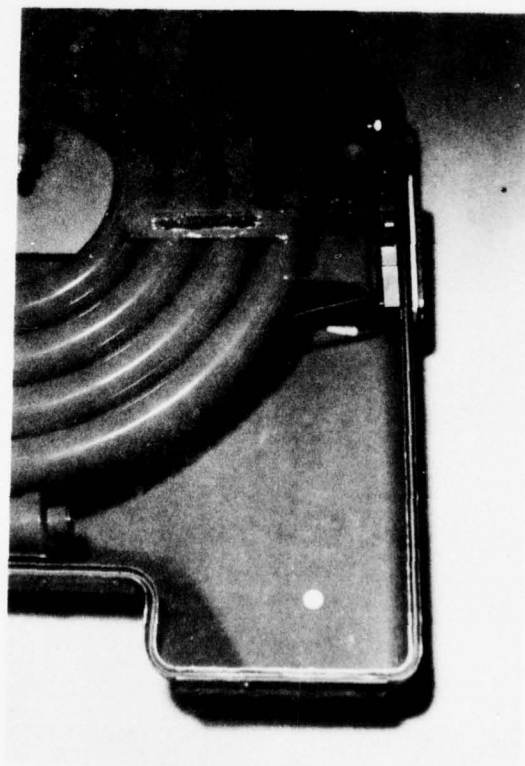


Figure 9b
East/West

mounting bracketry. (Figures 6 and 7) Rocket Jet (Figure 8) rotates the orientation of this oxygen coil by 180° precluding the use of the space under the mounting bracketry due to the non-symmetrical nature of the bracket with respect to the coil. This design does, however, allow a larger void volume in that the final wrap of the oxygen coil ends outside the area suitable for DAPS mounting (see Figure 8).

This additional space was of no value to ESC in its task as it was not common to the other kit design as fabricated by Scott and East/West. Only that volume common to all three kits could be utilized if the intent of the contract was to be fulfilled. Figures 9a and 9b are photographs of the differences between oxygen tank mounting configuration.

Based on the above study, a least common denominator of void volume configuration was determined. The determination of this volume was the first step in the completion of the design.

2.2 Impact on DAPS Configuration

Once the available common void volume was determined it was apparent that major changes would have to be made in the basic DAPS design if the function of the DAPS was not to be compromised.

Two components in the DAPS that were considered non-essential to the unit performance were the fluid temperature gauge and the fuel pressure gauge. These components, although useful from an operating view point, were deemed to be expendable without affecting system performance.

The deletion of the temperature gauge did not require any further changes to the unit to compensate for its removal. It was decided that the level of comfort could be safely controlled by the operator seeing that this comfort level is a relative state varying markedly from individual to individual.

The removal of the pressure gauge required that some means of knowing at what rate fuel was being consumed be supplied.

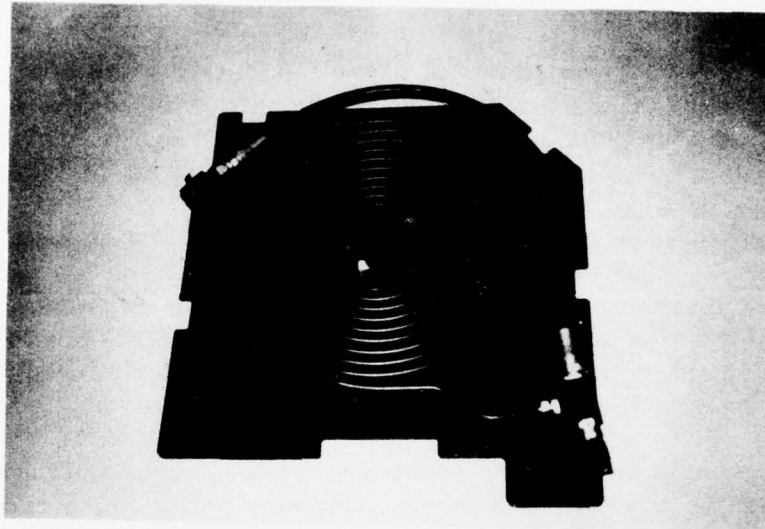
This was accomplished by modifying the lead of the thread on the regulator shaft, thereby allowing the full range of fuel rates to be obtained in one 360° rotation of the regulator control knob. This knob is equipped with a calibrated numerical face plate with numbers ranging arbitrarily from 0 through 10. The unit is delivered with a decal informing the operator of the approximate fuel duration that can be expected at the various numerical settings.

This information should enable the downed airman to select a proper balance between degree of comfort and fuel duration.

2.3 Fuel Supply Comparison & Design

2.3.1 Fuel Supply Design

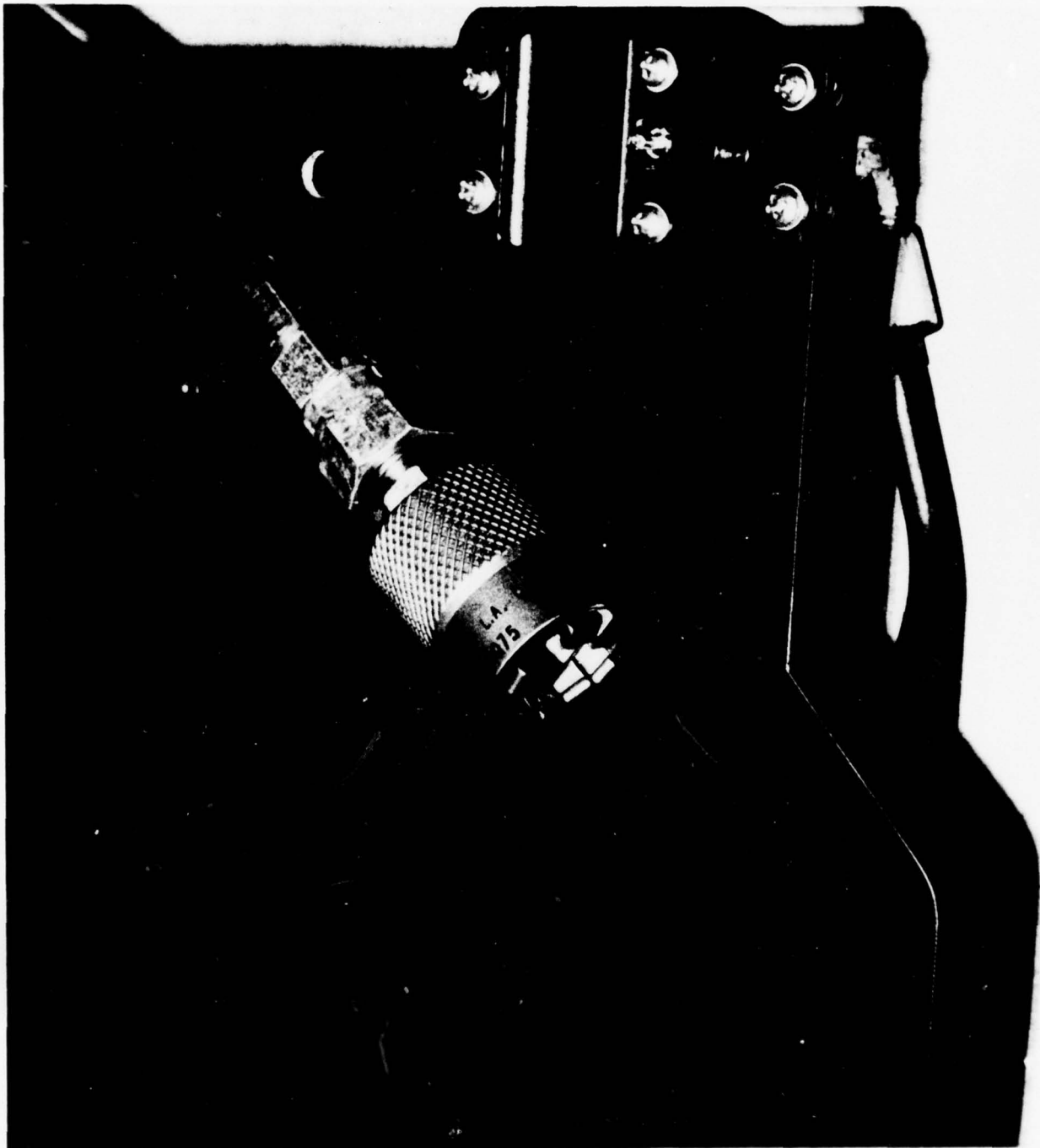
The fuel supply (Figure 10) as delivered with this system is similar to that supplied with previous units. The fuel tank consists of a spiral coil fabricated from .438 inch diameter with .035 inch thick wall aluminum tubing. One end is capped with a Joint Industry Conference on Hydraulic Standards for Industrial Equipment (JIC) 37° flared plug. The other end is provided with a 37° male pipe connector. (Both fittings are aluminum) This male connector is terminated at a manifold (also aluminum) into which is installed

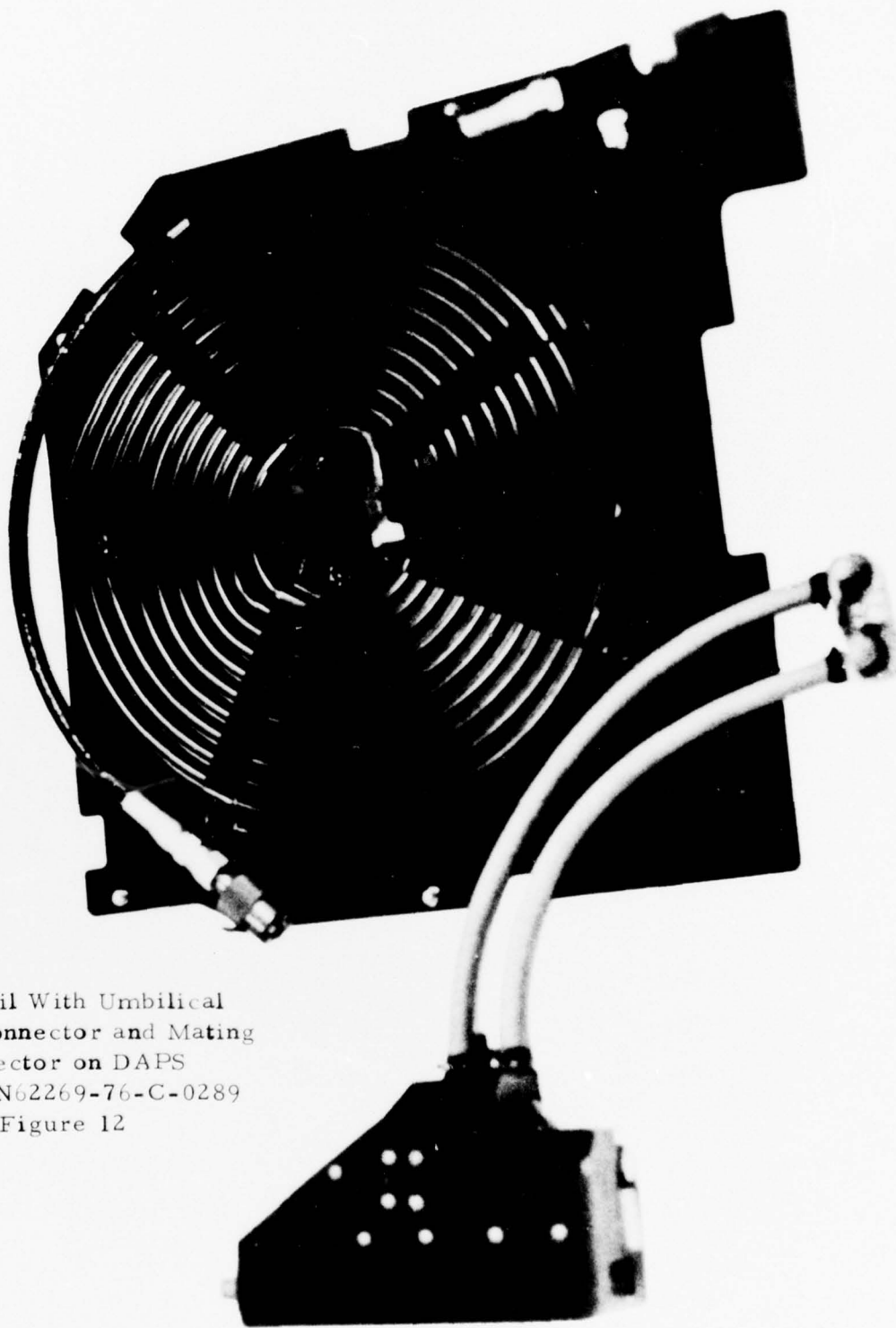


Fuel Coil as Delivered
Under Contract N62269-76-C-0289

Figure 10

Fuel Plate
and Umbilical
Contract N62269-75-C-0444
Figure 11





Fuel Coil With Umbilical
Mounted connector and Mating
Connector on DAPS
Contract N62269-76-C-0289
Figure 12

a preset pressure relief valve (250 PSIG) and a flexible fuel umbilical line. The umbilical line is approximately two feet long with a male pipe thread on one end and a Wiggins Quick Disconnect on the other end. This coil is in turn fastened to a flat 1/16 inch thick aluminum alloy plate (Figure 10).

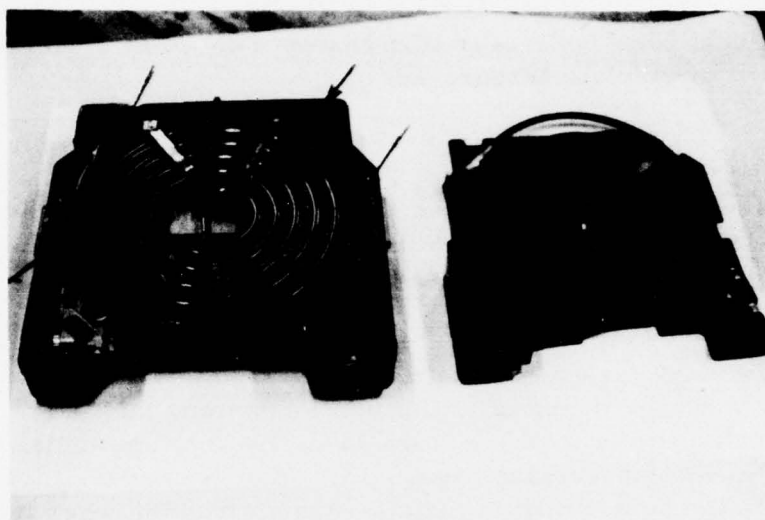
This plate serves a three fold function: first, it serves to make the fuel coil a more rigid assembly; second, it serves as a mounting surface for the life raft; and third, it serves as a mounting surface for the DAPS heater itself. The previous design did not have the latter feature.

There have been, though, several design improvements from the first design. The previous design had the hard mounted fuel connector mounted to the fuel supply and the fuel umbilical mounted to the DAPS (Figure 11). The system as delivered reverses these two connectors (Figure 12). Removal of the fuel umbilical from the heater will facilitate vacuum packing when these systems are prepared for field deployment.

The method of mounting the fuel supply to the plate has also been significantly improved by eliminating all protrusions above the level of the mounting plate that could cause potential damage to the life-raft during storage, deployment, and heater removal and utilization.

Another improvement incorporated into this design is the elimination of all through holes within that area on which the encapsulating life-raft is expected to be vacuum heat sealed. The elimination of these holes reduces significantly the number of leak paths through which the seal could be lost.

The method of attachment consists of four relatively equally distributed snap slides mounted on the underside of the fuel plate. These snap slides hard mount the fuel supply to brackets which in turn mount to existing holes already in the kits. The only difference in the fuel supply/heater system among the three manufacturer's kits is the retrofit package consisting of brackets to mount the fuel coil. These bracket kits were required due to the difference among the kits in question. It was determined that a kit of this type would minimize the retrofit effort by requiring only a change in mounting bracketry.



Scott RSK-1A/DAPS
Mounting Bracketry

Figure 13

The fuel coil in all kits is removed by a simple push or pull motion on tabs located on the coil/seat kit mounting bracketry (Figure 13).

A study of various available latching mechanisms to determine the degree of manual dexterity and coordination required to operate them resulted in the selection of the snap slide type manufactured by DIMCO GRAY Corporation.

These catches have been assigned military specification identification numbers (MS 21332) which also made their selection preferable to other types. The forces on the catches due to catapult launch, high speed maneuvers and seat ejection, were determined to be within the strength capabilities of the parts.

An additional feature incorporated into the design was a 3/8 inch thick compressible flame retardant foam rubber pad. The function of this pad is two-fold. It serves as a shock absorbing medium and also prevents vibration induced abrasion that could damage the fuel and/or oxygen coils.

The fuel coil delivered with this design contains nominally 187 grams. This corresponds to a time duration of 7.4 hours at the fuel flow rate of 25 grams per hour.

2.3.2 Stress Analysis

The stress analysis of the fuel coil was facilitated by the fact that it consists of a spirally wrapped circular cross section tube.

The internal pressure capacity of tubes of various diameters and alloys is well known. Based on available industrial data on tubing, keeping in mind the fuel duration requirement, it was decided to use 0.437 inch O.D. 6061-T6 aluminum tubing with a 0.035 inch wall. This tubing has a working pressure of 1000 PSI continuous. The maximum expected pressure based on a storage temperature of 125°F maximum, is 260 PSIG. This results in a minimum factor of safety of four (4). This figure is an extremely conservative one as the coil when operating at its rated pressure of 1000 PSI already has a safety factor figured into it.

The pressure relief valve used is a Nupro valve, part number 4-CPA-2-150 rated for a working pressure of 2500 PSIG.

The umbilical is Synflex medium pressure tubing Part No. 3130-03 rated for 2500 PSIG continuous duty.

The Fuel Connectors are manufactured by Wiggins Connector Co., Los Angeles, California. The Part Nos. are VS100D4 and VN100E4. Both are rated for 1500 PSIG continuous duty.

2.3.3 Fuel Tank Leak Rate Test

A prototype tank using parts identical to those of deliverable units has been assembled and filled with propane. The purpose of this assembly is to monitor fuel leakage rates with respect to time.

Measured leakage rates have been on the order of 0.2 grams/month, coinciding with the leakage rates of commercially available tanks. The leakage rate of these commercial tanks was determined experimentally by actually monitoring the leakage rates of 12 tanks purchased specifically for this purpose (See Figure 14).

These leakage rate tests were mandated by the apparently high leakage rates encountered in past fuel tank designs. Test results to date indicate that the components selected will eliminate the leakage encountered in past designs.

The fuel coil of the new design exhibited a marked decrease in leak rate. The leak rate decreased from a low factor of 3 to a high factor of 20. A leak rate of .15 grams per month would require a maintenance inspection schedule on the order of five years.

2.4 Combustion Chamber

2.4.1 Purpose of Redesign

After generating several design layouts it became apparent that the existing RSSK-1A DAPS combustion chamber could not be packaged within the available RSSK-1A void configuration as determined by the seat kit study. Combustion chamber redesign was required, and an effort of this magnitude was definitely beyond the scope of the contract. Fortunately, a lower profile

COMMERCIAL FUEL BOTTLE LEAK RATE

(weights in grams)

Bottle No. Date Weighed	1	2	3	4	5	6	7	8	9	10	11	12
12 July 1976	970.6	962.9	970.1	953.0	970.3	961.05	937.2	950.8	955.25	952.05	945.55	966.7
12 Aug 1976	970.5	962.7	969.9	952.9	970.2	961.05	937.15	950.6	954.95	951.9	945.45	966.6
13 Sept 1976	970.4	962.6	969.9	952.9	970.2	961.15	937.05	950.6	954.95	951.9	945.45	966.6
13 Oct 1976	969.9	962.5	969.5	952.6	970.1	960.9	936.9	950.5	954.6	951.7	945.1	966.3
12 Nov 1976	969.9	962.5	969.5	952.6	970.0	960.8	936.8	950.5	954.6	951.7	945.05	966.3
Avg. Leak. (gr./mo.)	9.18	0.10	0.15	0.10	0.08	0.06	0.15	0.08	0.16	0.09	0.13	0.10

FIGURE 14

combustion chamber was being developed by ESC for NADC under a concurrent contract to design a RSSK-8A DAPS. It was determined that this new design combustion chamber could in fact be packaged to fit the RSSK-1A void.

The extensive combustion chamber design and developmental test program which resulted is described in the following sections.

2.4.2 Comparison of Two Designs

A comparison of the two designs together with the design analyses involved in developing the new design follows.

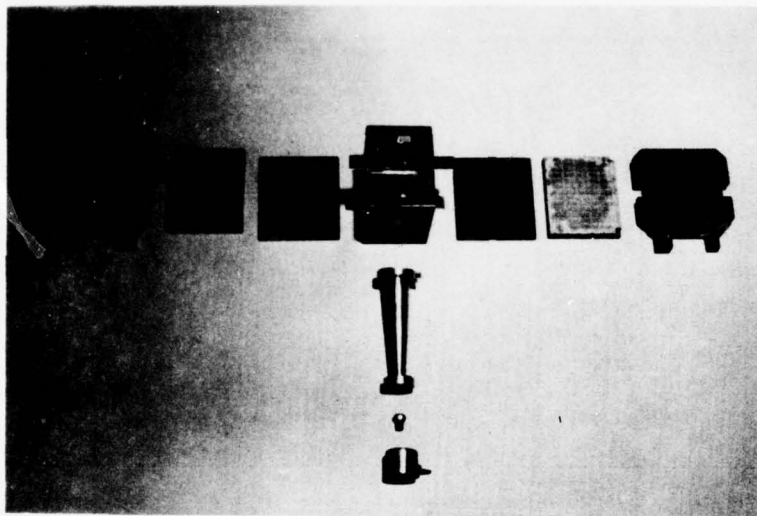
The combustion chamber used in all one man heaters to date (DAPS and Arctic heater) consist of a cubical combustion chamber to which were mounted pin plates on either side. (Figure 15 Exploded View) On each of these hot plates are mounted a thermoelectric module and heat exchanger, the thermoelectric module being sandwiched between the heat exchanger and pin plate (Figure 16).

The new design markedly changes this configuration (Figure 17 Exploded View). The new configuration uses only one hot plate and heat exchanger although it still utilizes two (2) thermoelectric modules. Several advantages were realized with the design. Component costs were reduced slightly and assembly time was reduced by 50%. (Figure 18)

2.4.3 Developmental Combustion Chamber Analysis and Testing

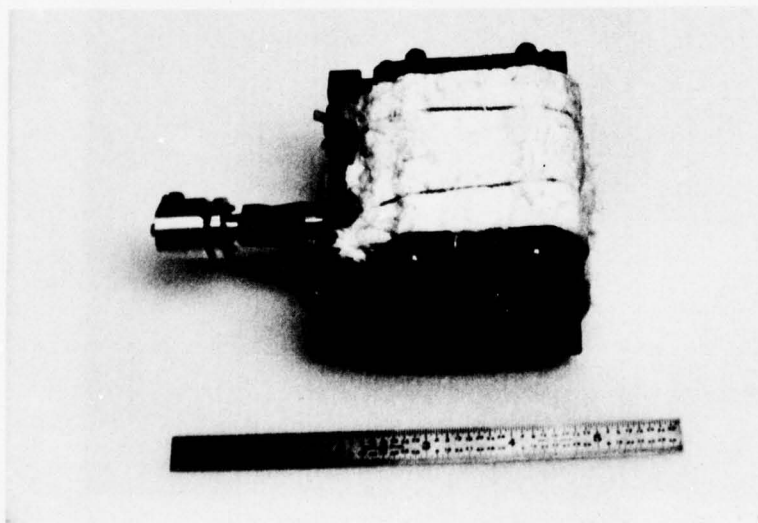
Before arriving at a final design, extensive developmental testing had to be performed. The four major testing programs performed on this combustion chamber design are listed below:

- A. Temperature profile as a function of catalytic bed size
- B. Temperature profile as a function of catalytic bed location



Exploded View of Old Combustion Chamber

Figure 15



Assembled View of Old Combustion Chamber

Figure 16

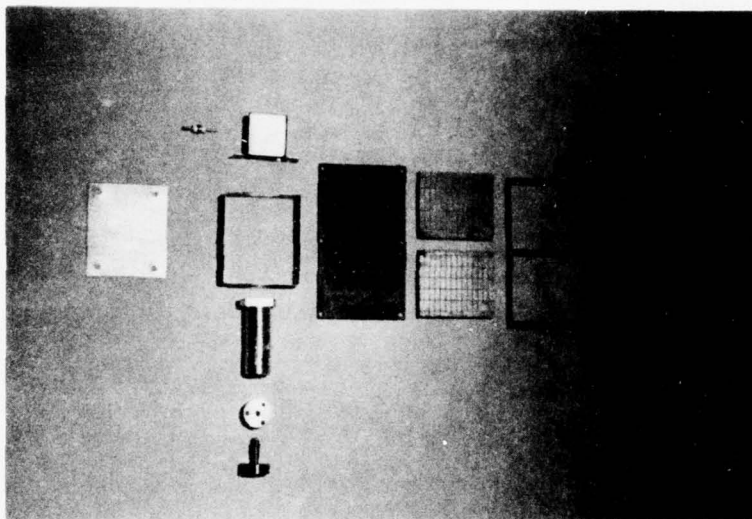


Figure 17

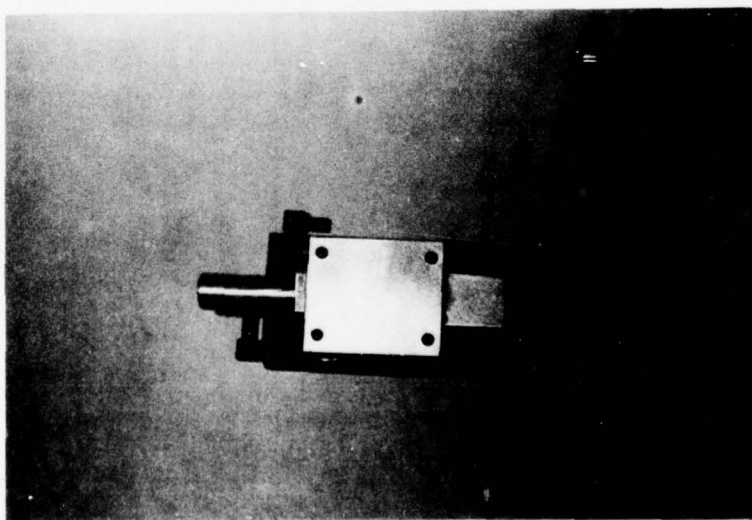


Figure 18

- C. Power generation ability
- D. Heat exchanger efficiency

A brief description of each test along with test results follows:

- A. Temperature Profile as a Function of Catalytic Bed Size

The temperature and combustion efficiency of the catalytic bed is directly related to its size. If the bed is too small, i.e., not enough catalyst present, all the fuel that is supplied to the chamber cannot be completely oxidized. This results in unburned fuel, therefore, wasted potential energy. This unburned fuel results in a net decrease in hot plate temperature.

Efficiency is also decreased if the bed size is too large. The major effect of too large a catalytic bed is the recombination of exhaust product in an extremely endothermic reaction. These reversed reactions possible in the presence of excess catalyst, or insufficient oxygen, absorb large amount of heat thereby reducing the hot plate temperatures.

In order to measure these effects, a combustion chamber was instrumented with thermocouple wires at six equally spaced locations along the hot side pin plate (See Figure 19) and the temperature profile plotted at 10, 20 and 30 PSIG fuel pressures. Figures 23 - a, b, c show the positions and relative sizes of the various beds tested.

Three plots were made for bed size of 7.15 grams, 12.4 grams and 28.5 grams of catalyst.

Results of these test (shown in Figures 20, 21 & 22) indicate that maximum temperatures are attained with the 12.5 gram bed and that too much or too little results in lower temperatures and, hence, a lower power output due to a decreased temperature difference across the thermoelectric modules.

Figure 19 shows the location of the thermocouple leads on the assembly. Figures 20 and 21 show how the temperature profile of the hot side changes as a function of catalytic bed size. From this data we see that of the three bed sizes used, the 12.5 gram bed yields the highest temperatures and, therefore, best results.

B. Temperature Profile as a Function of Bed Location

The thermoelectric modules generate the greatest electrical output if the temperature on the hot side is uniformly maintained across the entire surface. Although this is the ideal situation it is difficult to achieve in actual practice. Tests were performed to attempt to locate the hottest area symmetrically with respect to the two modules.

Referring to the location of peak temperatures with respect to the thermoelectric modules, it was observed that the maximum temperature is located at the front of the catalytic bed. This is shown by comparing the peak temperatures obtained in Figure 21 and Figure 22 and correlating these temperatures to the bed locations.

By examining the temperature profiles resulting from the tests it was possible to optimize catalyst bed location. (See Table 1 for Raw Data)

C. Power Generation Ability

Power generation output of the modules was monitored in the testing described above and it was found that the maximum power was generated once optimum catalytic bed size and location were determined.

D. Heat Exchanger Efficiency

The efficiency of the heat exchanger used in previous designs had been optimized at the time of original design. The change to a new design required that additional testing be performed to optimize the new configuration.

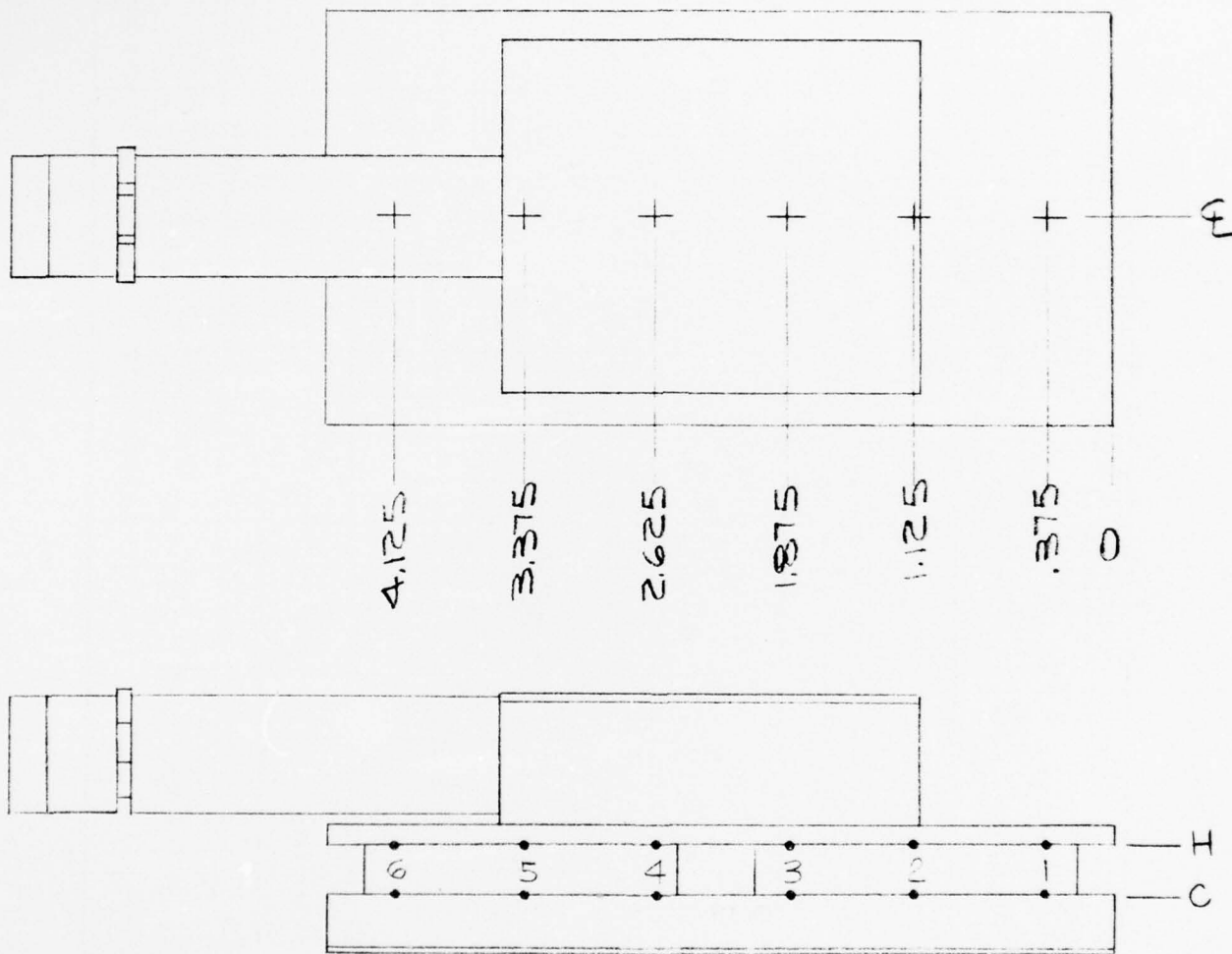
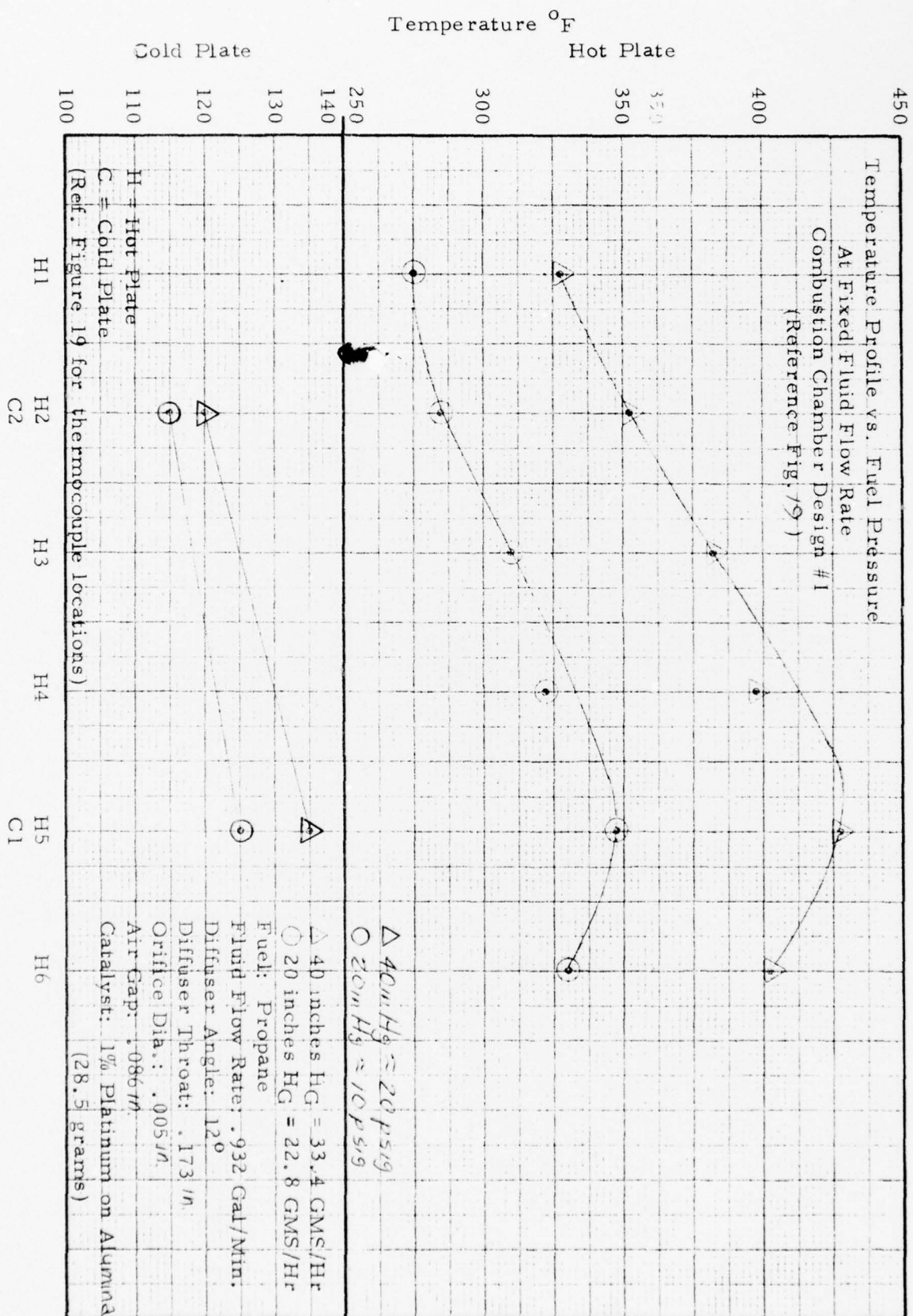
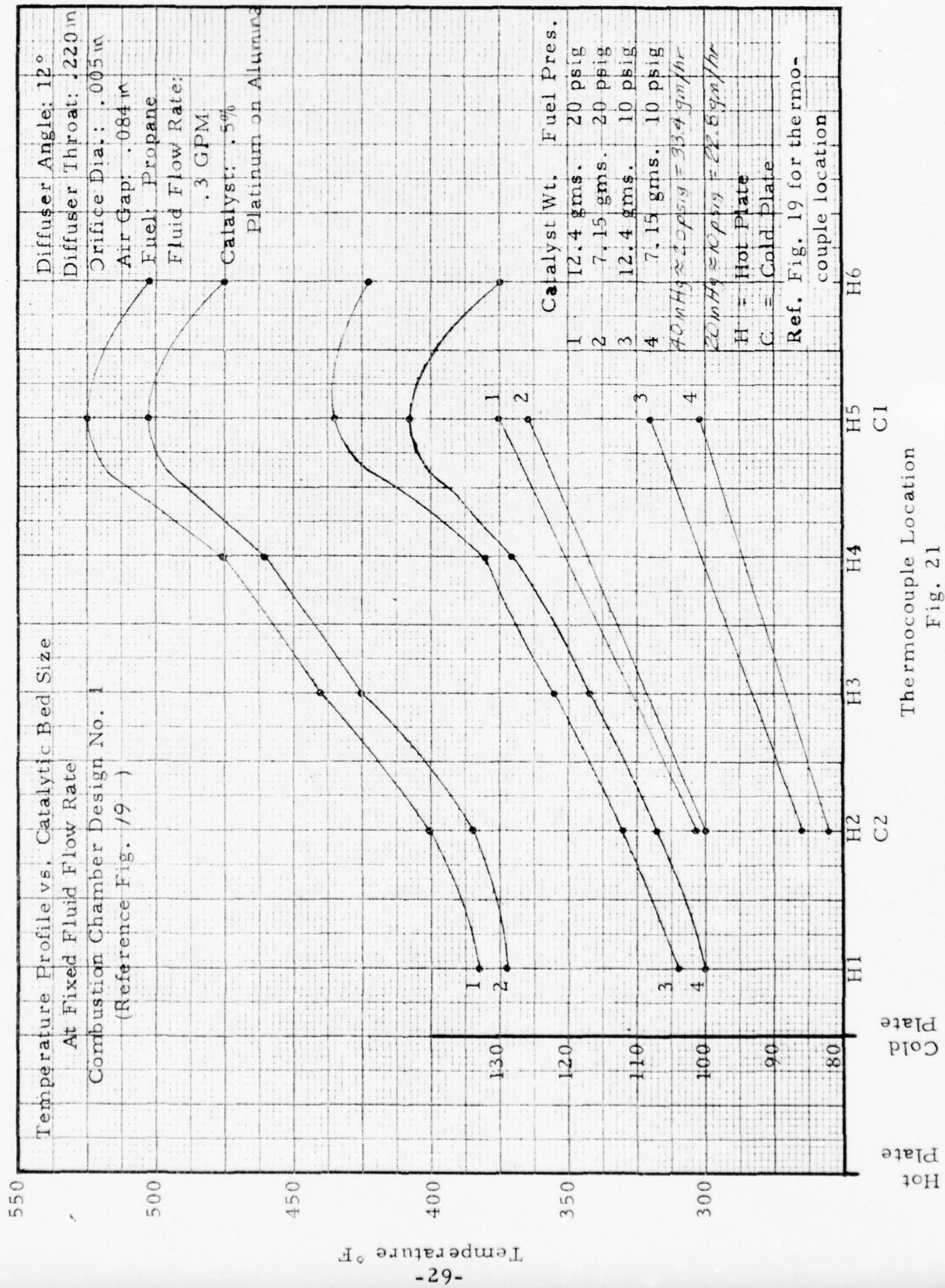


Figure 19





Thermocouple Location
Fig. 21

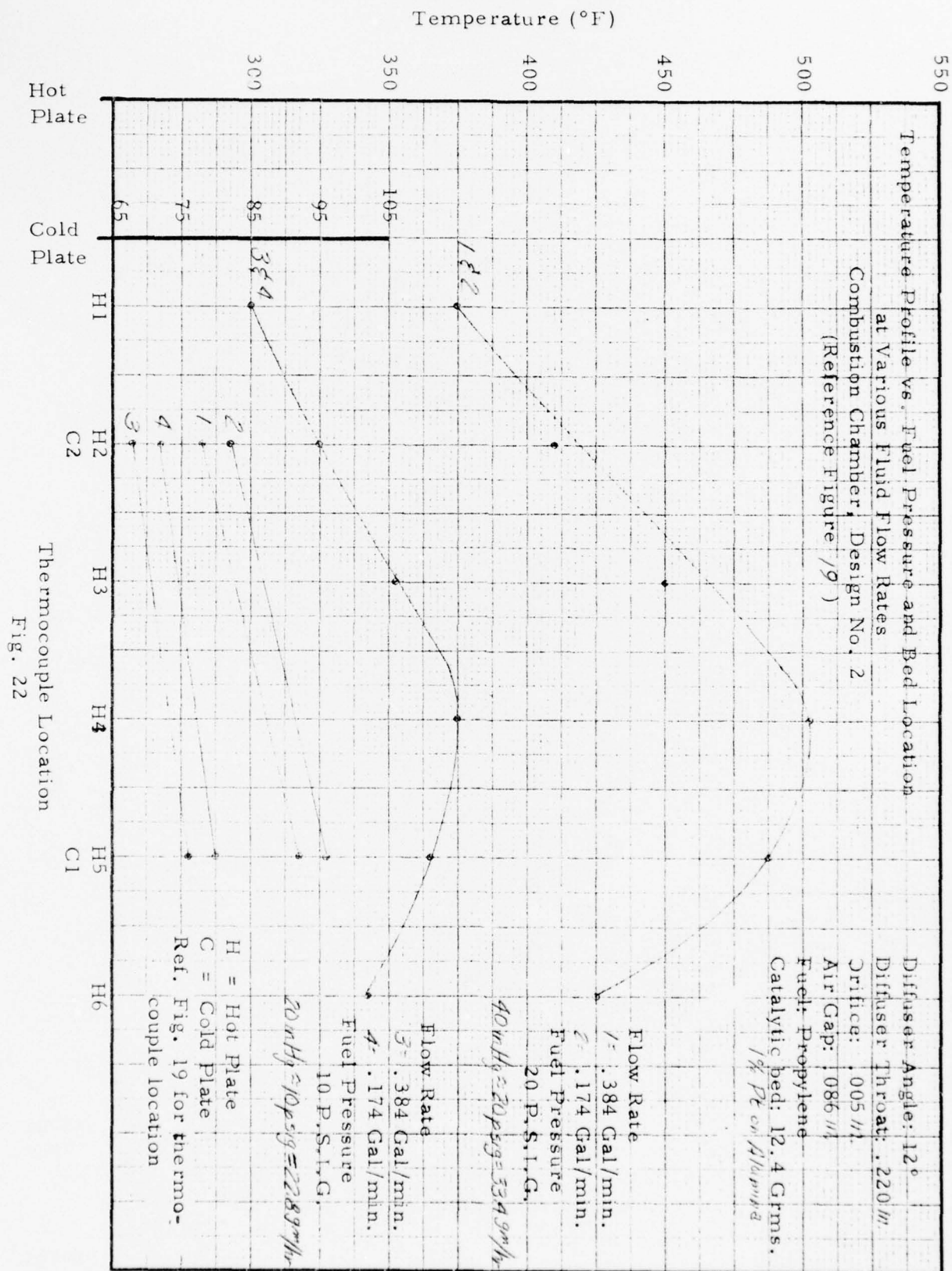


TABLE 1

RAW DATA FOR TEMPERATURE PROFILE
USED TO GENERATE PLOTS IN FIGURES 20, 21, & 22

Ref. Fig.	Fuel Pressure	Fluid Flow Rate	Catalytic Bed Size	Thermocouple Location							
				$\frac{H1}{mv}$	$\frac{H2}{mv}$	$\frac{H3}{mv}$	$\frac{H4}{mv}$	$\frac{H5}{mv}$	$\frac{H6}{mv}$	$\frac{C1}{mv}$	$\frac{C2}{mv}$
20 23c	20 psig	.932 gpm	28.5 gms	5.45 272	5.75 284	6.27 308	6.55 521	7.15 347	6.77 331	212 127	1.87 116
	10 psig	.932 gpm	28.5 gms	6.7 327	7.25 352	7.9 382	8.25 397	8.9 427	8.35 402	2.3 134	1.9 117
21, 23a	20 psig	.3 gpm	12.4 gms	7.7 373	8.32 401	9.15 438	9.9 477	11.22 529	10.65 504	7.2 130	1.5 99
23b	20 psig	.3 gpm	7.15 gms	7.61 370	8.34 402	9.07 433	9.77 465	10.80 510	10.00 475	2.10 125	1.50 100
	10 psig	.3 gpm	12.4 gms	6.25 308	6.7 328	7.25 357	7.9 381	9.05 433	8.62 414	1.68 108	1.18 85
	10 psig	.3 gpm	7.15 gms	6.05 298	6.55 321	7.1 345	7.60 370	8.5 440	7.77 375	1.55 122	1.16 82
22 23b	20 psig	.384 gpm	12.4 gms	7.76 375	8.58 412	4.55 455	10.85 512	10.05 477	8.96 430	1.42 96	1.16 82
		.174 gpm									
	10 psig	.784 gpm	12.4 gms	6.04 297	6.62 325	7.35 357	8.42 405	7.90 380	7.08 345	1.06 80	.90 73
		.174 gpm									

Heat exchanger efficiency depends directly on the heat transfer coefficient "h" and the surface area "A" as evidenced by the well known relationship:

$$q = h A \Delta T$$

where

- q = heat transferred from the heat exchanger to the water (BTU/Hr)
- h = heat transfer coefficient (BTU/Hr - ft² - °F)
- A = effective heat transfer area (ft²)
- ΔT = temperature difference between fluid and heat exchanger walls (°F)

Clearly, heat transfer into the water can be increased by increasing either h or A. Heat transfer coefficient, h, is a function of Reynolds Number, R_N, determined by the equation:

$$\text{Reynolds No. (RN)} = \frac{\rho V D}{\mu}$$

where:

- ρ = density (lbs/ft³)
- V = speed (ft/hr)
- D = Hydraulic diameter (ft)
- μ = viscosity of fluid (LBS/hr ft)

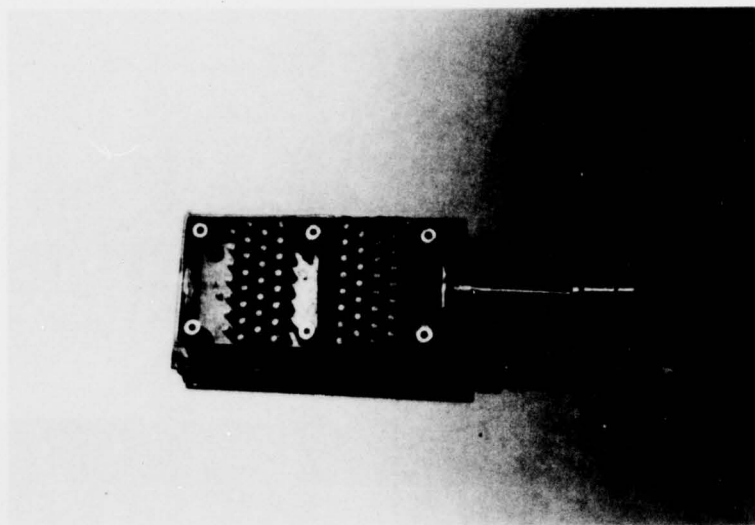
The velocity used to determine R_N is calculated by the equation:

$$V = Q/A_c$$

where:

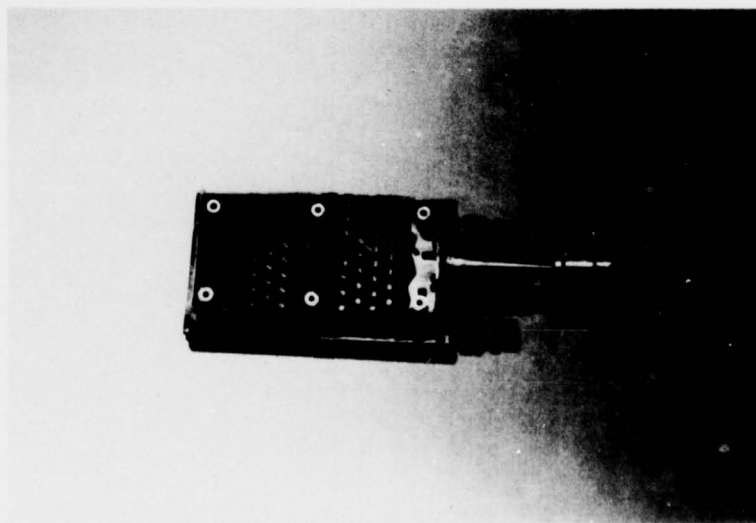
- Q = flow rate (ft³/hr)
- A_c = flow channel area (ft²)
- V = average flow velocity (ft/hr)

The test set-up consisted of a combustion chamber, heat exchanger and thermoelectric modules. The modules in this case were used only to simulate actual heat transfer and not for power generation. This was done so the flow rate could be varied independently of the level of power generation by the modules.



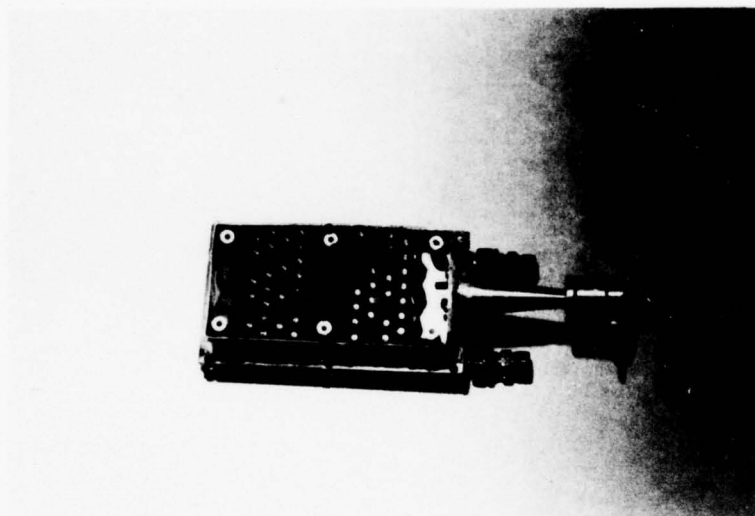
7.15 Gram Catalytic Bed Size

Figure 23a



12.4 Gram Catalytic Bed Size

Figure 23b



28.5 Gram Catalytic Bed Size

Figure 23c

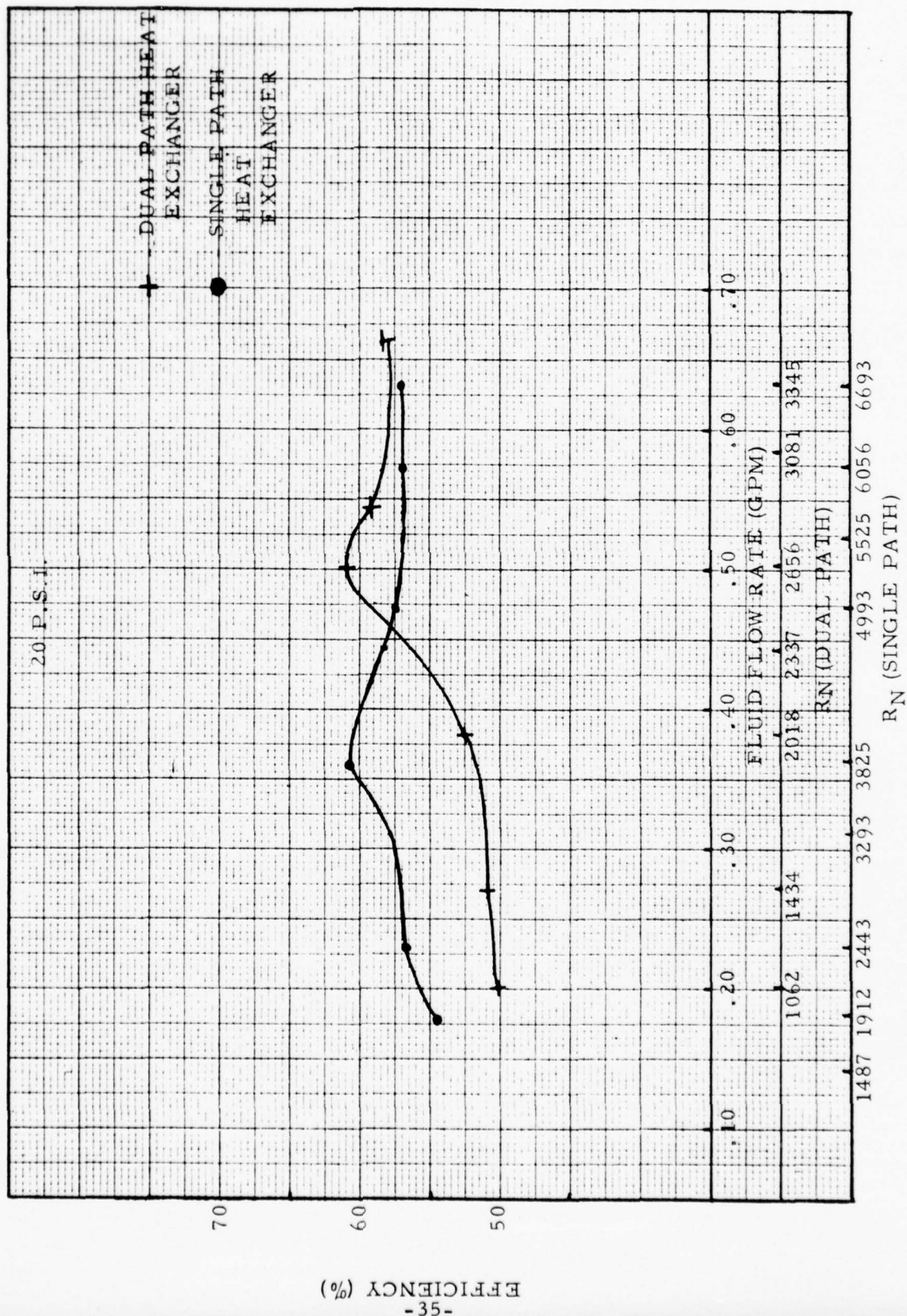


FIGURE 24

Three fuel rates were used. These fuel rates along with their corresponding heat rates are tabulated below.

<u>Fuel Pressure</u>	<u>Fuel Flow Rate</u>	<u>Fuel Energy Content</u>
9.82 psig	27.8 gms/hr	1005 BTU/hr
20.13 psig	33.4 gms/hr	1470 BTU/hr
30.0 psig	40.6 gms/hr	1787 BTU/hr

At each fuel flow rate cooling fluid was circulated through the heat exchanger using a pump driven by an auxilliary power supply. The water flow rate and temperature difference between the fluid into and out of the heat exchanger was measured and the heat into the water was calculated by the equation:

$$q = \dot{m} C_p \Delta T$$

where:

q = heat into water (BTU/Hr)

\dot{m} = mass flow rate of water (LB/Hr)

C_p = Specific heat of water (BTU/Lb-°F) = 1.0

ΔT = difference between inlet and outlet temperatures (°F)

Figure 24 shows a plot of system efficiency as a function of fluid flow rate showing that efficiency increases as flow rate increases. For each of these flow rates, the corresponding Reynolds number was calculated and plotted along the same axis. Clearly, system efficiency can be increased by increasing the Reynolds number independently of the flow rate. This could be done by decreasing the flow path diameter, thereby, increasing the velocity.

A second generation dual path heat exchanger with a smaller total cross sectional area was fabricated and the test was repeated. These results are plotted in Figure 24 and correlate very well with what was theoretically predicted, i.e., a higher efficiency can be obtained at a lower flow rate by increasing the fluid velocity.

The major drawback with attempting to increase heat transfer by increased heat transfer coefficient "h" is that a disproportionate increase in power to pump the fluid is required to achieve a relatively small increase in flow velocity. This is due to the exponential increase in pressure drop across the system as the flow rate Q or velocity V is increased.

Analysis of the test results obtained from this second generation heat exchanger leads to the conclusion that the greater part of the increase in heat transfer was achieved because of a large increase in the surface area available for heat transfer and not to a large increase in the heat transfer coefficient, h .

Tests indicate that the dual path heat exchanger resulted in a 4% increase in heat picked up by the water. These results are adequate to satisfy the requirements of the design.

Once the results of the performance test were reduced it was possible to compare what effects varying h and A had on the two configurations. The change in the surface area was easily determined by examining the drawings but the values for h were not as easily determined.

This determination was made using the empirical Sieder-Tate correlation of the heat transfer coefficient, h , with Reynolds Number (See Figure 25).

Table 2 shows a comparison of the values of this test on both heat exchangers.

TABLE 2

	Heat Exchanger #1 (Single Pass)			Heat Exchanger #2 (Dual Pass)		
Fuel Pressure	10psig	20psig	30psig	10psig	20psig	30psig
R_N	3825	3825	4462	3612	2656	3346
h	251	251	282	238	150	213
A	20	20	20	30	30	30
% Eff.	65.7	65.6	59.5	74.0	65.6	59.5
L/D_e	86.6	86.6	86.6	145	145	145

where:

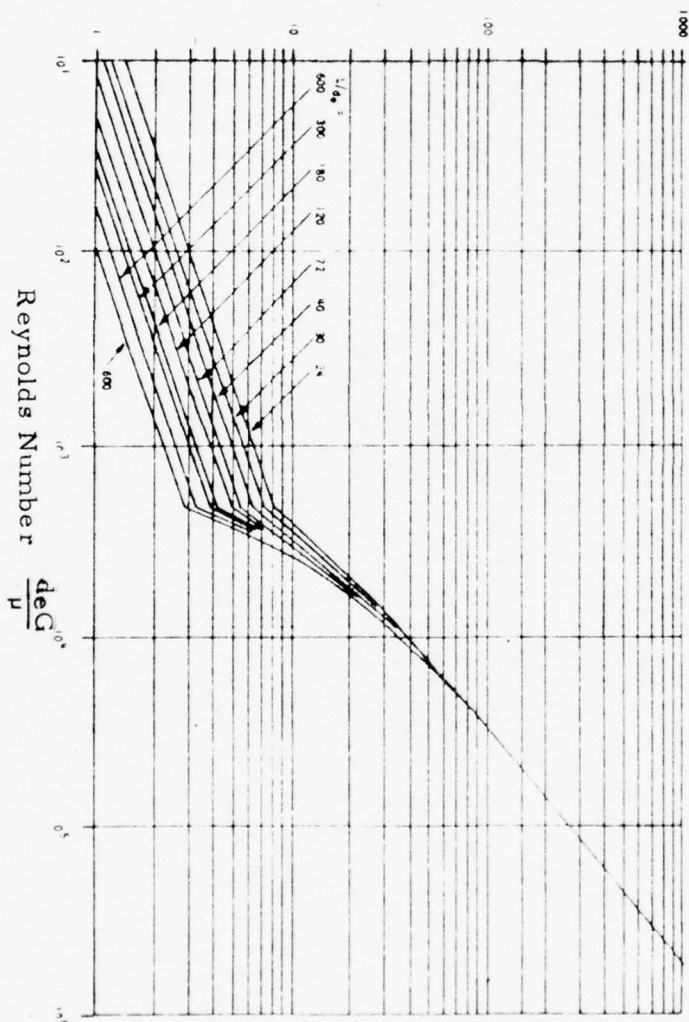
- R_N = Reynolds Number
- h = heat transfer coefficient ($B.T.U./Hr-ft^2-^{\circ}F$)
- A = Effective surface area (in^2)
- %Eff. = Efficiency of unit
- L/D_e = Path length/Equivalent Diameter

J = Sieder Tate Factor (Dimensionless)
 G = Mass Velocity (lb/hr. ft)
 h = Heat Transfer Coefficient (BTU/hr ft² °F)
 d_e = Equivalent Path Dia. (ft)
 k = Thermal Conductivity of Fluid (BTU/Hr ft °F)
 C_p = Specific Heat of Fluid (BTU/lb °F)
 μ = Dynamic Viscosity of Fluid (lb/hr ft)

Subscript b = Bulk Fluid Property
 Subscript w = Fluid Characteristics at wall

$$J = K_b \frac{h d_e}{C_p \mu} \left(\frac{K}{K_b} \right)^b \left(\frac{\mu}{\mu_w} \right)^{-0.33} \left(\frac{\mu}{\mu_w} \right)^{-0.14}$$

Sieder Tate Factor:



Graphical representation of Sieder Tate correlation for the heat transfer coefficient for fluids flowing within tubes, ducts, pipes, and annuli. (Kraus, A.D., Cooling Electronic Equipment, p. 139)

Sieder-Tate Correlation

Figure 25

Examination of these results indicate that the increase in efficiency was due to an increase in heat transfer surface area, rather than a significant increase in h .

Several other test and analyses were performed on other components of the DAPS. Those of major interest are listed below.

- Fuel/Air Mixture Ratios as a Function of Diffuser Geometry
- DC Motor Evaluation
- Exhaust Gas Concentration

A description of these tests and test results follows:

2.5 Venturi Analysis & Tests

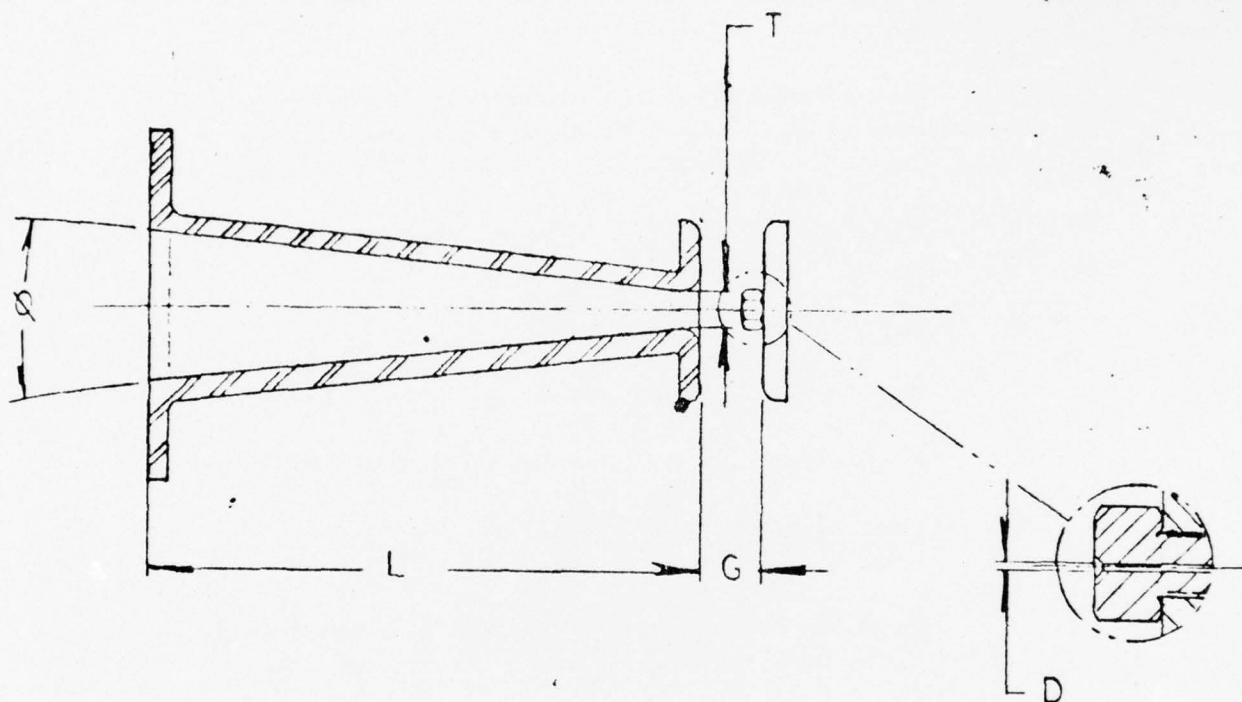
Optimum combustion efficiency is obtained when the air/fuel ratio is in the order of 4-4.5% fuel to air by volume.

This fuel/air ratio is affected by diffuser-orifice geometry and extensive tests were performed to determine the optimum diffuser geometry. Figure 26 defines the parameters affecting fuel/air ratios.

Figure 27 is a plot of the fuel/air ratio vs. the air gap ("G" dimension on Figure 26). Tables 3, 4 & 5 present the raw data from which the plots were generated.

Although the 7° diffuser gives the best results, the length "L" is too long and precludes its use in the system. The 12° diffuser gives satisfactory results and will be used in these systems.

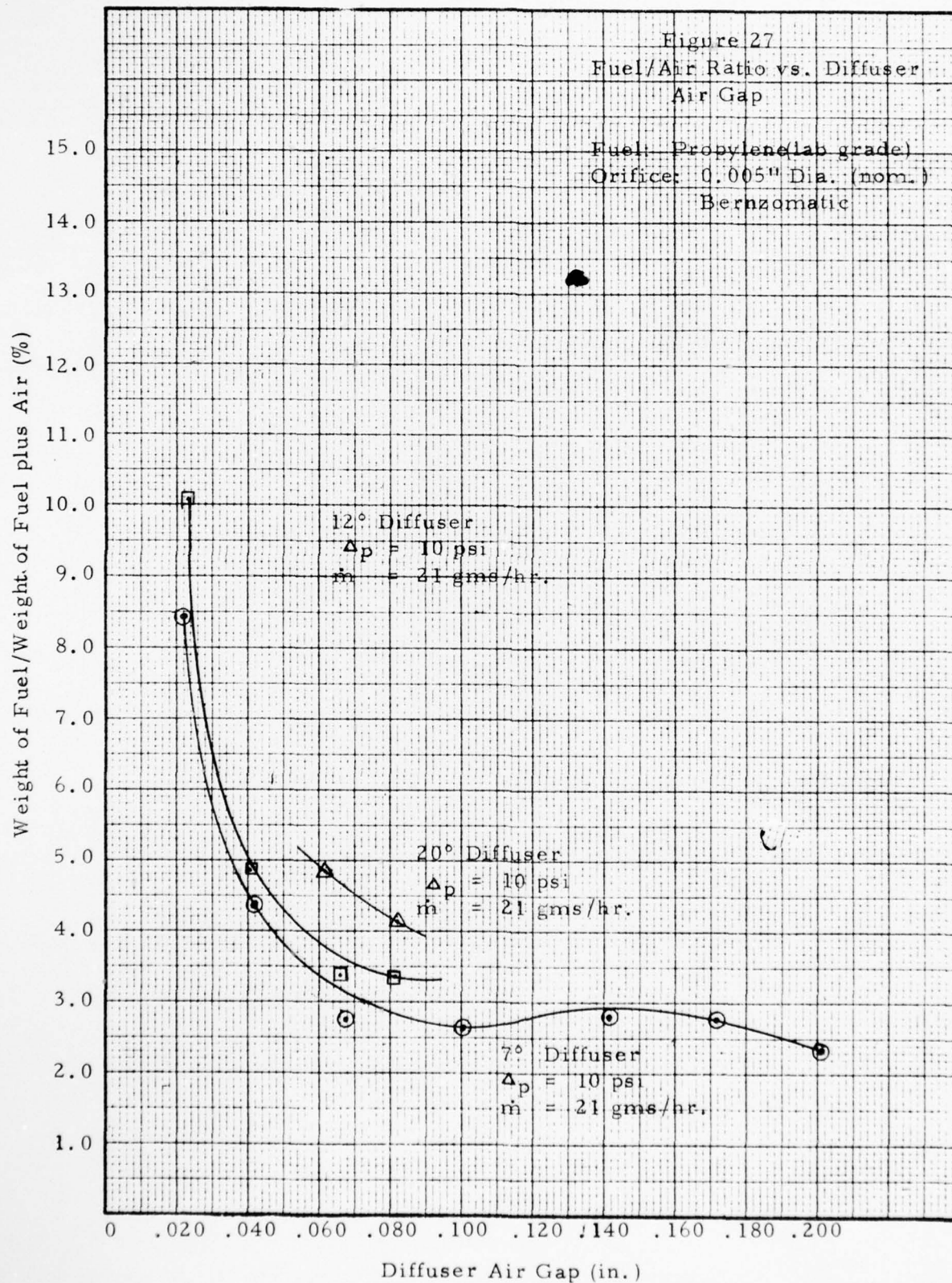
The fuel/air ratios were measured using a Miran Infrared Spectrometer. This device detects a gas concentration by measuring the absorption of this infrared energy as compared to the absorption of the pure gas.



- Q = Included Angle
 G = Air Gap
 L = Diffuser Length
 D = Orifice Dia.
 T = Throat Dia.

Orifice - Diffuser Geometric Variables

Figure 26



Venturi/Diffuser Fuel-Air Mixing Tests

Diffuser: 7°
 Orifice: 0.005 " Dia. Nominal - Bernzomatic
 Fuel: Propylene,** Laboratory Grade

Air Gap (Inches)	Pressure (In. Hg)	Pressure (psig)	Mass Flow (gm/hr)	Fuel/Air Ratio (%)
0.200	41.2	20.2*	30.7	2.3
	20.7	10.1	21.0	2.3
0.150	40.2	19.7 *	30.3°	2.7
	20.9	10.2	21.0	2.7
0.124	20.4	10.0	21.0	2.7
0.100	41.0	20.1 *	30.6	2.7
	30.7	15.0 *	26.1	2.7
	20.5	10.0	21.0	2.6
0.067	20.9	10.2	21.0	2.7
	10.5	5.1	19.4	2.7
0.066	10.5	5.1	19.4	3.0
	4.5	2.2	15.3	3.1
	2.1	1.0	11.3	3.3
	1.2	.6	9.0	3.9
0.041	40.5	19.8 *	30.3	4.1
	21.0	10.3	21.0	4.3
0.022	20.7	10.1	21.0	8.4
	10.6	5.2	19.5	8.8
	4.0	2.0	14.8	9.9

* Choked flow (occurs when pressure greater than 25.5 psia or 10.8 psig)

** Commercially available Propane can contain a significant amount of other hydrocarbon compounds which would significantly increase the difficulty of accurate air fuel analysis. Therefore because the fuel values of commercial propane is within 5% of laboratory grade, Propylene was used.

Air Gap Data
 7° Diffuser
 TABLE 3

Venturi/Diffuser Fuel-Air Mixing Tests

Diffuser: 12°
 Orifice: 0.005 " Dia. Nominal - Bernzomatic
 Fuel: Propylene, Laboratory Grade

Air Gap (Inches)	Pressure (In. Hg.)	Pressure (psig)	Mass Flow (gm/hr)	Fuel/Air Ratio (%)
0.080	40.9	20.0*	30.5	3.5
	19.7	9.7	21.0	3.3
0.065	41.4	20.3*	30.8	3.5
	20.3	9.9	21.0	3.3
	6.2	3.0	16.9	3.2
	1.5	.7	9.6	3.6
0.040	40.1	19.6*	29.7	5.0
	20.5	10.0	21.0	4.8
	6.4	3.1	17.1	5.0
	2.3	1.1	11.7	5.2
0.022	40.8	20.0*	30.5	9.9
	21.1	10.3	21.0	10.0
	2.6	1.3	12.5	13.0

* Choked flow (pressure greater than 10.8 psig)

Air Gap Data

12° Diffuser

TABLE 4

Venturi/Diffuser Fuel-Air Mixing Tests

Diffuser: 20°
 Orifice: 0.005" Dia. Nominal - Bernzomatic
 Fuel: Propylene, Laboratory Grade

Air Gap (Inches)	Pressure (In. Hg.)	Pressure (psig)	Mass Flow (gm/hr)	Fuel/Air Ratio (%)
0.081	41.3	20.2*	30.7	4.4
	20.8	10.2	21.0	4.1
	10.8	5.3	19.6	3.6
	5.6	2.7	16.4	3.9
	2.2	1.1	11.7	3.5
0.061	40.0	19.6*	29.7	4.5
	21.0	10.3	21.0	4.8
	10.5	5.1	19.4	4.5
0.061	40.0	19.6*	29.7	25.3**

* Choked flow (occurs when pressure greater than 10.8 psig)

** Combustion chamber exhaust hole closed off - through flow due to leakage only. No measurable pressure in chamber (inches of alcohol).
 An attempt was made to measure pressure recover thru the diffuser so that the maximum back pressure against which the air/fuel mixture could be passed could be determined. Alcohol was used due to its lower specific gravity. The significant data was derived from this test.

Air Gap Data
 20° Diffuser

TABLE 5

As an example, assume that a 3000 microliter sample of the pure gas, propylene in this case, results in a Miran meter reading of .497 absorption units. A 3000 microliter sample of mixture of unknown concentration of the gas in question can be determined, i.e., $.0174/.497 \times 100\% = 3.5\%$.

These fuel/air mixtures were measured for a wide variety of diffuser configurations, the best*of which was incorporated into the system.

2.6 DC Motor Evaluation

In order to determine which of the many DC motors available would be best suited for the DAPS, tests were performed to determine the pumping rate and power consumption of each type.

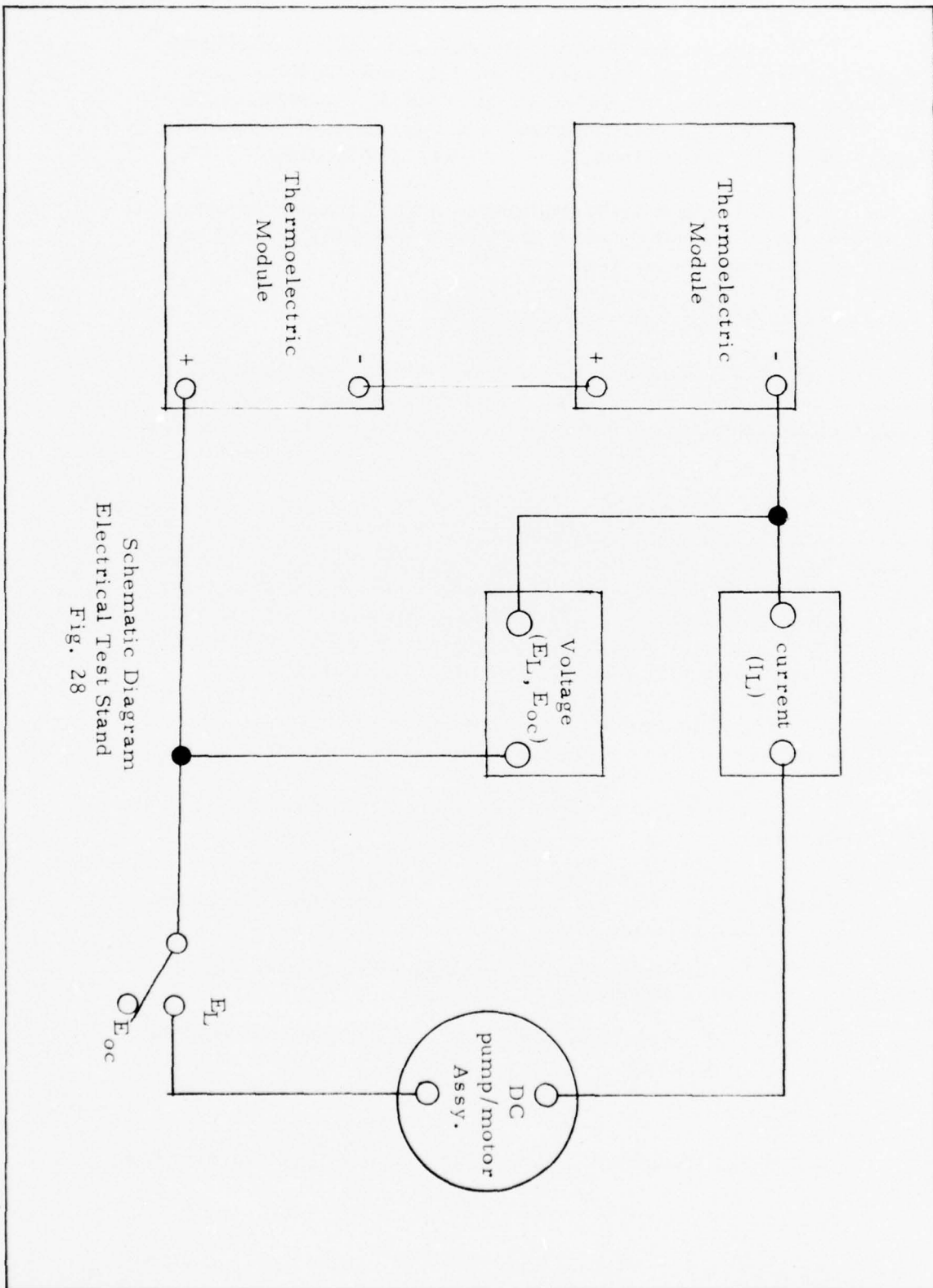
For this test, six motors were individually coupled to the same Micro-pump and this pump/motor assembly in turn connected to the combustion chamber equipped with live thermoelectric modules for power. The system was run at three fuel pressures (10, 20 and 30 PSIG) and load voltage, load current, open circuit voltage, and fluid flow rate were measured. This test set-up is schematically represented in Figures 28 & 29.

Figures 30 and 31 are plots of flow rate vs. current and flow rate vs. power consumption respectively.

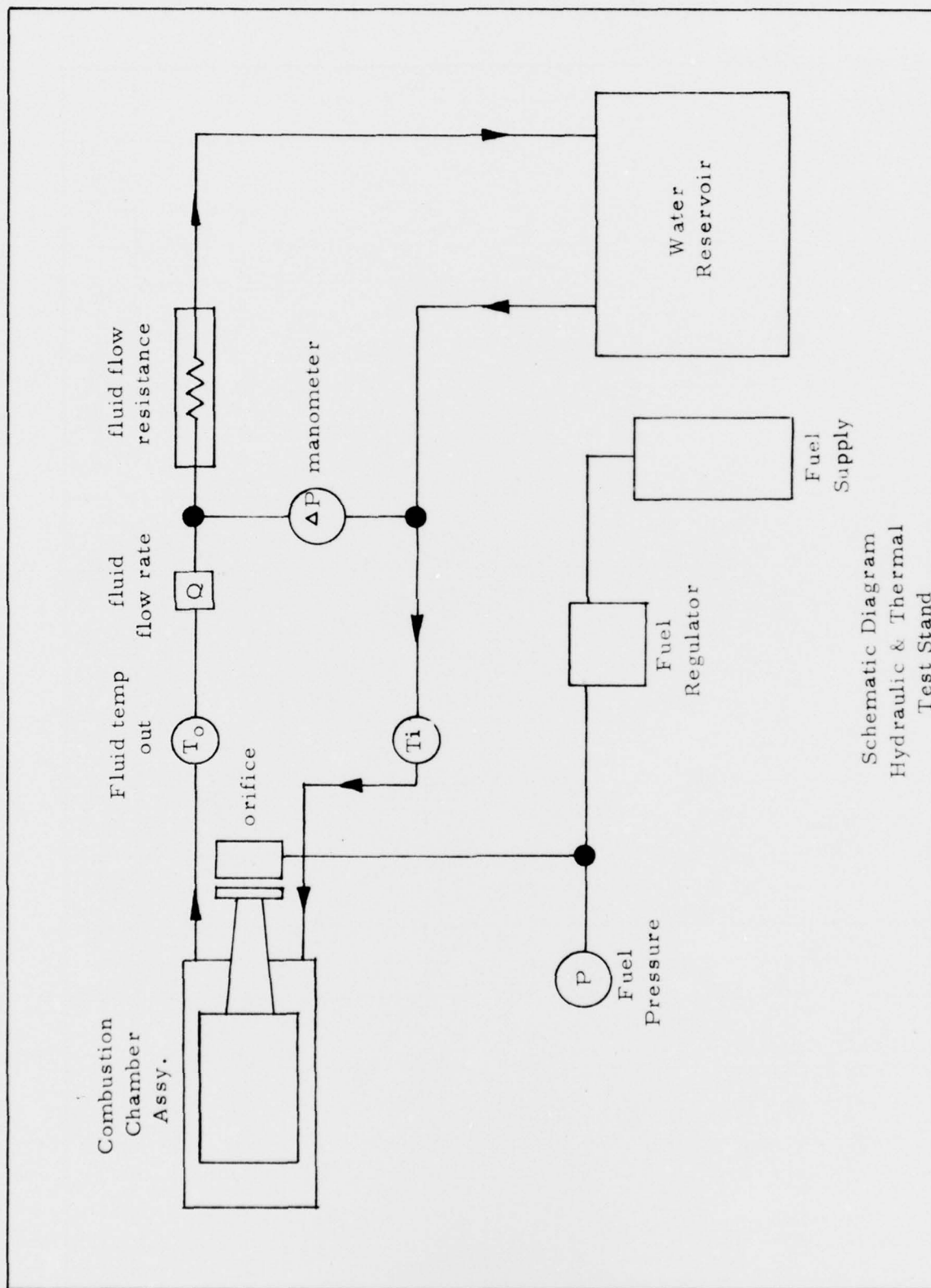
The prime considerations in the selection of a DC motor are:

1. Obtaining a good match between the motor internal resistance and the internal resistance of the modules.
2. Obtaining a sufficient fluid flow rate to satisfy the requirement for heat.
3. A current demand that will not over-stress the motor.

* 12° Diffuser; .005 in. Dia. orifice; .100 in Air Gap



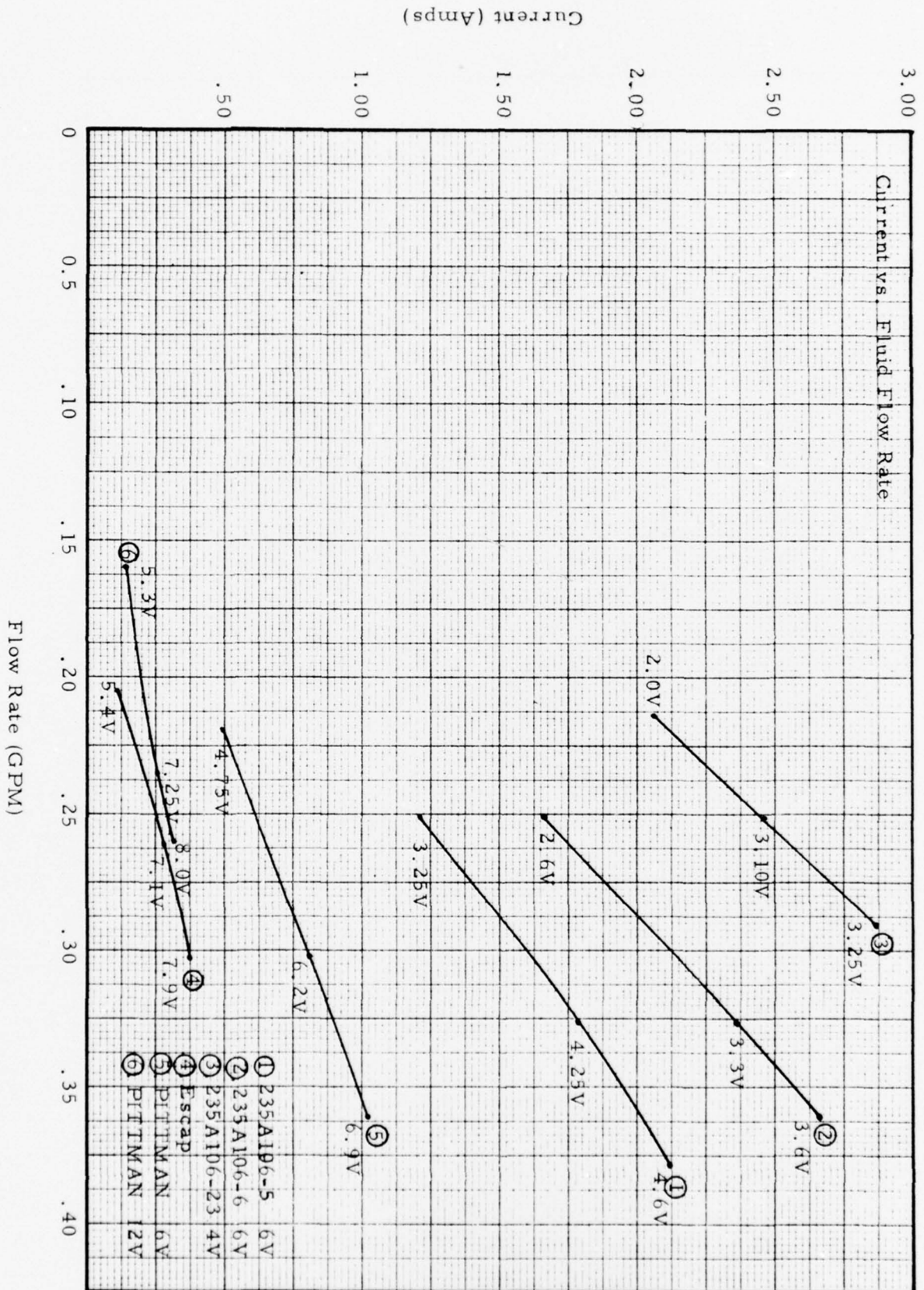
Schematic Diagram
Electrical Test Stand
Fig. 28

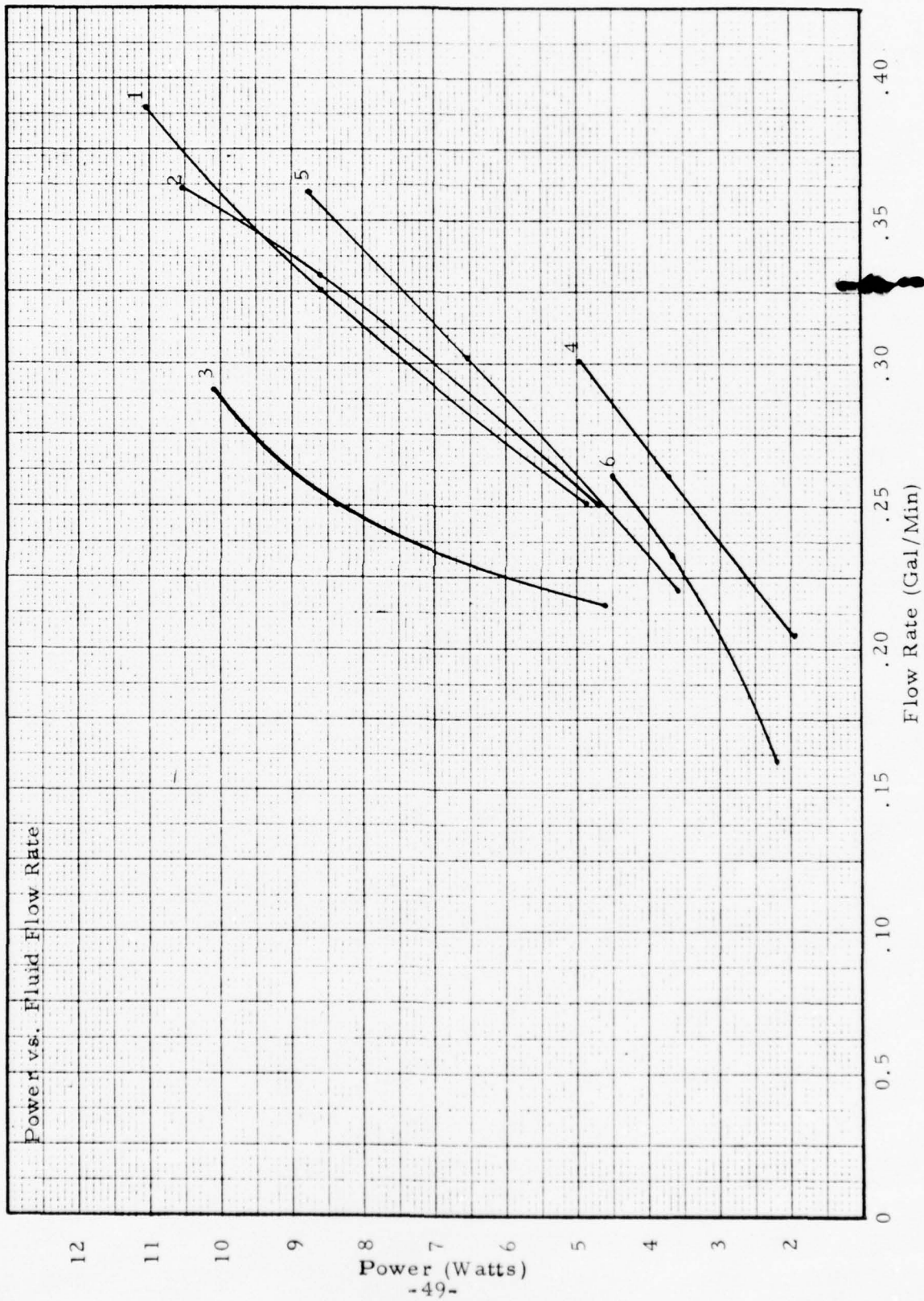


Schematic Diagram
Hydraulic & Thermal
Test Stand

Fig. 29

Figure 30





The results indicate that the TRW Globe motor number 235A106-5 gives the best flow characteristics for a realistic current demand. Further analysis indicates that the internal resistance is almost identical to that of the modules, typically five to six ohms.

2.7 Exhaust Gas Analysis

A series of tests were performed on the DAPS exhaust gas. The purpose of the test was to determine what the exhaust gas constituents are and the concentration of each.

The tests were performed using a portable infrared (IR) instrument manufactured by Wilks Scientific Corp., South Norwalk, Conn. The instrument is a single-beam scanning spectrophotometer with solid state electronics and a variable pathlength gas cell (0.75 to 20 meters). The gas cell can be pressurized to 10 atmosphere (150 PSIA) for increased sensitivity although this feature was not required in our application. The usable IR range for the instrument is from 2.5 to 14.5 μ (4000 to 690 cm^{-1}) which can be scanned automatically or manually in three segments. The output of the instrument can be observed on a meter or plotted on a strip chart.

The instrument detects the presence of a particular gas in the exhaust by measuring the amount of energy absorbed by the gas at a specific wavelength.

Each gas has a unique bandwidth in which it absorbs IR energy and by setting the instrument to the specific absorption wave length of a gas its presence can be detected.

The absorption of radiation at a particular wavelength by an absorbing material is given by the Beer-Lambert Law:

$$T = \frac{I}{I_0} = e^{-\epsilon lc}$$

or given as a function of absorbance A:

$$A = -\log_{10} T = \frac{\epsilon lc}{2.303}$$

This data is supplied as theoretical background data. All data is read directly from the meter on the instrument.

Referring to a calibration chart the concentration in parts per million (PPM) can be determined as a function of absorbance, (read directly from the meter or strip chart).

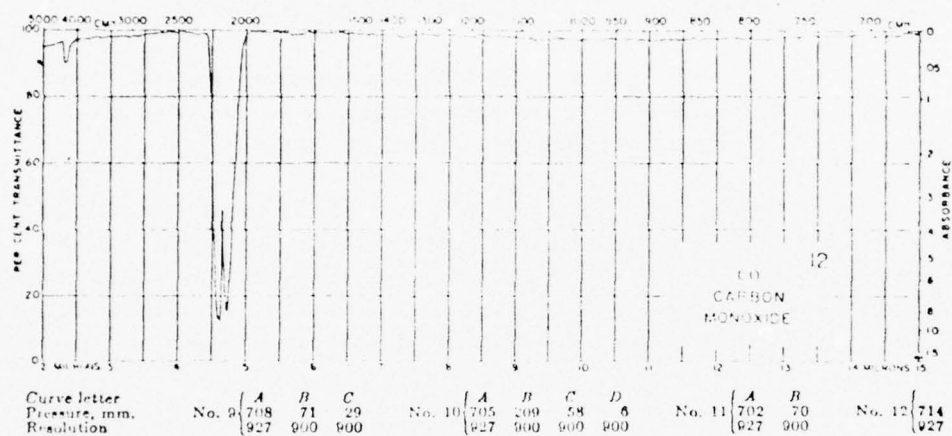
Figures 32 and 33 are plots of the total absorption spectra of carbon monoxide and propane. These plots indicate the particular wave length at which infrared energy is best absorbed. By selecting a strong absorption wavelength that is not adjacent to other compounds in the same frequency, interference can be eliminated.

Based on the spectral plots, calibration charts were generated for carbon monoxide (CO) and propane (C_3H_8) so as to accurately determine the concentration of these two gases in PPM (See figures 34 & 35). Plots of the exhaust gases of each unit were generated at 10, 20 and 30 PSI fuel pressure so as to maintain a permanent copy of the test results and also to facilitate comparing changes in exhaust gas constituents concentration as a function of fuel pressure.

A secondary benefit that could be determined from these plots, over and above determining the concentration of these two potentially dangerous compounds, was an indication of fuel combustion efficiency.

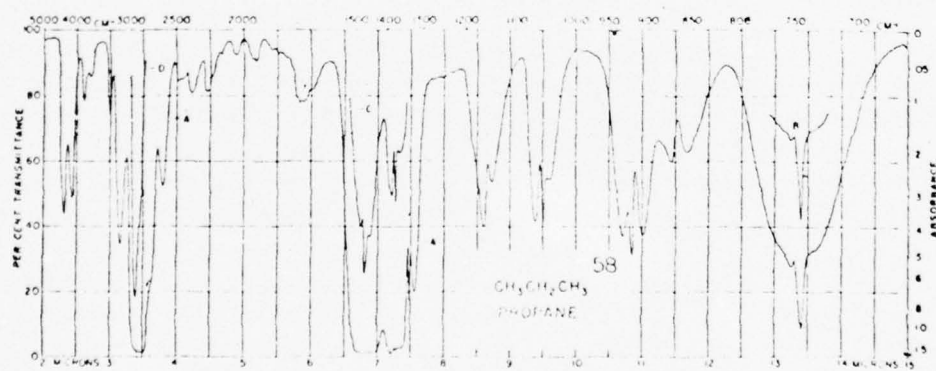
In complete combustion there would only be carbon dioxide (CO_2) and water (H_2O) in the exhaust gas. Because catalytic combustion is not a perfectly efficient method of combustion, some incomplete products of combustion are produced, i.e., carbon monoxide (CO) and propane (C_3H_8). The smaller the concentrations of these products the more efficient is the combustion process.

The concentration of carbon monoxide in the exhaust gas has been the subject of much debate in the past. To clarify this question, a study of exhaust gas concentration build-up rate has been performed.



CO Absorption Spectra

Figure 32



C₃H₈ Absorption Spectra

Figure 33

Figure 34
Carbon Monoxide Calibration Curve
Concentration Vs. Absorption

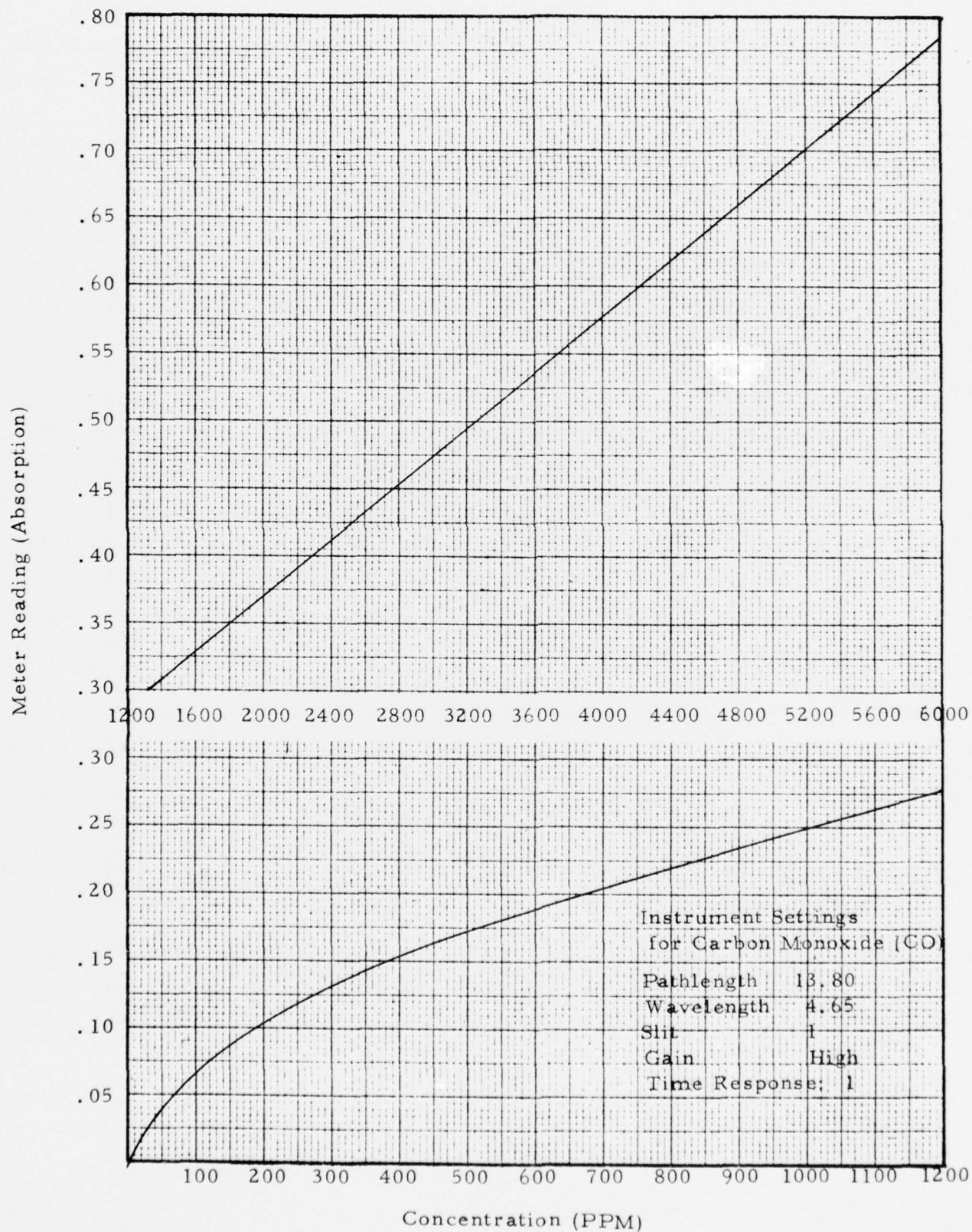
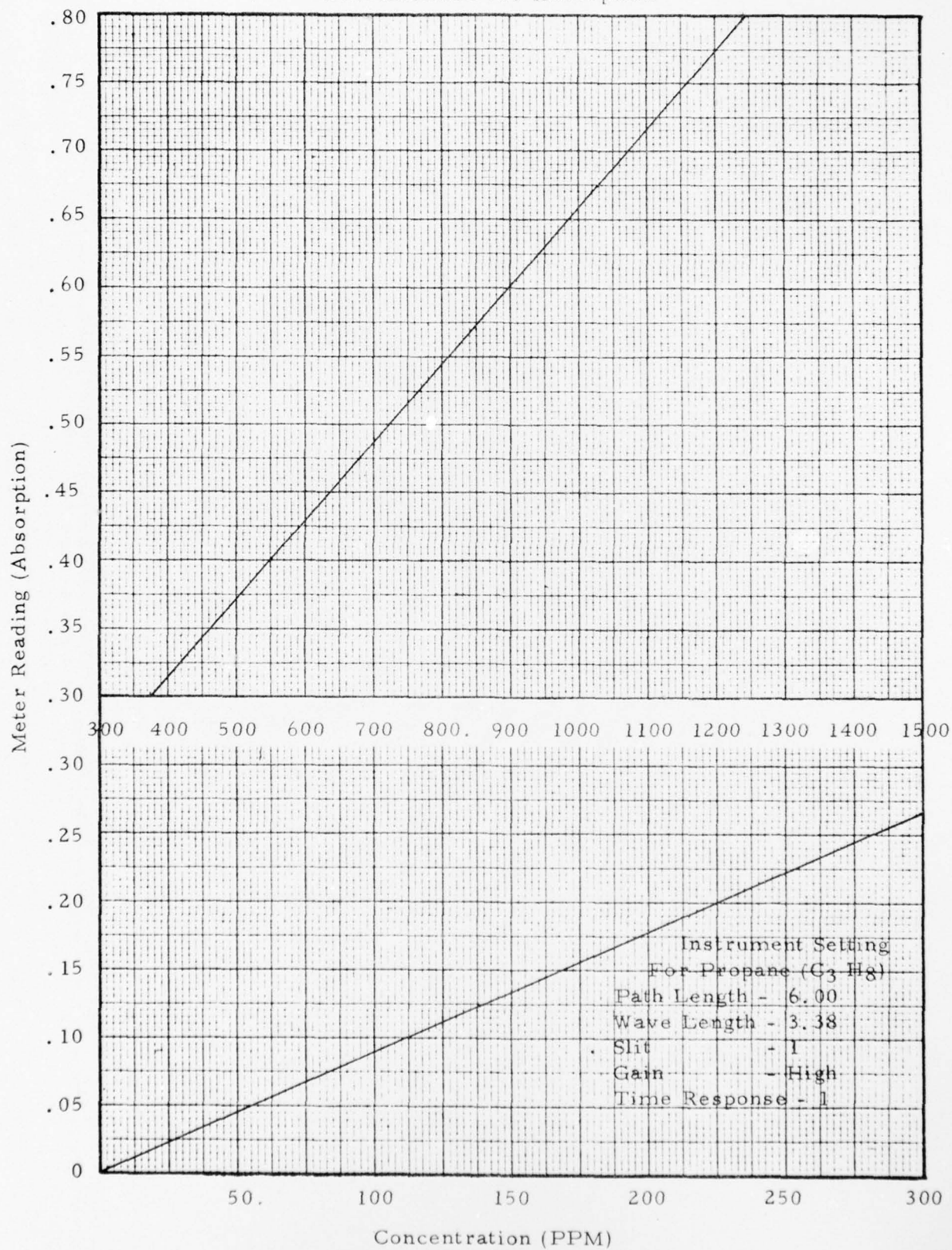


Fig. 35
Propane Calibration Curve
Concentration vs. Absorption



The typical concentrations of CO in the exhaust stream of the DAPS unit is on the order of 400 PPM. On first inspection, this may seem high, but when the rate of CO production is considered, the concentration can be viewed with better perspective.

At a fuel flow rate of 40 grams per hour based on a 20 to 1 ratio of air to fuel, exhaust gas is generated at the rate of approximately 550 grams per hour.

400 PPM of CO based on 550 grams per hour is the equivalent of .22 grams per hour of CO.

An enclosure $6' \times 6' \times 6'$ has a volume of 216 ft^3 . Air has a density of .074 LBS/ ft^3 or 34.1 grams/ ft^3 . The total weight of air in the enclosure is $216 \text{ ft}^3 \times 34.1 \text{ grams}/\text{ft}^3 = 7365.6$ grams. A CO production rate of .22 gms/hr diffused in this chamber would result in a CO build-up rate of $\frac{.22 \text{ gms/hr}}{7365.6 \text{ gms}} = 29.8 \text{ PPM/Hr}$ which is well within the OSHA recommended safety limits.

The above analysis is based on a closed chamber in which there is no exchange of air and the building up of exhaust products increases at a constant rate.

In an actual life-raft situation the life-raft will not be sealed tightly and the raft will also be flexible. These two factors will allow the life-raft to "breathe". This breathing results in an exchange of air that will be induced by the airman motion inside the raft and/or by wave motion. These factors preclude the possibility of an excessively high concentration of exhaust gas build-up inside the raft.

3.0 DAPS DESIGN

3.1 RSSK 1A DAPS Requirements

3.1.1 General Requirements

The Downed Airman Power Source (DAPS) must integrate functionally with and enable the proper operation of all interfacing elements of the modular Downed Airman Integrated

Survival system. These interfacing elements are the airman and his clothing most specifically a liquid loop thermal garment, his parachute, and encapsulating liferaft, and the ejection seat kit (into which are incorporated an emergency descent oxygen supply and miscellaneous survival kit elements, DAPS and the liferaft).

The DAPS must heat and circulate heated fluid through a full length liquid loop garment worn by the airman. Operation is airman initiated upon entry to the water in his liferaft. Subsequent thereto DAPS must provide this principle function for up to twenty-four hours. An additional subsidiary function of DAPS shall be electrical power generation for operation of survival communications equipment.

In addition, the DAPS System must be interchangeable among the seat kits as manufactured by the three (3) major suppliers with minimum modification or rework to the kits.

These suppliers are:

- (1) Scott Aviation
- (2) Rocket Jet Division of American Safety Flight System, Inc.
- (3) East/West Industries, Inc.

3.1.2 Specific Requirements

3.1.2.1 System Operation

Operation

- (a) Thermal output shall be initiated by the airman.
- (b) A minimum capability for five re-starts of operation shall be provided. No resort to auxiliary re-start means shall be permitted in meeting this requirement.
- (c) The airman will be provided means to modulate DAPS thermal output in the minimum range of 100 to 300 watts.
- (d) Emergency operation must be possible when sea water is used in the fluid loops of DAPS and the airman's liquid loop thermal garment.

Controls

Those necessary to provide Operations as indicated above are required. Visual indicators to facilitate airman in-raft operation may be included.

Ignition

A ceramic piezoelectric crystal generates a high voltage spark when struck by a spring loaded button. The spark ignites the fuel/air mixture. No batteries shall be used in the system. A built-in restart capability shall be provided.

Temperature of Fluid at DAPS Outlet

The temperature of fluid exiting DAPS shall be adjustable by the operator.

3.1.2.2 Design

Weight

The DAPS less fuel supply and liquid umbilicals shall weigh three pounds or less.

Configuration

The DAPS with a minimum six (6) hour fuel supply @ 25 GMS/hr shall fit within the lid of a Scott Aviation, Rocket Jet Engineering, or East/West Industries RSSK-1A. Components currently mounted within seat kit lids must be retained without their relocation to accommodate the DAPS.

3.1.2.3 Performance

3.1.2.3.1 Thermal

Thermal Output

- (a) DAPS shall supply a minimum of 250 watts of thermal output from an ambient air source for a minimum of twenty-four hours, one time, following a separation of the airman from the aircraft in any emergency abort situation.
- (b) DAPS shall be capable of supplying a minimum of 6000 thermal watt-hours of output from an ambient air supply over a twenty-four hour period, one time, following performance as in (a) above.

Fuel Consumption Rate

At a fuel rate of 25 grams per hour of propane sufficient fuel shall be available to allow DAPS Operation for six (6) hours. At this fuel flow rate a minimum of 200 thermal watts shall be supplied to the airman.

Fuel

Propane shall be the fuel of use; a minimum of 150 grams shall be storable in the seat kit lid.

Combustion Products

These shall consist of water vapor, carbon dioxide, and non-toxic concentrations of other products of incomplete combustion.

Insulation

System components shall be insulated as necessary to obtain specified performance. Insulation shall insure against hot spots that may cause injury to the airman, his life raft and other interfacing items.

3.1.2.3.2 Hydraulic

Hydraulic Output

DAPS shall provide the necessary fluid flow rate to deliver required thermal outputs at an airman's liquid loop garment inlet maximum temperature of 110°F. The foregoing requirement must be met when the liquid loop garment pressure drop at 0.25 gpm flow rate does not exceed five (5) psi at normal operating temperature with water the fluid of reference.

Fluid

The fluid stored in DAPS will be of a type to prevent freezing at low temperature, vaporization at high temperature, and corrosion of interfacing surfaces.

Disconnects

The DAPS, as mounted in the seat kit, must interface external fluid loops via manually operated quick disconnects. In addition to performing the foregoing functions:

- (a) Quick disconnects will not leak fluid out or admit air to the fluid subsystem in an amount detrimental to system operation.
- (b) Quick disconnects will be light weight, low volume, standard parts of materials compatible with liquid loop system fluids.
- (c) The quick disconnect to interface the liquid loop garment to the DAPS umbilical shall be provided as GFE.

3.1.2.3.3 Electrical

Electrical Outputs

DAPS connectors shall be readily accessible and protectively capped in the as-stored condition. Each shall be connectable to but one specific, identified, auxiliary load.

Auxiliaries

Fuel required in auxiliaries operation shall be an allowable addition to fuel required to meet specified thermal outputs.

Survival communications transceiver input power shall be within specified limits when DAPS thermal output is in the range 150 to 300 watts. Specified limits are:

- (1) Output voltage 12 volts ± 5 percent when load is varied from 10 ma to 100 ma and
- (2) Ripple voltage 150 mv peak to peak

3.1.2.4 Storage

Exhaust and Air Inlet Ports

These shall be capped in the unit as-stored condition to prevent introduction of foreign matter. The exhaust shall be vapor sealed from the unit insulation to prevent condensate degradation of insulation.

3.1.2.5 Environment

The system shall be designed to withstand the following conditions:

- (a) Pressure Altitude Non-operating; sea level to 100,000 ft. Operating, sea level to 5,000 ft.
- (b) Hydrostatic Pressure - Non-operating without leakage; 30 psia.
- (c) Operating Ambient Temperature - in air; 20° to plus 80°F.
- (d) Storage Ambient Temperature - -20°F to + 125°F.
- (e) Shock - Operable after drop of ten (10) feet to concrete surface, all axes, as mounted in seat kit. Operable after drop of four (4) feet to concrete surface, all axes, as packaged for delivery.
- (f) Other - Consider that aircraft vibration spectrum will be imposed in period preceeding DAPS use. Consider that relative humidity will be high in in-raft operation and air required for combustion will be salt laden; unit will be subject to salt spray.

3.2 Final Daps Configuration

As a result of the design analysis as described in Section 2.0 of this report a final RSSK-1A DAPS design was determined. Figure 36 is a photograph of the heater assembly with cover in place while figure 37 is a photograph of the unit with cover removed. Figure 38 shows the DAPS heater with fuel system as mounted in the Scott Kit.

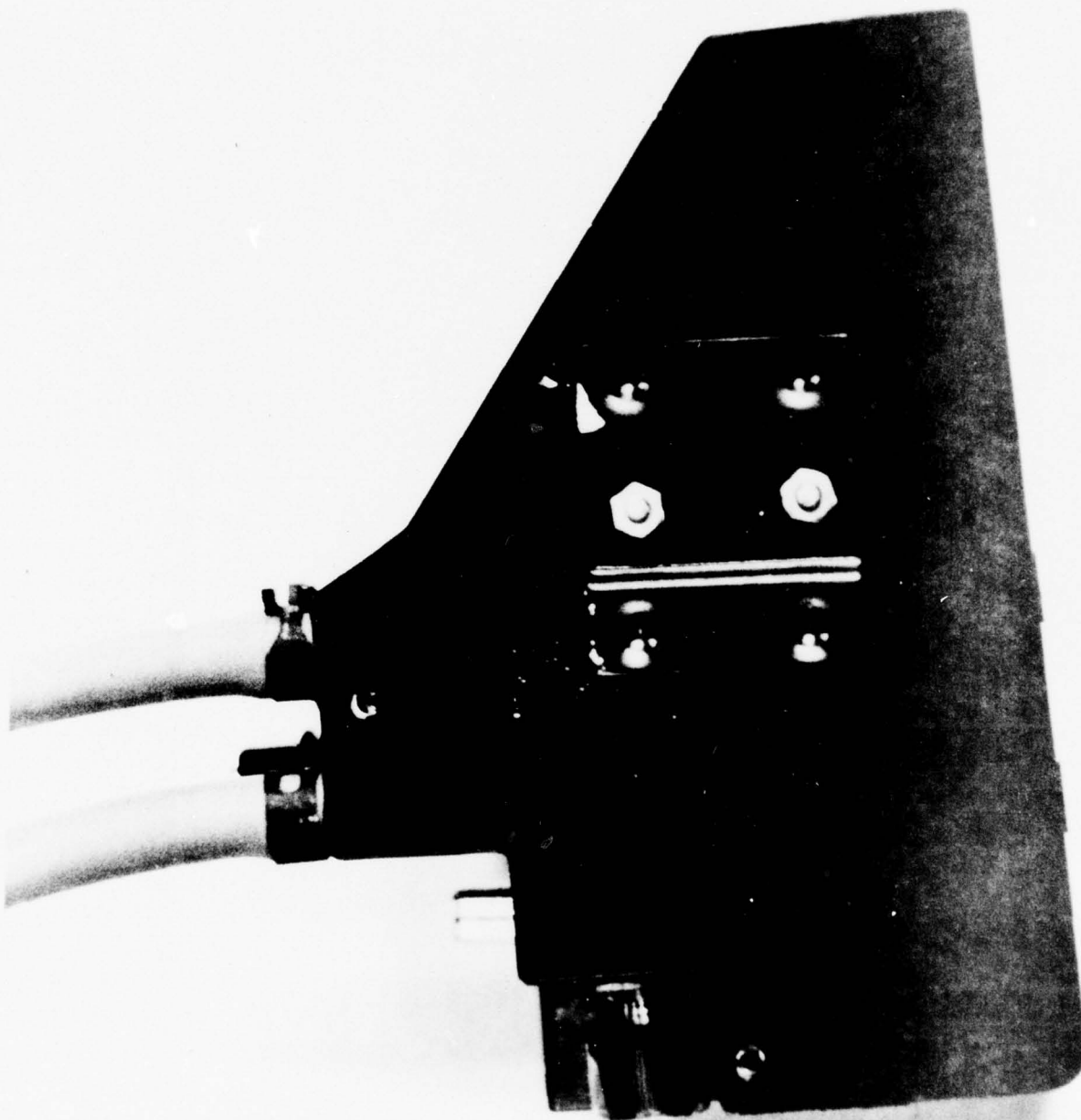
The major components called out on the photograph of Figure 37 are listed below:

- (1) Pump/motor assembly
- (2) Combustion chamber assembly
- (3) DC-DC converter
- (4) Fuel regulators
- (5) Fluid Manifold
- (6) Fuel input connector

A description of these major components together with their operating characteristics are presented below:

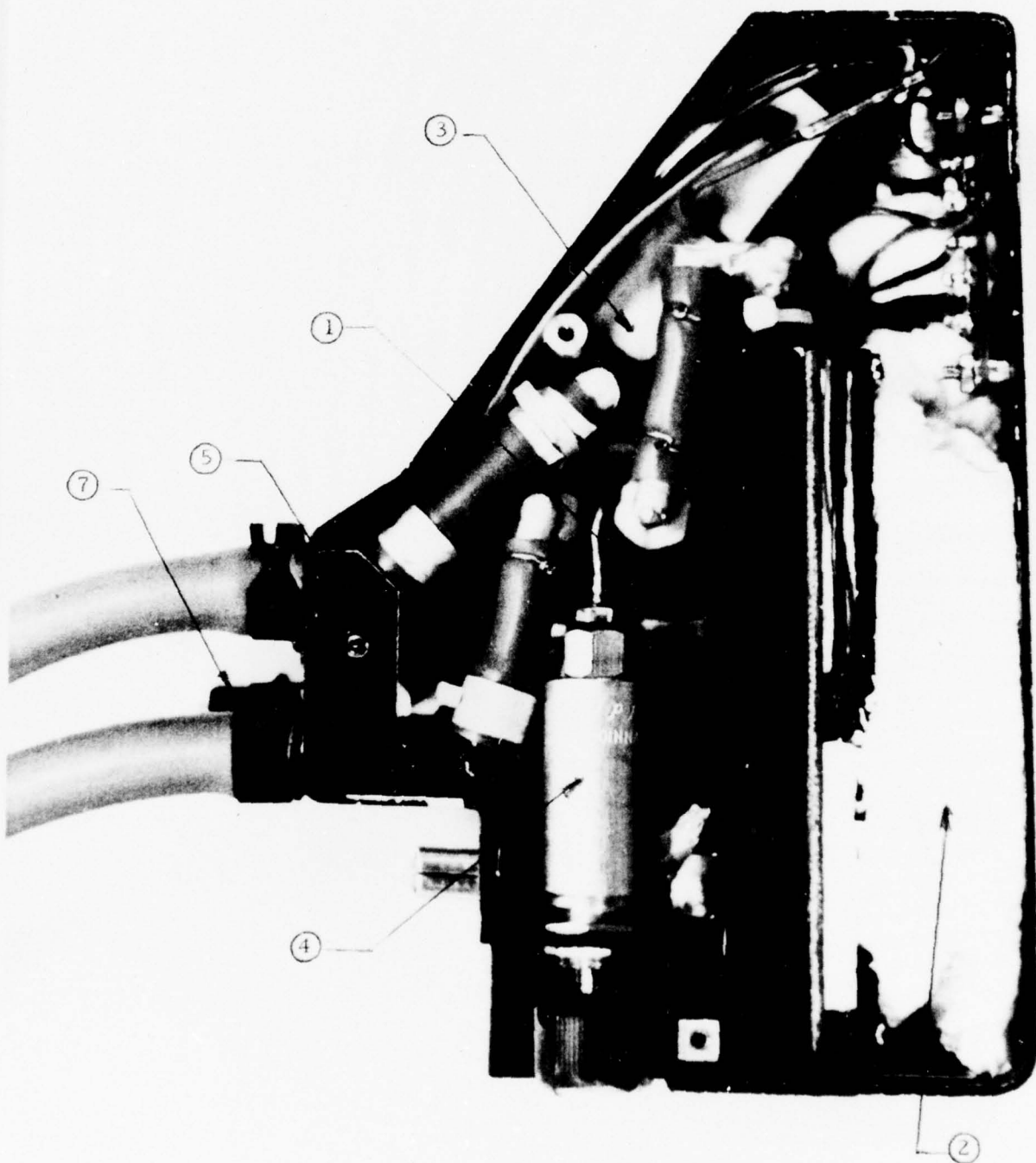
3.2.1 Pump/Motor Assembly

The pump is manufactured by Micro Pump Corporation Part No. 08-00-103. It is a positive displacement gear pump comprised of a delrin plastic housing with teflon gears. It requires no dynamic seals as the drive mechanism utilizes a magnetic drive requiring only static seals. The pump is capable of pumping approximately 30 gph at 0 psi head.



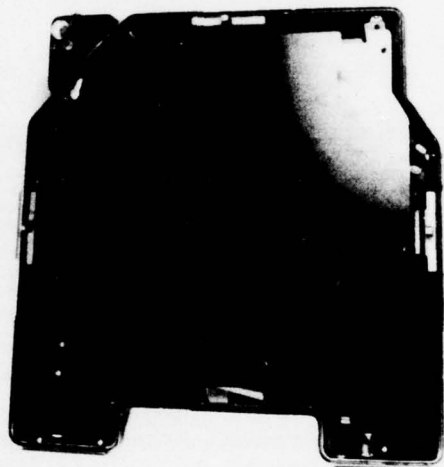
DAPS With Cover

Figure 36



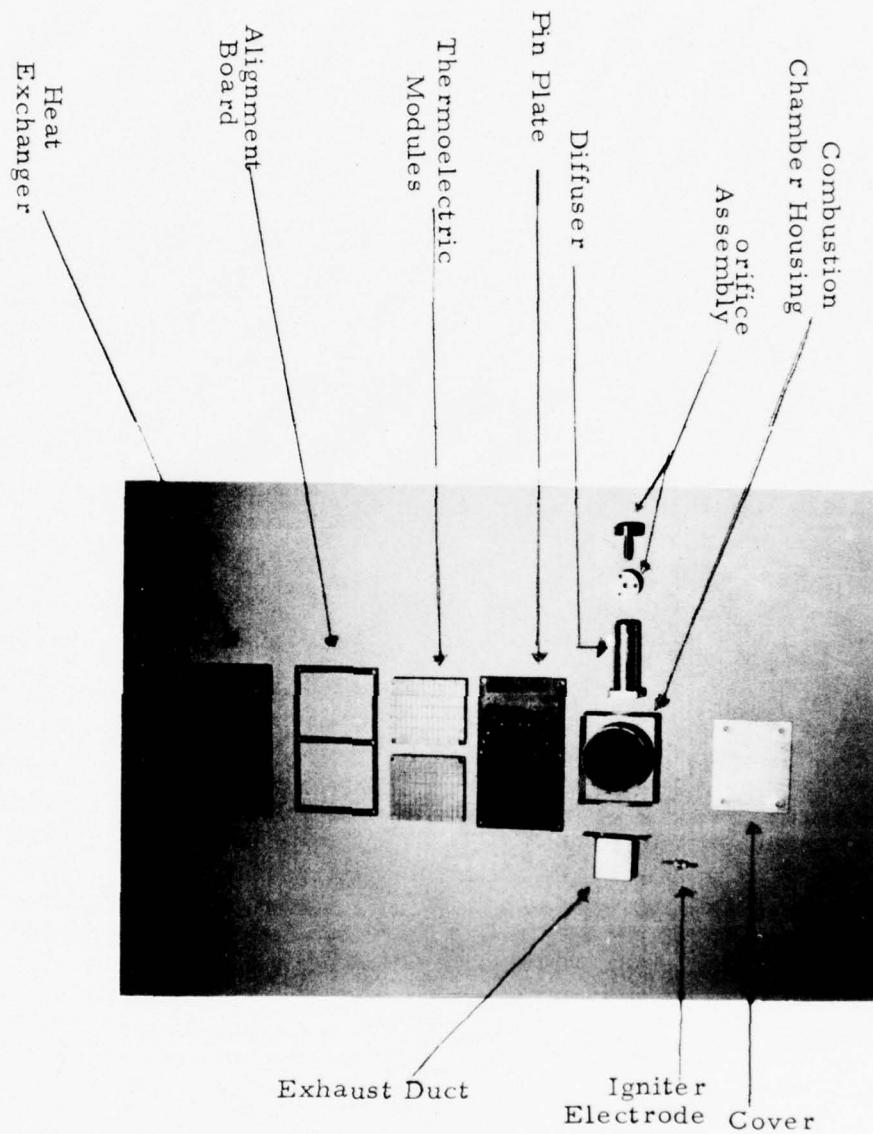
DAPS Without Cover

Figure 37



RSK-1A with Fuel Supply as Packed for
Delivery in the Scott RSK-1A Kit

Figure 38



Exploded View of Combustion Chamber
As Delivery Under Contract N62269-76-C-0239

Figure 39

The pump is coupled to a TRW Globe 6 VDC motor (Part No. 235A106-5) with a no-load speed of from 12000 RPM to 14000 RPM.

This pump/motor combination is capable of pumping .25 GPM (15 GPH) against a 4 PSI head.

3.2.2 Combustion Chamber Assembly

The combustion chamber assembly consists of a pin plate, 2 thermoelectric modules, heat exchanger, combustion chamber housing and cover, diffuser and catalyst, alignment board, exhaust duct, igniter electrode and orifice assembly. (See Figure 39)

Fuel is admitted to the unit through a precision .005 inch orifice manufactured by The Lee Company (Part No. JETA1872240H). The orifice assembly has a filter in front of the orifice to prevent blockage from impurities in the fuel. The gas leaves the orifice and enters the diffuser where the velocity head is converted to pressure head thereby allowing the gas to diffuse through the catalytic bed. The diffuser also is responsible for obtaining the proper air fuel mixture.

The air-fuel mixture contacts the catalytic bed and reacts, thereby liberating its stored thermal energy.

The catalyst is 1% platinum deposited on an alumina matrix. The catalyst is manufactured by Matthey Bishop Corporation. The advantage of using platinum catalyst lies in the fact that the stored energy is released at a slower rate resulting in a lower combustion temperature.

The liberated heat is picked up by the pins in the pin plate and conducted through the thermoelectric modules.

These modules are made of bismuth telluride semi-conductor material. Each module is capable of delivering 5.5 watts of electrical power at $2.5 \pm .25$ volts provided a hot junction temperature of 270°C and cold junction temperature of 70°C is maintained.

The heat liberated in the catalytic reaction is conducted through the modules to the heat exchanger where it is picked up by the circulating heat transfer fluid and pumped to the man.

3.2.3 DC-DC Converter

The DC-DC converter (output converter) manufactured by Vintor Electrical Associates, Part No. CV2-12 accepts an input voltage of between 2.6 and 5 VDC and produces a regulated 12 VDC \pm 5% at 100 milliamps. This output can be used to operate an emergency transmitter or xenon flasher. The connector is capable of being wired either with a floating ground or common ground and is wired into the system such that there is power consumption only when a load is attached to the DAPS.

This is accomplished by completing the input circuit of the DC-DC converter at the time of connecting the load (See Figure 40).

The output connector is a four pin bulkhead mountable type manufactured by Bendix Connector Corporation, Part No. PT02E-8-4S.

3.2.4 Fuel Regulator

The fuel regulator is manufactured by Clippard Controls Corporation, Part No. MAR1-NR. The major function of the regulator is to step down the vapor pressure of the fuel in the tank to a pressure compatible with the DAPS design.

3.2.5 Fluid Manifold

The fluid manifold consists of an aluminum block to which have been dip brazed aluminum tubing.

The manifold serves the function of eliminating difficult flexible tubing lines which require additional space for runs and are also susceptible to kinking and rupture.

3.2.6 Fuel Input Connector

The fuel input connector is manufactured by Wiggins Connector Co., Part No. VF11004. It comes with a Mil specification end connection per MS33656-4. The operating temperature is from -65°F to +400°F and has an operating pressure of 1500 psi continuous.

3.2.7 Piezoelectric Starter

Ignition of the air fuel mixture is accomplished by the use of a piezoelectric igniter. Ignition is initiated by depressing a spring loaded hammer which strikes a ceramic crystal releasing a high voltage arc across an air gap through which the fuel mixture is flowing. The voltage rating of the device is 13 KV minimum. The part number of the device is EF1-AF27 and it is manufactured by Matsushita Electric Corporation of America.

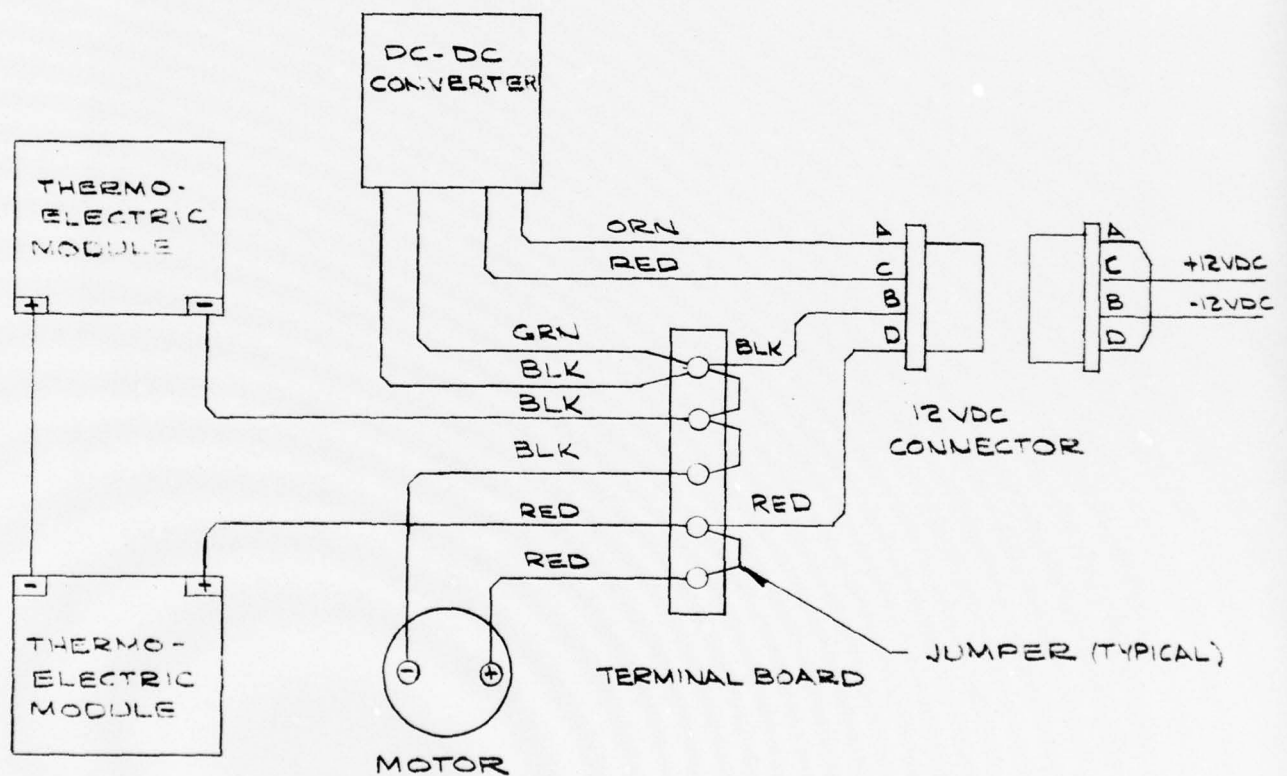
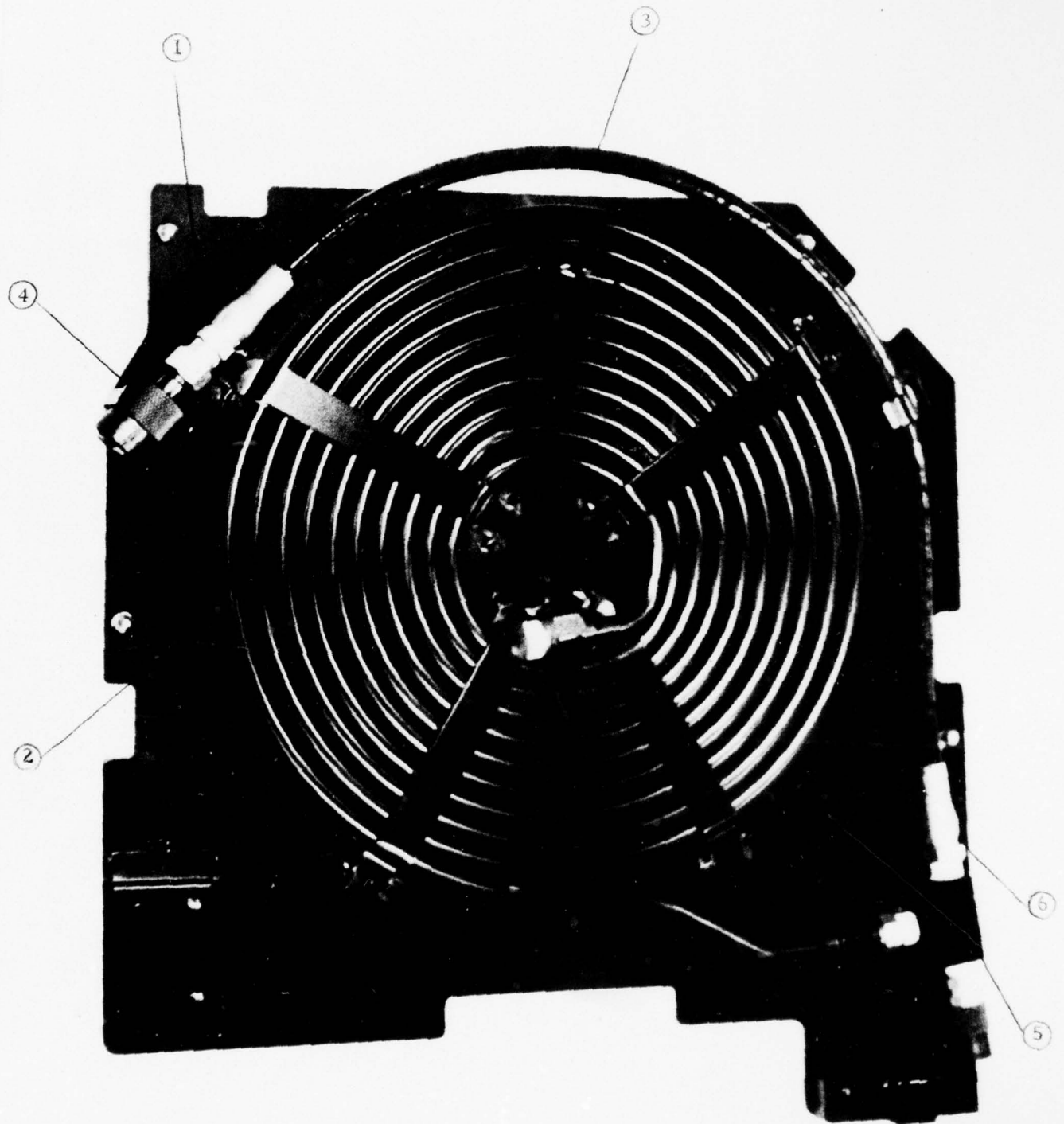


Figure 40



Fuel Coil
(N62269-76-C-0789)

Figure 41

3.2.8 12 VDC Output Connector

A 4 pin, 12 VDC output connector is supplied with each DAPS. The purpose of the connector is to make available a convenient way of obtaining regulated 12 VDC output to operate an emergency flasher or transmitter.

The mating connector is coupled to it by a simple push motion and disconnected via a pull action. Both operations can be accomplished using only one hand.

3.3 Fuel Tank

A photograph of the deliverable fuel tank is shown in Figure 41. The major components are flagged out in the photograph.

The major components are listed below together with a description of each of them:

- (1) Mounting Plate
- (2) Fuel coil
- (3) Fuel umbilical
- (4) Fuel connector
- (5) Manifold block
- (6) Pressure relief valve

3.3.1 Mounting Plate

The mounting plate is made of 6061-T6 aluminum alloy .062 inches thick. It serves as a mounting surface for the fuel coil on one side and as a mounting surface for the liferaft on the other side. It also gives a large degree of rigidity to the final assembly.

3.3.2 Fuel Coil

The actual fuel tank consists of a coil of .437 inch O.D. x .035 inch wall 6061-T6 aluminum alloy draw seamless tubing. The inside of the fuel coil is terminated with a 37° flare plug. The outside of the coil terminates at the fuel manifold.

3.3.3 Fuel Umbilical

The fuel umbilical is synflex tubing Part No 3130-03, 3/16 I.D. x .4200 D. The tubing consists of three layers. The inner tube is nylon. This inner core is covered with a nylon braid which in turn is covered with a polyurethane outer cover. The tubing has a continuous working pressure of 2500 PSI with a minimum burst of 10000 PSI. The tubing has swaged-on end connections. One end attaches to the fuel manifold by a 1/4 inch NPT male pipe fitting. The other end of the fuel umbilical has a 1/4 inch Joint Industry Conference on Hydraulic Standards for Industrial (JIC) Equipment 37° female flare fitting that mates to a valved fuel connector.

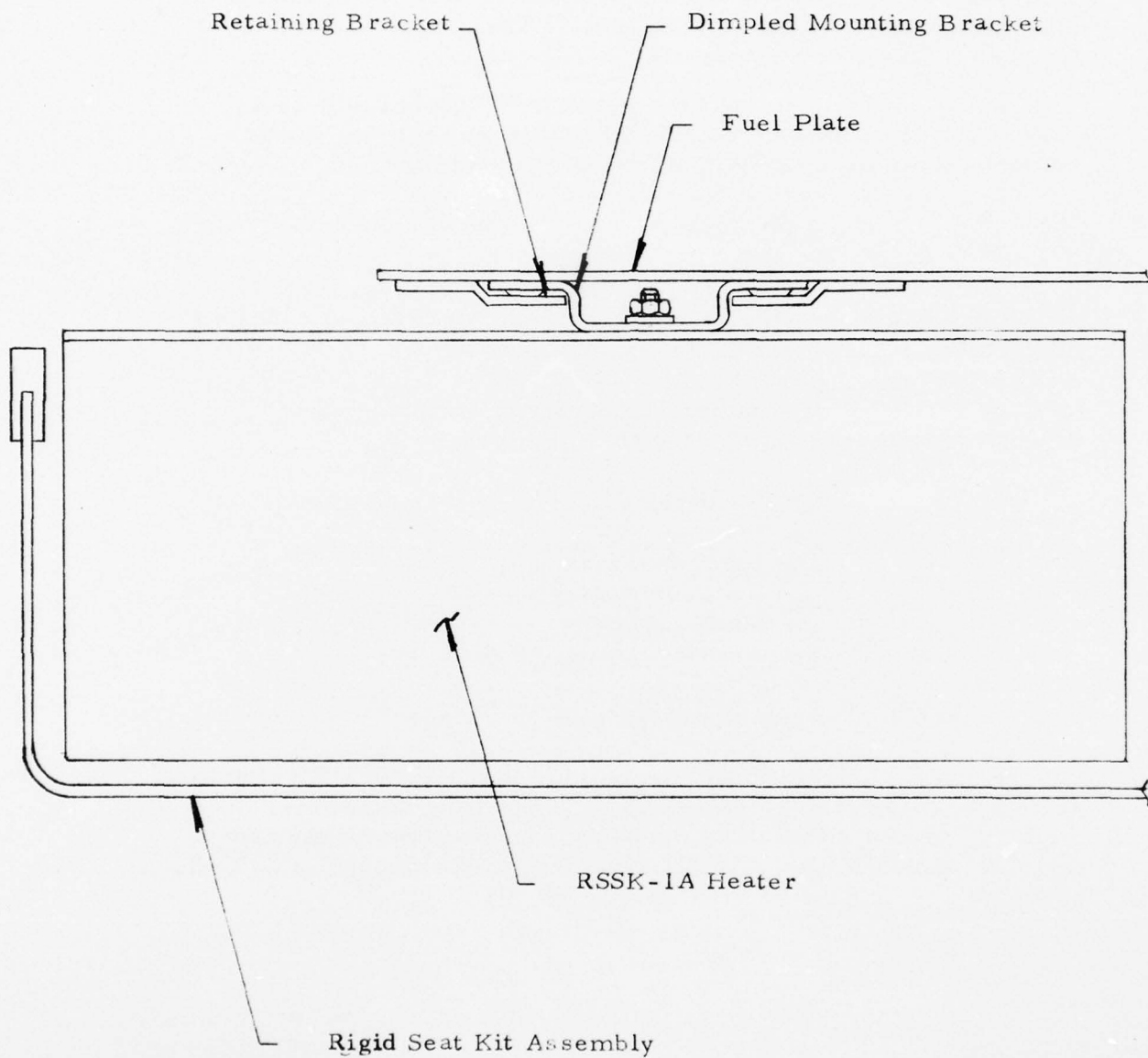


Figure 42

3.3.4 Fuel Connector

The fuel umbilical is terminated with a Wiggins Connector Corporation connector, Part No. VS100D4. This connector has an operating temperature range of from -65°F to +400°F and a pressure rating of 1500 PSI.

3.3.5 Manifold Block

The manifold block serves a three-fold function. The block has 3 ports. One port terminates the fuel coil, the second port terminates the fuel umbilical and the third port is used to mount a pressure relief valve.

3.3.6 Pressure Relief Valve

The pressure relief valve is manufactured by Nupro Co., Part No. A-4CPA2-150DC. It is pre-set to release at 250 psig. This pressure would be reached if the ambient temperature corresponds to the maximum storage as specified by the contract.

3.4 Interface of DAPS System With the Fuel Coil to the Seat Kit

The DAPS heater and fuel supply mount to the seat kit via bracketry that is attached to existing mounting hardware. The utilization of existing hardware eliminates the necessity for reworking the kit. The only exception to this is that in several cases longer screws are required to accommodate the added brackets.

4.0 RELIABILITY AND MAINTAINABILITY

4.1 Introduction

As required by the RSSK-1A contract, production models of these units shall have a success probability of .976. This value is based on a MTBF (Mean Time Between Failures) of 1000 hours and an operational life of 24 hours. The current Reliability and Maintainability Program was incorporated into the RSSK-1A Design Program to provide information to the designer which would help him achieve this success probability.

The major effort, during this contract, was in developing a Reliability Program Plan that could be used interchangeably with each of the Navy heater systems, and includes the following:

- . Identification of the system mission profile
- . Reliability Dependency Diagram
- . Math Model
- . A Failure Mode, Effects and Criticality Analysis
- . Current reliability and maintainability predictions
- . Recommendations for future reliability programs

4.2 Reliability Program Description

The Reliability Program was broken down into three major tasks, per paragraphs 5.1 through 5.3 of MIL-STD-785A (Reliability Program for Systems and Equipment. Development and Production): (1) Reliability Program Management, (2) Reliability Design and Evaluation, and (3) Reliability Testing. The following is a description of work performed under each task.

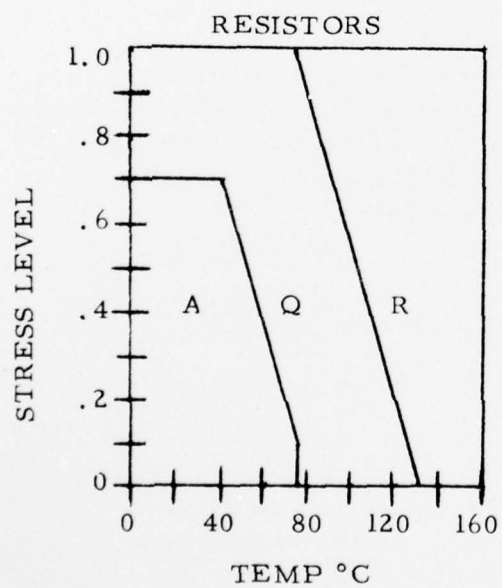
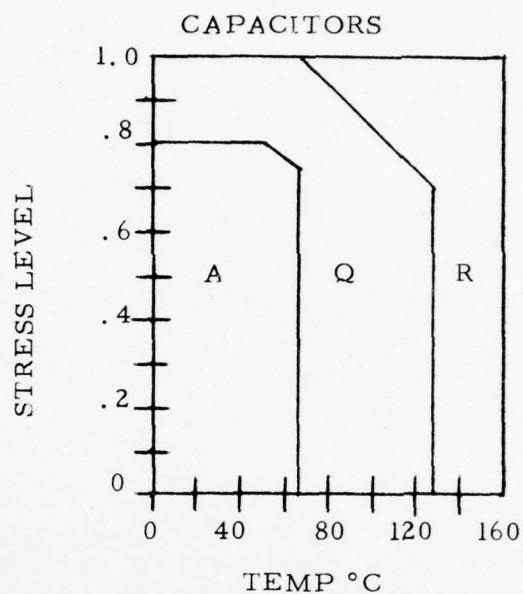
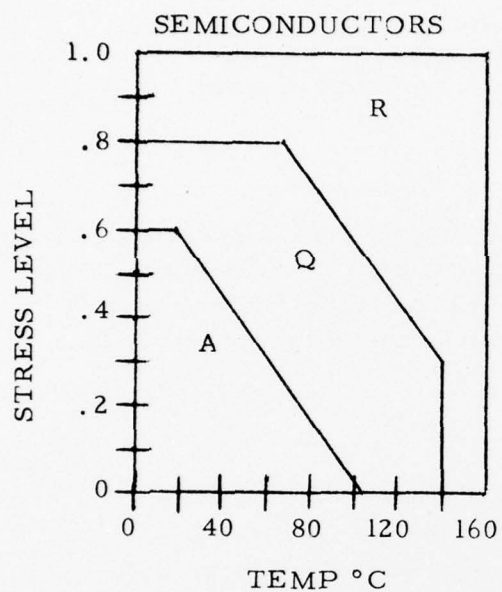
4.2.1 Reliability Program Management

A Reliability Program Manager was assigned to the program on a full time basis and was responsible for organizing, coordinating, and carrying out the work required for each of the three major tasks. To assist in this early program phase, a reliability consultant, with considerable experience in Navy hardware Reliability and Maintainability Programs, was retained. He assisted at the beginning of the program in defining the analytic effort that was pursued. At the end of the program he assisted in drafting the future Reliability and Maintainability Program Plan.

4.2.2 Reliability Design and Evaluation

4.2.2.1 Design Techniques

An improvement in part and equipment reliability can be realized by applying the techniques of stress derating. The failure rate of most parts is dependent upon the applied stress. As the applied stress is reduced, the failure rate decreases. The reverse is also true. Therefore, by increasing the strength of the part, the failure rate can be reduced, and the reliability improved.



A = Acceptable
 Q = Questionable
 R = Restricted

D.C. D.C. CONVERTER DERATING GUIDELINES

Figure 43

Those components in the RSSK-1A DAPS for which stress derating is necessary include: (1) D.C. motor, (2) DC-DC converter, (3) fuel lines, (4) fluid lines, (5) thermoelectrics, and (6) fuel tank. Following is a brief list of these parts and their operational loads.

(1) DC Motor

The DC motor currently being used is operated at 125 percent of its rated load. This tends to reduce the useful life and the reliability of the motor. Several alternate motors have been tested to date; no motor operable satisfactorily in a derated mode has been found.

(2) DC-DC Converter

The DC-DC converter is operated at a stress level of 80 percent. The major components of the converter are: (a) Silicon transistors, (b) silicon diodes, (c) CSR capacitors, and (d) carbon composition resistors. Assuming a ground application, Figure 43 shows the derating guidelines for these parts, as presented by the IIT Research Institute in the Reliability Design Handbook.

(3) Fuel Line

The fuel lines are copper on the high pressure (input) side of the pressure regulator and urethane hose on the low pressure (output) side. The copper is used at 10 percent of its rated working pressure while the urethane hose is used at 25 percent of its rated working pressure (according to manufacturers data).

(4) Fluid Lines

The fluid lines are used at 15 percent of the rated working pressure.

(5) Thermoelectrics

The maximum recommended operating temperature is 550°F. Using the thermoelectrics at temperatures higher than this will cause the solder joints to melt. The thermoelectrics in the RSSK-1A DAPS see a maximum temperature of 500°F.

(6) Fuel Tank

The fuel tank is rated for a continuous working pressure of 1000 psi. The maximum pressure seen by the fuel tank, at the maximum storage temperature (125°F), is 260 psi. For a complete analysis of the fuel tank see Section 2.3.2 of this report.

(7) Pressure Regulator

The pressure regulator has a working range of 0-300 p.s.i., and a delivery pressure of 0-100 p.s.i. The maximum input pressure seen by the regulator is 250 p.s.i. and the maximum delivery pressure is 20 p.s.i.

The working temperature range is from -30°F to +230°F. The temperatures seen by the regulator range from +20°F to +80°F. Therefore, it is felt that this regulator is sufficient for use in the RSSK-1A system.

(8) 12 VDC Connector

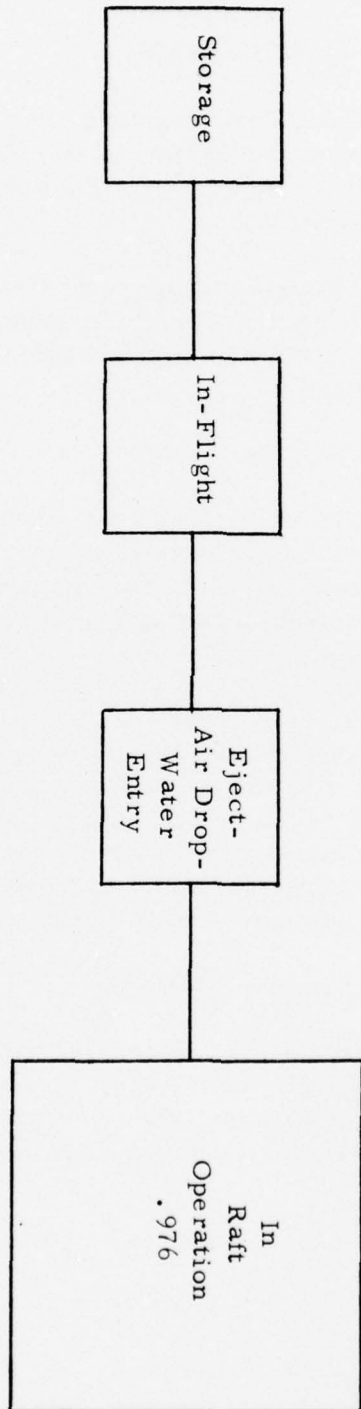
The 12 VDC electrical connector in the DAPS has a contact rating of 7.5 amps. The maximum current seen by the connector is 100 milliamps. With a success probability of .99994, the connector should function properly for the entire life of the unit.

(9) Pump

The pump used is a miniature, magnetic drive, gear pump. This pump utilizes a Viton o-ring seal which is compatible with ethylene glycol and has a working temperature range from -15°F to +400°F. The temperature range seen by the pump is +20°F to +110°F. Since the pump is non-operational during the storage stage the -50°F storage temperature is not expected to cause any problems.

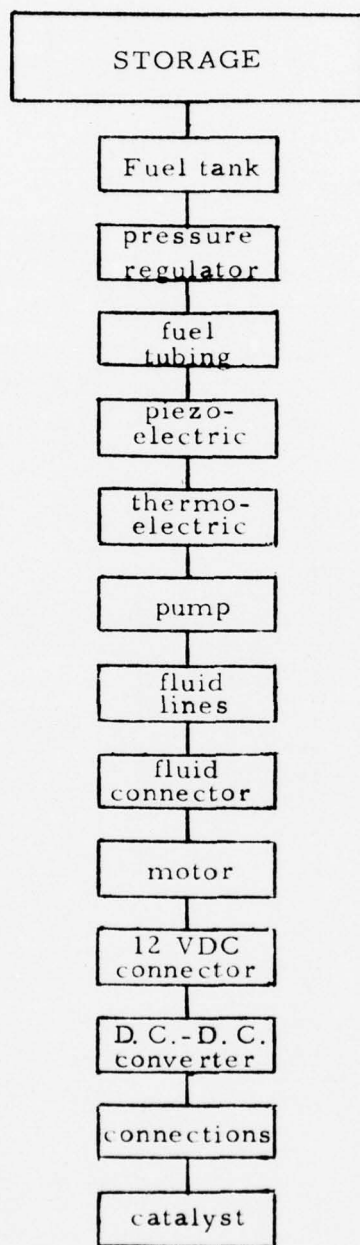
(10) Fluid Connectors

The fluid connectors used for the RSSK-1A DAPS were supplied to Energy Systems Corporation as government furnished equipment. Data available indicates no degradation in the temperature range of -65°F to +180°F using a 60 percent ethylene glycol solution.



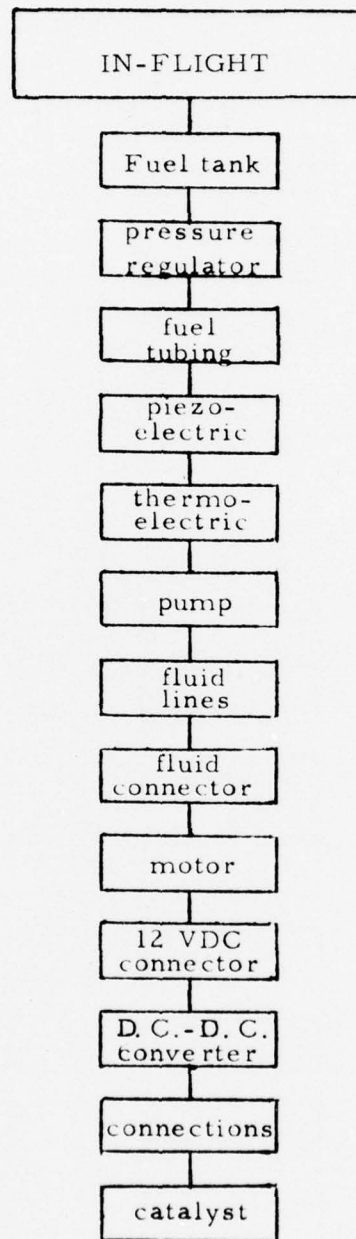
System Mission Profile

Figure 44



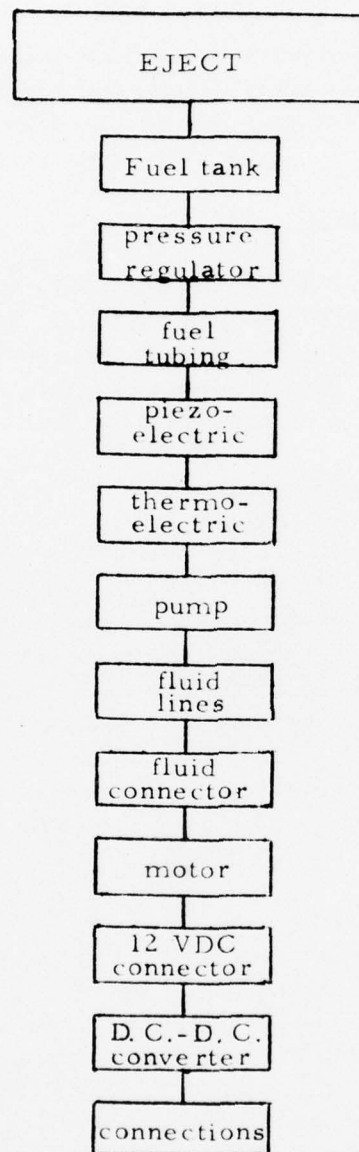
Reliability Dependency Diagram - Storage Stage

Figure 45a



Reliability Dependency Diagram - In-Flight Stage

Figure 45b



Reliability Dependency Diagram - Eject Stage

Figure 45c.

Redundancy is another design technique used to improve system reliability. However, due to the small size, limited space, and operational life of the RSSK-1A DAPS, no redundant parts or sub-systems have been included.

4.2.2.2 Reliability Analysis

A reliability dependency diagram showing the dependency of the overall RSSK-1A DAPS reliability on the reliability of the individual components was generated during this program. The diagram was broken down into three separate stages, to represent the stages of the mission profile:

- (1) Storage
- (2) In Flight
- (3) Eject-Air Drop-Water Entry

Figure 44 gives a visual representation of the system mission profile. Each of the three mission profile stages was then broken down to show the series reliability configuration of the individual components (Figures 45a, 45b, 45c).

Expected replacement schedules, Table 6, have been assigned to each part, based on available data, during the Storage and the In-Flight stages, as the unit is non-operational during these times.

Initially required failure rates were assigned to each component, in the Eject-Air Drop-Water Entry stage, based on an overall success probability of .976 (see Table 7). The calculations for the required failure rates are included in this report as Appendix A. As reliability data was obtained, the success probability for each component was updated. These predicted failure rates are also shown in Table 7. The calculation for the predicted failure rates are included as Appendix B.

The math model used to calculate each success probability is essentially a mathematical statement of the relationship depicted in the reliability dependency diagram. Since a series configuration model was used to evaluate the reliability of the unit, the probability of success of the mission (.976) is equal to the product of the success probabilities of each component.

$$P_m = P_{c_1} \cdot P_{c_2} \cdot P_{c_3} \cdot \dots \cdot P_{c_N}$$

	STORAGE	IN-FLIGHT
FUEL TANK	10 years	5 years
PRESSURE REGULATOR	5 years	5 years
FUEL TUBING	5 years	5 years
PIEZOELECTRIC	indefinite	indefinite
THERMOELECTRIC	20 years	5 years
PUMP	15 years	15 years
FLUID LINES	5 years	5 years
FLUID CONNECTOR	15 years	15 years
MOTOR	2 years	2 years
12 VDC CONNECTOR	5 years	5 years
D.C. -D.C. CONVERTER	indefinite	indefinite
CATALYST	10 years	5 years
CONNECTIONS (solder, dip braze, weld, pipe, clamps)	indefinite	indefinite

RSSK-1A Component Replacement Schedule

Table 6.

	REQUIRED ($\times 10^{-6}$)	PREDICTED ($\times 10^{-6}$)	ACTUAL ($\times 10^{-6}$)
FUEL TANK	100	100	
PRESSURE REGULATOR	30	15	
FUEL TUBING	50	50	
PIEZOELEC- TRIC	100	100	
THERMO- ELECTRIC	100	328	
PUMP	80	80	
FLUID LINES	20	20	
FLUID CONNECTOR	180	100	
MOTOR	80	25.1	
12 VDC CONNECTOR	30	1.9	
D. C. -D. C. CONVERTER	30	11.2	
CONNECTIONS (solder, dip, braze, weld, pipe, clamps)	2.6	2.6	

RSSK-1A FAILURE RATE DATA

Table 7.

AD-A044 481

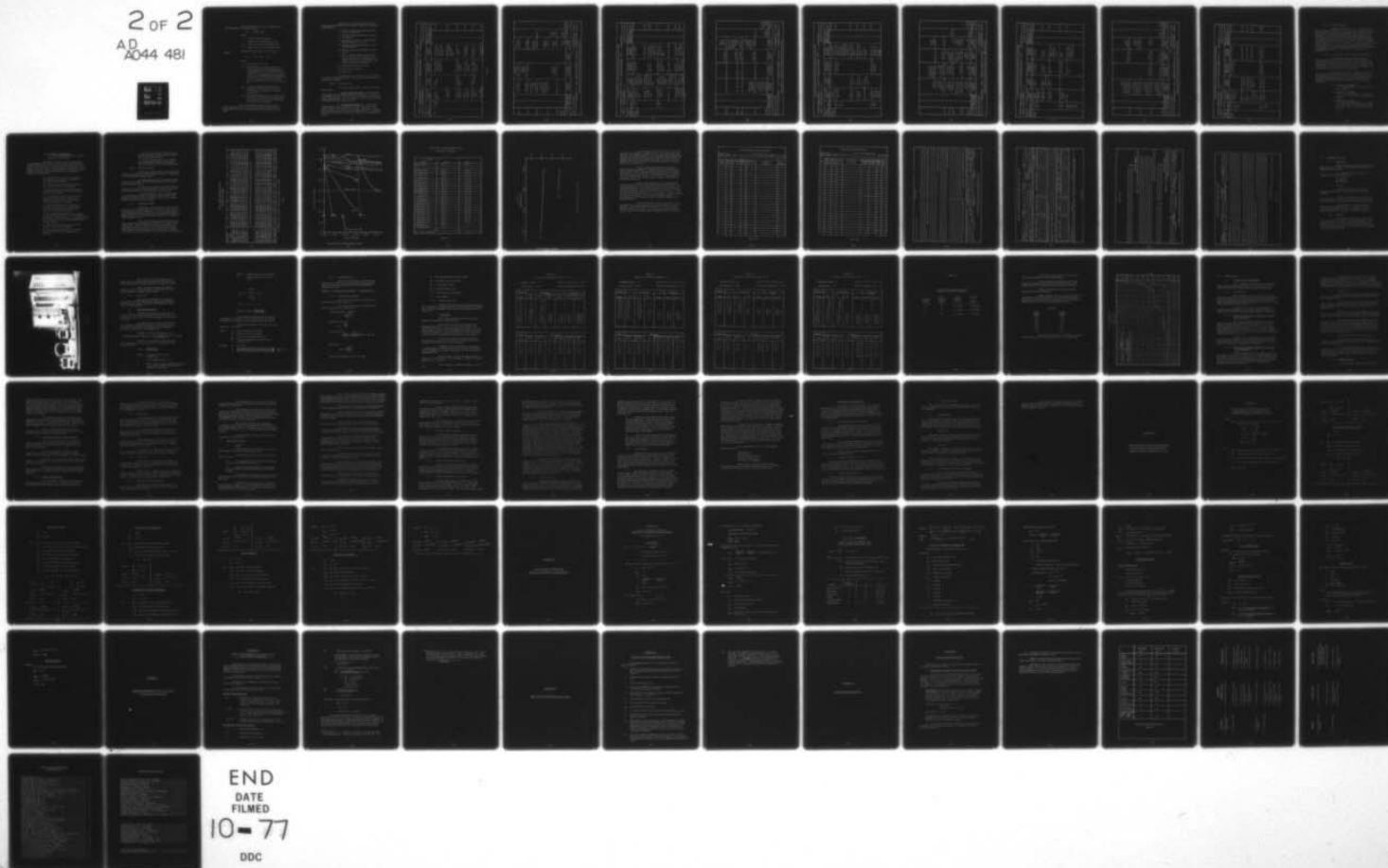
ENERGY SYSTEMS CORP NASHUA N H
DOWNED AIRMAN POWER SOURCE (DAPS) FOR INCLUSION INTO THE RSSK-1--ETC(U)
JAN 77 R E LECOMPTE, R S CHRISTIE
ESC-0289-1FR

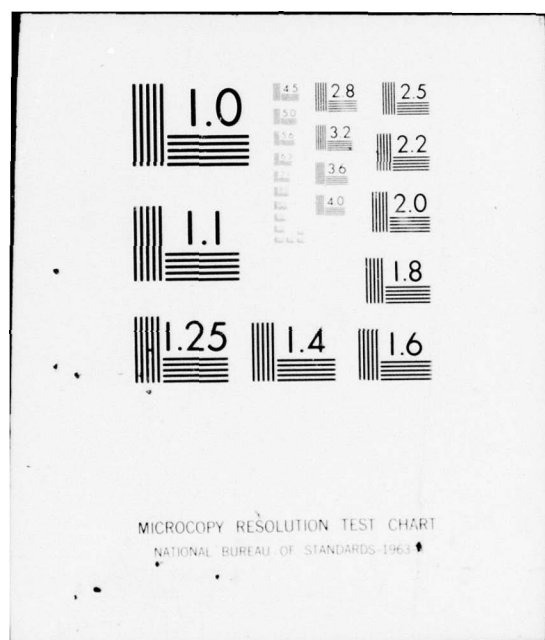
F/G 13/1
N62269-76-C-0289
NL

UNCLASSIFIED

NADC-76045-40

2 OF 2
AD
A044 481





The calculation of the success probability for each component proceeded as follows:

$$P_c = e^{-(\lambda_1 t + \lambda_2 c)}$$

where:

t = time of operation in hours

c = number of cycles during operation

λ_1 = failure rate of time dependent parts

λ_2 = failure rate of cyclic dependent parts

Component failure rates were calculated as follows:

$$\lambda_p = (\lambda_b) (\pi_E) (\pi_Q)$$

where:

λ_p = component failure rate

λ_b = base failure rate. These values were based on data from the following sources: (1) manufacturer, (2) MIL-HDBK-217B, (Reliability Prediction of Electronic Equipment), (3) the Reliability Design Handbook (published by the IIT Research Institute, (4) the Government-Industry Data Exchange Program (GIDEP), and (5) Nuclear Systems, Inc.

π_E = The environmental adjustment factor accounts for the influences of environments which the equipment is expected to experience.

π_Q = the quality adjustment factor, which is used to account for the degree of manufacturing control with which the part was fabricated and tested prior to shipment.

The environmental adjustment factor and the quality adjustment factor were used to alter the base failure rates so as to obtain a more accurate picture of the component failure rates.

During its life, the RSSK-1A DAPS will be subjected to the following environmental conditions, as specified in the contract:

- (1) Pressure altitude Non-Operating; sea level to 100,000 feet.
- (2) Pressure Altitude Operating; sea level to 5,000 feet.
- (3) Hydrostatic Pressure - Non-Operating without leakage; 30 p.s.i.a.
- (4) Operating Ambient Temperature, in air; +20°F to +80°F.
- (5) Storage Ambient Temperature; -50°F to +125°F.
- (6) Shock - Operable after drop of ten (10) feet to concrete surface, all axes, as mounted in seat kit. Operable after drop of four (4) feet to concrete surface, all axes, as packaged for delivery."
- (7) Vibration spectrum of aircraft
- (8) High relative humidity
- (9) Salt spray

Components were chosen for use in the RSSK-1A DAPS system that would survive and operate most satisfactorily under these conditions.

4.2.2.3 Problem Areas

Two major problems were encountered during this program:

1. Lack of failure rate data. At present time most suppliers of the RSSK-1A DAPS components are not involved in reliability testing. Therefore, failure rate data for the majority of the components has not been obtained. Other sources have been investigated with only limited success.

2. Limited unit life history. To date only a small amount of data is available for study. This lack of data greatly hinders the evaluation of the system components. There has also been a lack of accurate and complete failure documentation in the past which further hinders the evaluation of the components in use.

FAILURE MODE, EFFECTS AND CRITICALITY ANALYSIS							
SYSTEM		RSSK-LA DAPS		CONTRACT N62269-76-C-0289		DATE 20 July 1976	
ENG'R		R. S. Christie		PAGE		1 OF 9	
SUB SYSTEM	PART	FAILURE MODE	PART EFFECT	SUBSYSTEM EFFECT	SYSTEM EFFECT	FAIL. RATE (x10 ⁻⁶) FAIL. FREQ.	CRIT.
Fuel	1. Fuel Tank	A. Initial Supply too low	A. Tank leakage	A. Fuel supply may not last the required length of time	A. System will not operate for the required length of time.		A. Crit.
		B. Fuel tank empty			B. Combustion not sustained unit shuts down		B. Crit.
		C. Fuel is liquid; not gaseous	C. No vapor pressure in bottle.	C. No fuel to the combustion chamber	C. Unit will not operate		C. Mar.
		D. Vapor pressure too low.		D. Insufficient fuel to comb. chamber.	D. Combustion not sustained		D. Mar.
		E. Damaged fuel connector.	E. Possible fuel leakage	E. Tank cannot be interfaced with unit.	E. No fuel & no combustion		E. Crit.
		F. Gas valve sticks closed			F. No fuel and no combustion		F. Mar.

Table 8.

FAILURE MODE, EFFECTS AND CRITICALITY ANALYSIS

SYSTEM SSK-1A-DAPS CONTRACT N62269-76-C-0289 DATE 20 July 1976

ENG'R R. S. Christie

PAGE 2 OF 9

SUB SYSTEM	PART	FAILURE MODE	PART EFFECT	SUBSYSTEM EFFECT	SYSTEM EFFECT	FAIL. RATE (x10 ⁻⁶)	FAIL. FREQ.	CRIT.
Fuel	1. Fuel tank	G. Tank Bursts		A. No fuel to combustion chamber	A. No combustion			G. Catastrophic
	2. Pressure regulator	A. Sticks in closed position B. Fails to regulate properly			A. No combustion B. Can cause overheating and damage to the thermoelectrics			A. Major B. Major
	3. Tubing	A. Leakage thru end connections B. Breaks from vibration		B. Little or no fuel to combustion chamber	A. Unit may not operate for required length of time B. Little or no combustion			A. Major B. Critical
		C. Fuel line puncture		C. Insufficient fuel to combustion chamber	C. Little or no combustion			C. Critical

FAILURE MODE, EFFECTS AND CRITICALITY ANALYSIS										
SYSTEM		RSSK-1A- DAPS		CONTRACT		N62269-76-C-0289		DATE	20 July 1976	
ENG'R		R. S. Christie		PAGE		3		OF		9
SUB SYSTEM	PART	FAILURE MODE	PART EFFECT	SUBSYSTEM EFFECT	SYSTEM EFFECT	FAIL. RATE (x10 ⁻⁶)	FAIL. FREQ.	CRIT.		
Com-bustion chamber	1. Ori-fice	A. Blockage by impuri-ties or frost.	A. Will not allow fuel to pass into combustion chamber	A. No fuel for combustion	A. No combust-ion; no heat			A. Crit.		
		B. Partial blockage by impur-ities.	B. (1) Reduced fuel flow rate (2) change in the air/fuel ratio	2. Decreased efficiency	B. Reduced Heat 2. Fuel supply will not last the required length of time			B. Mar. 2. Mar. Crit.		
	2. Cata-lyst	A. Break-up caused by vibration	A. Catalyst settles and packs into bottom of chamber.	A. Gas passes over top of catalyst & not thru it.	A. Little or no combustion; little or no heat.			A. Crit.		
	B. Wetted		B. Catalytic combustion not initiated	B. No combust-ion	B. No heat output			B. Mar.		
	C. Leaks out of combust-ion cham-ber and in to the dif-		C. Insufficient amt. of catalyst for optimum combustion.	C. Partially blocks air gap causing a change in the air/fuel ratio.	C. (1) decreased efficiency; (2) increased fuel consump-tion.			(1)Mar. (2)Mar.		

FAILURE MODE, EFFECTS AND CRITICALITY ANALYSIS

SYSTEM RSSK-1A DAPS CONTRACT N62269-76-C-0289 DATE 20 July 1976

ENG'R R. S. Christie PAGE 4 OF 9

SUB SYSTEM	PART	FAILURE MODE	PART EFFECT	SUBSYSTEM EFFECT	SYSTEM EFFECT	FAIL. RATE (x10 ⁻⁶)	FAIL. FREQ.	CRIT.
Com- bustion Chamber	2. Cata- lyst				C. (3) Possibility of excess carbon mon- oxide in ex- haust gas.			(3) Crit.
	3. Piezo	A. Spring hammer not strong enough to generate spark.	A. No spark to ignite gas.	A. No combustion	A. No heat unless combustion initiated by other means			A. Mar.
		B. Spark gap too great	B. No spark to ignite gas.	B. No combustion	B. No heat, etc.			B. Mar.
		C. Spark shorting back along electrode to duct wall	C. No spark to ignite gas	C. No combustion	C. No heat, etc.			C. Mar.
		D. Wire lead to elec- trode breaks.	D. No spark to ignite gas	D. No combustion	D. No heat, etc.			D. Mar.

FAILURE MODE, EFFECTS AND CRITICALITY ANALYSIS								
SYSTEM RSK-1A DAPS			CONTRACT N62269-76-C-0289		DATE		20 July 1976	
ENG'R R. S. Christie					PAGE		5 OF 9	
SUB SYSTEM	PART	FAILURE MODE	PART EFFECT	SUBSYSTEM EFFECT	SYSTEM EFFECT	FAIL. RATE (x10 ⁻⁶)	FAIL. FREQ.	CRIT.
Combustion Chamber	3. Piezo	E. Button Sticking	E. No spark	E. No ignition	E. No combustion and no heat.			E. Mar.
	4. Thermoelectrics	A. Low voltage output		A. Reduced output voltage	A. No DC motor start or reduced operating speed; inefficient or non operating auxiliaries.			A. Mar.
		B. Broken lead or tab	B. No electrical output		B. Motor will not start; no auxiliaries			B. Crit.
		C. Cracked module	C. No electrical output		C. Motor will not start; no auxiliaries.			C. Crit.
		D. Overheated	D. No electrical output.		D. No heat to airman.			D. Crit.
5. Exhaust duct		A. Breaking away or disconnecting from housing.		A. Exhaust gases fill inside of housing	A. Insufficient fresh air to sustain combustion -- No heat to airman			A. Mar.

FAILURE MODE, EFFECTS AND CRITICALITY ANALYSIS

SYSTEM RSSK-1A-DAPS CONTRACT N62269-76-C-0289 DATE 20 July 1976

ENG'R R. S. Christie

PAGE 6 OF 9

SUB SYSTEM	PART	FAILURE MODE	PART EFFECT	SUBSYSTEM EFFECT	SYSTEM EFFECT	FAIL. RATE (x10 ⁻⁶)	FAIL. FREQ.	CRIT.
Fluid System	1. Pump	A. Flow blockage	A. Reduced pumping action	A. Reduced fluid flow	A. Possible overheating of thermo.			A. Mar. Crit.
		B. Excess friction on gear shafts	B. Excessive wear and decreased life of pump	B. Reduced or no fluid flow	B. (1) Excessive load on motor (2) Little or no heat to airman			B. Mar. Crit.
		A. Leak	A. (1) Loose end connection. (2) break in line	A. (1) Excessive fluid loss (2) Excessive fluid loss	A. (1) System overheating (2) System overheat			(1) Mar. (2) Crit.
	2. Fluid lines	B. Collapse	B. Restricts fluid flow	Pressure build-up; thermoelectrics overheat	B. Loss of electric power, no heat to airman			B. Crit.
		C. Complete open circuit	C. No fluid flow	C. Thermoelectrics overheat & prevent DC motor start	C. No heat to airman			

FAILURE MODE, EFFECTS AND CRITICALITY ANALYSIS

SYSTEM RSK-JA DAPS CONTRACT N62269-76-C-0289 DATE 20 July 1976

ENG'R R. S. Christie PAGE 7 OF 9

SUB SYSTEM	PART	FAILURE MODE	PART EFFECT	SUBSYSTEM EFFECT	SYSTEM EFFECT	FAIL. RATE (x10 ⁻⁶)	FAIL. FREQ.	CRIT.
Fluid System	3. Fluid connectors	A. Frozen fluid or moisture in connector	A. Will not connect	A. No heated fluid to airman	A. Unit not operable			A. Mar.
		B. Damaged connector	B. Cannot connect mating halves	B. No heat to airman	B. Unit not operable			B. Crit.
		C. Seal malfunction	C. Connector leaks	C. Excessive fluid loss	C. System overheats causing damage to thermoelectrics.			C. Mar.
4. Anti-freeze	A. Not capable of being pumped	A. Leaks	A. Too viscous	A. No heat transfer to airman	A. System overheats			A. Crit.
5. Internal fluid connections				A. Excessive fluid loss	A. System overheats causing damage to thermoelectrics			A. Crit.

FAILURE MODE, EFFECTS AND CRITICALITY ANALYSIS

SYSTEM RSK-1A DAPS CONTRACT N62269-76-C-0289 DATE 20 July 1976

ENG'R R. S. Christie

PAGE 8 OF 9

SUB SYSTEM	PART	FAILURE MODE	PART EFFECT	SUBSYSTEM EFFECT	SYSTEM EFFECT	FAIL. RATE (x10 ⁻⁶)	FAIL. FREQ.	CRIT.
Elec- trical	1. DC- motor	A. Overload	A. Motor stops functioning	A. No power to drive the pump	A. No heat to air- man; unit over- heats damaging the thermo- electrics			A. Crit.
		B. Broken Lead	B. No DC motor operation	B. No power to drive pump	B. No heat to air- man; unit over- heats damaging the thermo- electrics			B. Crit.
		C. Failure to operate at design speed			C. Reduced fluid flow, possibly causing over- heat of thermo- electrics			C. Mar.
		D. Operates at too high a speed	D. Decreased life of motor		D. Fluid delivered at lower than normal temp- erature to air- man.			D. Mar.

FAILURE MODE, EFFECTS AND CRITICALITY ANALYSIS								
SYSTEM <u>RSSK-1A DAPS</u>		CONTRACT <u>N62269-76-C-0289</u>		DATE <u>20 July 1976</u>		PAGE <u>9</u> OF <u>9</u>		
ENG'R <u>R. S. Christie</u>								
SUB SYSTEM	PART	FAILURE MODE	PART EFFECT	SUBSYSTEM EFFECT	SYSTEM EFFECT	FAIL. RATE (x10 ⁻⁶)	FAIL. FREQ.	CRIT.
Elec-trical	2. 12 VD C Con-nec-tor	A. Broken lead to the connector		A. No regulated 12 VDC output	A. No auxiliaries			A. Crit.
		B. Broken con pin	B. Connection not possible		B. No auxiliaries			B. Crit.
		C. Bent con. pin	C. Connection not possible		C. No auxiliaries			C. Crit.
		D. Ice in either half of connec-tor	D. Connection delayed		D. No auxiliaries			D. Mar.
3. DC-DC con-verter		A. Operation below design Spec.	A. Insufficient power into the converter	A. Thermoelectric output too low	A. Weakened or no auxiliaries			A. Mar-Crit.

4.2.2.4 Parts Reliability

A tabular presentation of the component failure rates is included as Table 7 of this report. The calculations, for the predicted failure rates and success probabilities of the individual components, are presented in Appendix B. Along with these calculations are the sources of information and the assumptions made. The calculation of the actual success probabilities for the individual components was hindered by the lack of accurate failure rate data. Until this data can be acquired, from either a central information agency such as GIDEP, or by actual testing, the predicted failure rates are assumed correct. Based on these predictions the current MTBF for the RSSK-1A DAPS is 960 hours and the current success probability .975.

4.2.2.5 Failure Mode, Effects and Criticality Analysis

A preliminary Failure Mode, Effects and Criticality Analysis (F.M.E.C.A.) Table 8, which identifies the basic faults at the part level and shows the effects on higher levels of assembly, was performed during this contract. Included in the F.M.E.C.A. are both actual failure modes from past testing, and hypothesized failure modes from design analysis.

Hazard levels have been assigned to each failure mode and indicate the effect of the failure on the downed airman. The hazard levels used for the failure criticality are those of MIL-STD-882 (System Safety Program for Systems and Associated Subsystems and Equipment: Requirements for) and are defined as follows:

- (a) Category I - Negligible
... will not result in personnel injury or system damage.
- (b) Category II - Marginal
... can be counteracted or controlled without injury to personnel or major system damage.
- (c) Category III - Critical
... will cause personnel injury or major system damage, or will require immediate corrective action for personnel or system survival.

(d) Category IV - Catastrophic

. . . . will cause death or severe injury to personnel, or system loss

During this contract, corrective actions and recommendations dealt solely with those failure modes labeled as critical. Most of the critical failure modes have had some form of corrective action taken. Further testing is required to determine whether or not the corrective actions taken were sufficient. A list of those corrective actions taken since the previous RSSK-1A contract is included below:

- A. The pressure relief valve on the spiral fuel tank has been changed, resulting in a decreased fuel leakage rate.
- B. Protective caps for the fuel, electrical, and fluid connectors have been added.
- C. Tubing and wires have been sufficiently supported or tied down, in order to minimize the effects of vibration.
- D. A fuel filter has been included on the upstream side of the orifice to reduce the number of impurities to the orifice thereby reducing the chances of clogging.
- E. The pin plate has been re-designed to eliminate the possibility of catalyst leaking out of the combustion chamber, past the front screen, and into the diffuser.
- F. The internal fluid lines have been changed from fluorocarbon to silicone. Fluorocarbon at low temperatures tends to become very brittle whereas the silicone tubing, at the same temperatures, remains flexible.
- G. Those fittings that had previously been epoxied are now being dip brazed.
- H. Hose clamps have been added to all fluid lines to help reduce fluid leakage and air inclusion.

- I. The fuel pressure and fluid temperature gauges have been removed, thereby eliminating four possible leak paths.
- J. The fluid connectors have been changed, thus reducing the amount of fluid leakage and air inclusion per connect disconnect cycle.

4.2.2.6 Effects of Storage

As the unit is scheduled to be heat sealed upon delivery, the effects of storage should be minimal. The following is a list of predicted storage effects:

(1) Demagnetization of the permanent magnet can occur if the RSSK-1A unit is stored in an area of excessive external magnetic field.

(2) The D.C. motor has a specified shelf life of two years, due to the bearing lubricant. However, the manufacturer feels that a five year shelf life is more accurate.

(3) The fuel tank does have a small leakage rate and should be checked periodically. The predicted refill schedule is shown in Table 6. Initially, however, the fuel tank should be checked on a yearly basis.

4.2.3 Reliability Testing

During this contract funds were not provided specifically for reliability testing and, therefore, only a minimal amount of testing was accomplished. The most extensive tests were conducted on the RSSK-1A spiral fuel tanks and the RSSK-1A DAPS units that were returned to Energy Systems Corporation by NADC on April 9, 1976.

The spiral fuel tanks, that had been delivered under Contract Number N62269-76-C-0444, were tested for their leakage rates. All nine tanks had relatively high leakage rates (see Table 9, and Figure 46). To correct this problem several design changes were incorporated into the new spiral fuel tank, (for details of the design changes refer to section 2.3 of this report).

FUEL TANK LEAKAGE RATE*
(WEIGHT IN GRAMS)

Serial No. DATE	0004	0005	0006	0007	0008	0009	0010	0011	0012
Empty Weight	1000.5	1005.0	1007.0	1005.0	1000.0	1005.0	1000.0	1007.0	1007.0
10 Dec. 1975	1171.5	1187.0	1190.0	1180.0	1176.0	1176.5	1178.0	1191.5	1182.0
12 April 1976	1184.8	1178.0	1186.0	1175.7	1144.2	1169.3	1176.3	1189.5	1060.2
12 May 1976	1184.6	1177.7	1185.6	1175.5	1137.5	1168.1	1176.0	1184.1	1059.9
11 June 1976	1184.1	1177.4	1185.2	1175.3	1132.0	1166.2	1175.5	1184.1	1059.9
22 June 1976	1184.1	1177.2	1185.2	1175.3	1130.9	1165.4	1175.5	1184.1	1059.9
Fuel tanks numbered 0008, 0009, and 0012 were refilled on 22 June 1976.									
22 June 1976	1184.1	1177.2	1185.2	1175.3	1184.1	1185.0	1175.5	1184.1	1182.3
12 July 1976	1183.9	1177.1	1185.0	1175.3	1174.8	1184.1	1175.5	1184.1	1123.9
12 August 1976	1183.9	1176.9	1184.8	1175.3	1162.5	1184.0	1175.5	1184.1	1110.4
13 September 76	1183.25	1175.8	1183.9	1174.65	1154.0	1182.75	1174.9	1184.05	1098.9
13 October 1976	1183.25	1175.5	1183.3	1174.65	1151.2	1182.4	1174.7	1183.9	1092.5
12 November 76	1183.25	1175.2	1183.0	1174.5	1149.05	1181.7	1174.4	1183.75	1086.95
Avg. Leak./Mo.	0.2	1.1	0.6	0.5	7.8	0.7	0.3	0.7	21.2

*Fuel tanks delivered under Contract No. N62269-76-C-0444

Table 9.

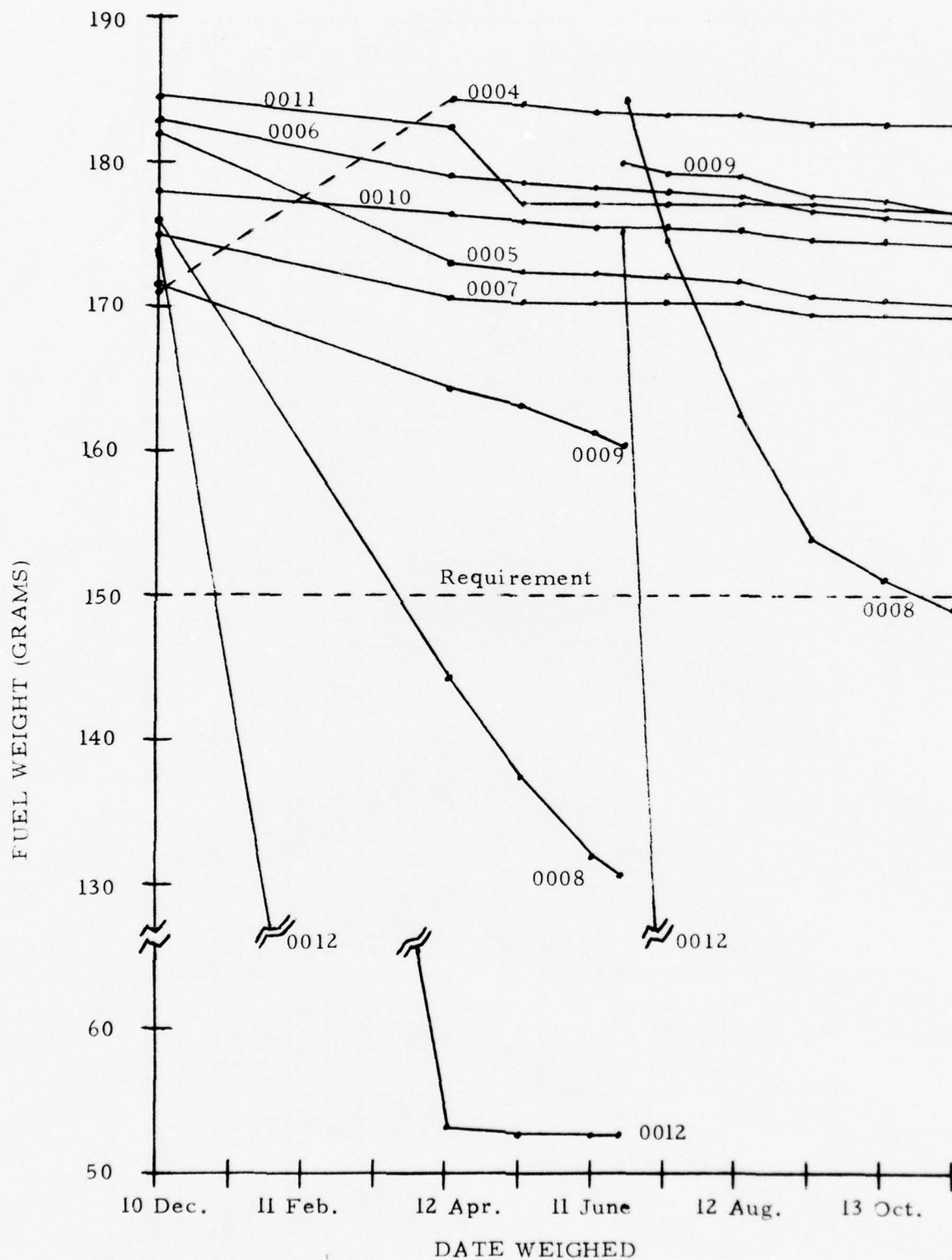


Figure.46.FUEL TANK LEAKAGE RATE

TEST FUEL TANK LEAKAGE RATE
(WEIGHTS IN GRAMS)

Serial No. DATE	0001	0002
Empty Weight	406.6	439.65
12 August 1976	432.8	467.4
13 August 1976	432.8	467.4
16 August 1976	432.8	467.35
17 August 1976	432.75	467.35
18 August 1976	432.75	467.35
19 August 1976	432.75	467.35
20 August 1976	432.75	467.35
23 August 1976	432.75	467.35
24 August 1976	432.75	467.30
25 August 1976	432.75	467.30
27 August 1976	432.75	467.30
30 August 1976	432.75	467.30
31 August 1976	432.75	467.25
1 September 1976	432.75	467.25
2 September 1976	432.75	467.25
3 September 1976	432.75	467.25
7 September 1976	432.75	467.25
8 September 1976	432.75	467.25
9 September 1976	432.75	467.25
10 September 1976	432.75	467.25
13 September 1976	432.75	467.25
13 October 1976	432.65	--
12 November 1976	432.50	--
Avg. Leak. (gr/month)	0.1	0.15

Table 10.

TEST FUEL TANK LEAKAGE RATE

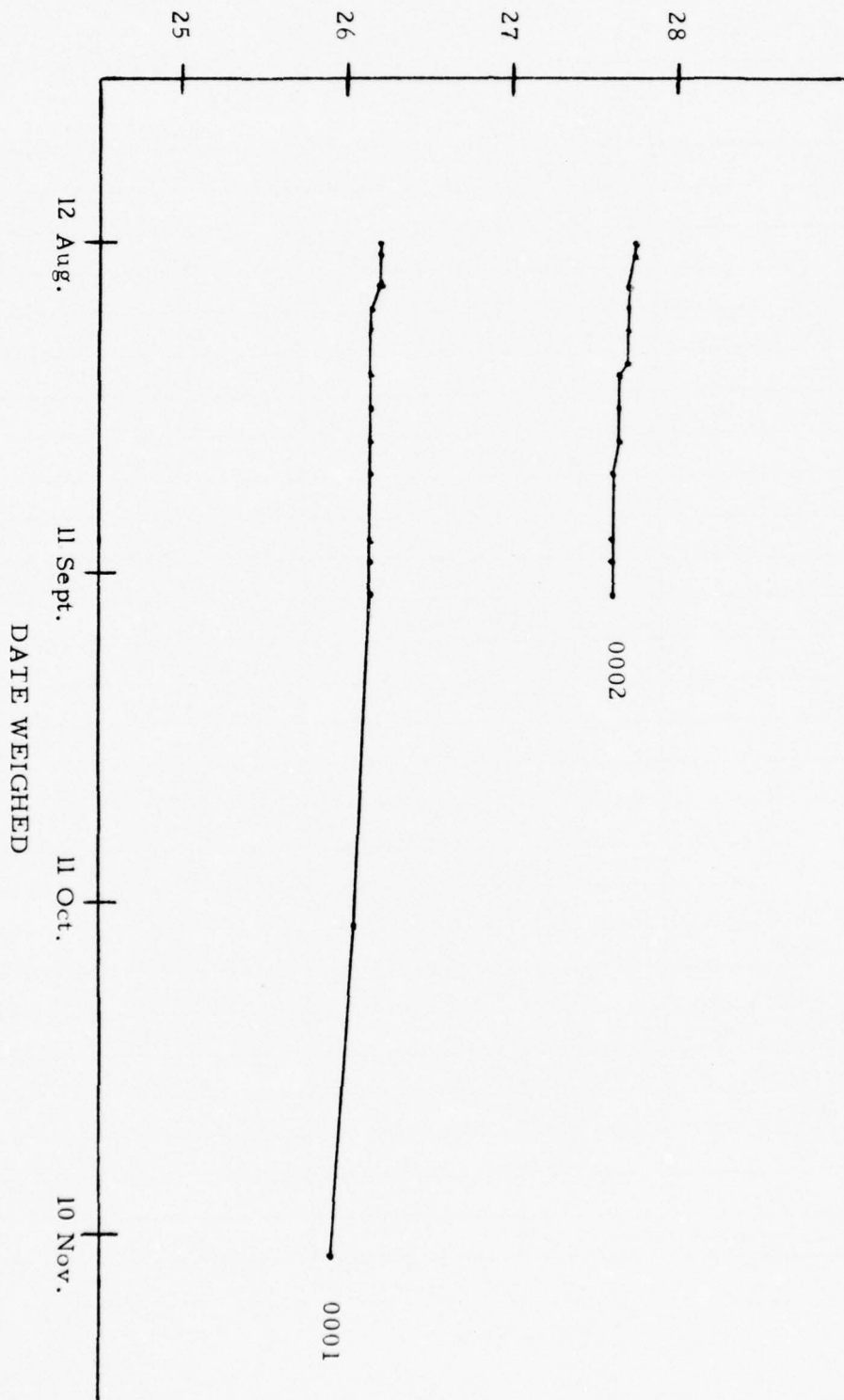


Figure 47.

Two test tanks of the new design were assembled and filled with propane on August 12, 1976. The leakage rates were monitored on a daily basis for the first month and on a monthly basis thereafter (See Table 10 and Figure 47). A marked improvement in the leakage rate was noticed over the old design. With this improved leakage rate it is expected that the fuel tank will have to be refilled only once every five years.

Nine of the RSSK-1A DAPS were returned to Energy Systems Corporation, along with the spiral fuel tanks, for further testing to determine the effects of storage on the operating performance. Three of the units exhibited an increase in efficiency over the original tests, three of the units had efficiencies approximately the same as the original results, and three units showed a decrease in efficiency.

After careful inspection it was found that those units with efficiencies the same or lower than original results, had catalyst leaking out of the combustion chamber, past the front screen, and into the diffuser. Some of this catalyst worked its way into the air gap and thus affected the air-fuel ratio and the efficiency. Those units which exhibited an increase in efficiency had no catalyst leakage. To correct this problem in future units the distance between the outside pin of the pin plate, and the combustion chamber wall, has been reduced.

Failure identification reports and failure record forms have been drawn up and are of the format of MIL-STD-7813 (Reliability Tests: Exponential Distribution). They will be used for all future testing to accurately record all failure modes encountered. Sample copies of these forms appear as Figures 48a, b, c, d, e, f.

[illegible]

- 102 -

[illegible]

- 103 -

FAILURE IDENTIFICATION REPORT (PART A)			
SYSTEM _____	ASSEMBLY _____	SUBASSEMBLY _____	PART NO. _____
COMPONENT _____	SERIAL NO. _____	DATE _____	TIME _____
TOTAL UNIT TEST TIME _____	TEST REFERENCE _____	REPORT NO. _____	_____
TEST TYPE _____	_____		
TEST AND ENVIRONMENTAL CONDITIONS _____		IDENTIFICATION OF TEST EQUIP: _____	
_____		_____	
_____		_____	
_____		_____	
FAILURE SYMPTOMS: _____		_____	
_____		_____	
_____		_____	
ADJUSTMENT REQUIRED _____		_____	
_____		_____	
_____		_____	
OTHER EQUIP. FAILURES OBSERVED SIMULTANEOUSLY WITH SUBJECT FAILURE _____		_____	
_____		_____	
_____		_____	
_____		_____	

Figure 48c.

FAILURE CONFIRMATION AND REPAIR REPORT (PART B)					
SYSTEM _____	ASSEMBLY _____	SUBASSEMBLY _____	PART NO. _____		
COMPONENT _____	SERIAL NO. _____	DATE _____	TIME _____		
FAILURE SYMPTOM _____	NAME _____		UNIT TIME _____		
TEST TYPE _____	TEST REFERENCE _____		REPORT NO. _____		
TEST EQUIP. USED	SERIAL NO.	TEST PERFORMED	DATE BEFORE REPAIR		
CONFIRMATION OF SYSTEMS REPORTED _____					
REASON FOR PART FAILURE _____					
TEST EQUIP. USED	SERIAL NO.	PART TEST USED TO ESTABLISH PART FAIL	DATE ON DEFECT. PART		
DEFECTIVE PART _____ PART NO. _____ MFG. _____					
Use copy of this form for each failure at this time. Check <input type="checkbox"/> if more than one failure found.					

Figure 48d.

FAILURE CONFIRMATION AND REPAIR REPORT (PART C)

SYSTEM _____ ASSEMBLY _____ SUBASSEMBLY _____ PART NO. _____
 COMPONENT _____ SERIAL NO. _____ REPORT NO. _____
 TEST TYPE _____ UNIT TIME _____ NAME _____

MULTIPLE PART FAILURE

IDENTIFICATION OF DEPENDENT FAILURES

PARTS FAILING

(1)	_____	(4)	_____
(2)	_____	(5)	_____
(3)	_____	(6)	_____

CAUSE OF MULTIPLE FAILURES

IDENTIFICATION OF INDEPENDENT FAILURES

PARTS FAILING

(1)	_____
(2)	_____
(3)	_____

Figure 48e.

FAILURE ANALYSIS REPORT (PART D)

SYSTEM _____ ASSEMBLY _____ SUBASSEMBLY _____ PART NO. _____
COMPONENT _____ SERIAL NO. _____ DATE _____ REPORT NO. _____
TEST TYPE _____ TEST REFERENCE _____

COMPONENT ANALYSIS _____

DESIGN ANALYSIS _____

RECOMMENDATIONS FOR CORRECTIVE ACTION _____

SIGNATURE _____

Figure 48f.

5.0 SYSTEM FINAL TEST

5.1 Test Set Up

System final testing was performed on a test stand designed specifically for the purpose of characterizing DAPS heater performance.

The test stand is shown in Figure 49. It consists of three major sub-systems.

- (1) Thermal
- (2) Hydraulic
- (3) Electrical

5.1.1 Thermal

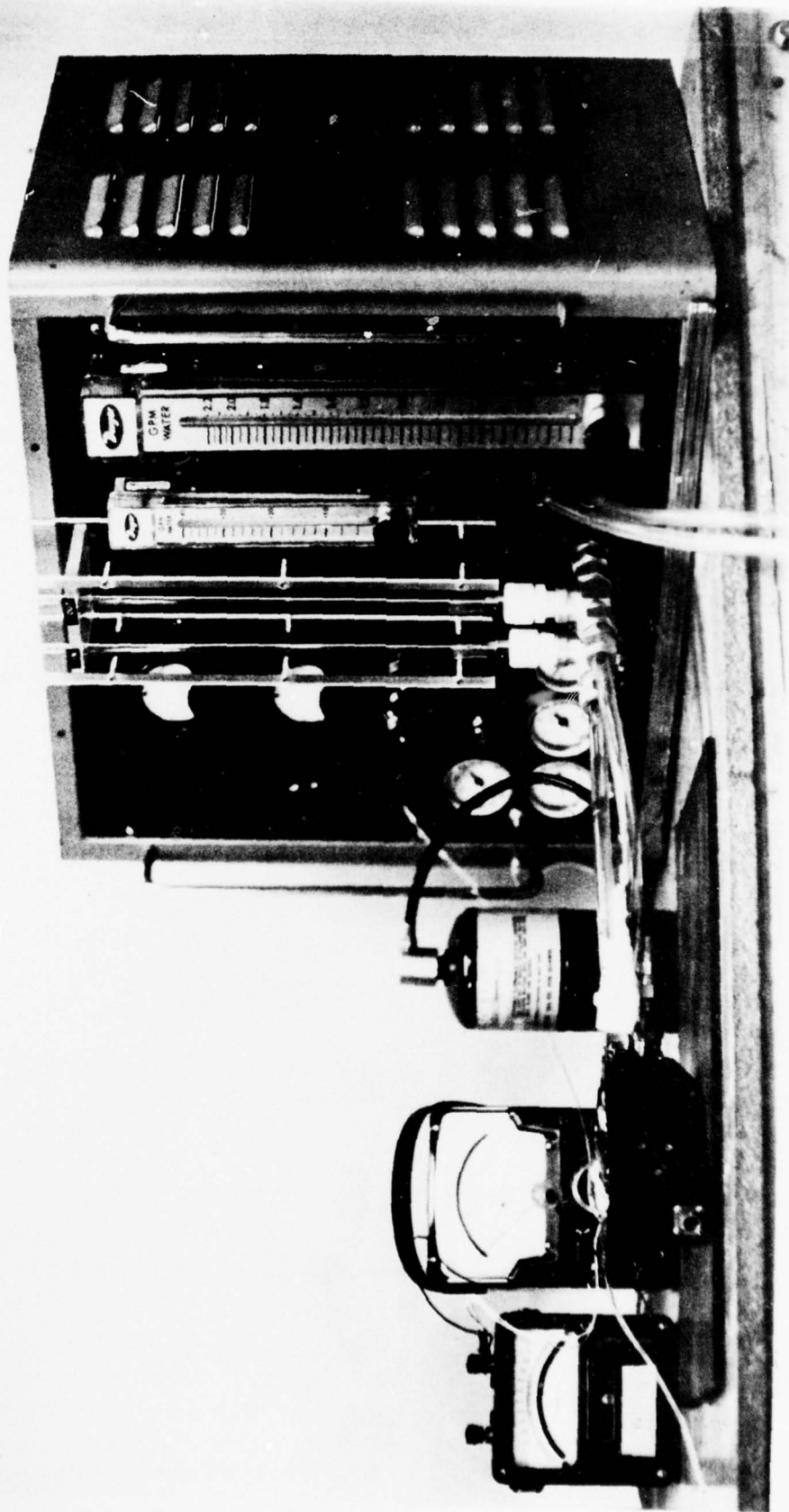
The thermal sub-system is designed to measure the temperature rise of the fluid across the heat exchanger.

Two precision thermometers are used for this measurement. They have a temperature range from 79°F to 116°F and have .2°F increments for accurate measurement.

The fuel flow rate is measured using a Dwyer flow meter Part No. RMA-1. This meter is capable of measuring the flow of air from .05 SCFH to .5 SCFH. This range converts to .05 SCFH to .40 SCFH for propane.

5.1.2 Hydraulic

The hydraulic sub-system is comprised of a mercury manometer, flow meter and flow resistance. The mercury manometer is used to measure the pressure drop against which the system must pump. The flow measurements are accomplished using either of two Dwyer flow meters depending upon the anticipated flow.



Test Stand

Figure 49

Dwyer flow meter Part No RMB-84 has a capacity of from 0 to 40 Gallons per hour while the Dwyer flow meter Part No. RMC-142 has a capacity of .2 GPM to 2.2 GPM.

A flow resistance is used in the system to simulate a pressure drop as would be realized when the system was pumping into a tubulated under garment.

5.1.3 Electrical

The electrical test stand is comprised of a volt meter, ammeter and normally closed switch with which to measure open circuit voltage of the thermoelectric modules under a no load condition.

5.2 Required Calculations

5.2.1 Thermal efficiency as used in this case is the ratio of potential heat available in the fuel in BTU/Hr. to the heat picked up by the water in the heat exchanger also measured in BTU/Hr.

The potential fuel heat value is determined by two methods. Method #1 is the most accurate and consists of actually measuring the weight change of the fuel supply at a given fuel pressure for a given length of time.

Example: 43 Grams of Propane per hour

$$\text{Heat Value (BTU/Hr)} = \left(43 \text{ Gms. / Hr} \right) \left(\frac{1 \text{ lb.}}{453.6 \text{ Gm}} \right) \left(19944 \text{ BTU/lb.} \right)$$

Method #2 uses an empirical formula derived by the manufacturers of the orifice used in the RSSK-1A DAPS System (Lee Co.)

$$\text{Lohms} = \frac{C \times F \times P_1}{\text{SCFM} \times \sqrt{T_1}}$$

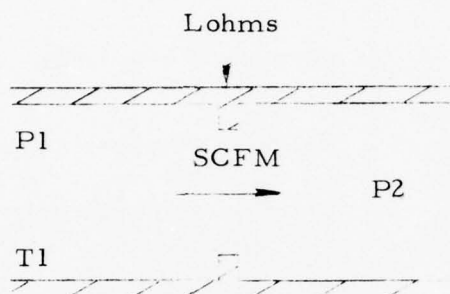
Lohms = Resistance as specified by manufacturer

C = Gas constant (Propane = 165)

F = Ratio of High Pressure (before orifice) to low Pressure(after orifice) = $(P_1/P_2)-1$; for $(P_1/P_2)-1 > 1$ use $F=1.0$

SCFM = Standard Cubic Feet per Minute

T1 = High Pressure side temp ($^{\circ}\text{R} = ^{\circ}\text{F} + 460$)



$$\text{Example: SCFM} = \frac{C \times F \times P1}{\text{Lohm} \times \sqrt{T1}}$$

From these two calculations we see that the correlation is very good. For the purposes of the calculation, the flow rate as determined from actual measurement is used.

The heat into the water is determined from the formula $q = \dot{m} C_p \Delta T$

Where:

- q = heat into the water (BTU/hr)
- \dot{m} = Mass flow rate of fluid (lb/Hr)
- C_p = Specific heat of fluid (BTU/lb $^{\circ}\text{F}$)
- ΔT = change in temperature through the heat exchanger ($^{\circ}\text{F}$).

$$\begin{aligned} \text{Example: } q &= \dot{m} C_p \Delta T \\ q &= \left(\frac{.25 \text{ Gal}}{\text{Min.}} \right) \left(\frac{8.34 \#}{\text{Gal.}} \right) \left(\frac{60 \text{ Min}}{\text{Hr.}} \right) \left(\frac{1 \text{ BTU}}{\text{lb}^{\circ}\text{F}} \right) (4.5^{\circ}\text{F}) = 562.95 \end{aligned}$$

5.2.2 System Efficiency

System overall efficiency is defined as the ratio the sum of the heat into the fluid plus the heat converted into electrical energy (typically 4%) to the heat potentially available in the fuel.

Example: (1.04) (heat into fluid) 100% = Total Efficiency

5.2.3 Electrical Performance

Electrical characteristics are measured to monitor thermoelectric efficiency.

The required formulae for determining the electrical parameter are listed below:

Internal Resistance of Module

$$R_i = \frac{E_{oc} - E_L}{I_L}$$

Resistance of Circuit

$$R_L = \frac{E_L}{I_L}$$

Power Delivered

$$P = \left[\frac{E_{oc}}{R_i + R_L} \right]^2 R_L = E_L I_L = I_L^2 R_L$$

Max Power

$$P_{max} = \frac{(E_{oc})^2}{4R_i}$$

System off design power ratio P/P_{max}

R_i = Internal resistance of module (ohms)

R_L = Resistance of circuit (ohms)

E_L = Load Voltage (volts)

E_{oc} = No load voltage (volts)

I_L = Current draw of Load (amps)

P = Power (watts)

5.2.4 Exhaust Gas Test

Exhaust gas tests were performed to determine the concentration of unburned fuel and carbon monoxide in the exhaust gas. A detailed explanation of the theory and equipment is found in Section 2.7.

5.3 Test Results

The results obtained from tests on the DAPS System are tabulated and explained below.

The fuel used for these tests was propylene although the systems are delivered for use with propane. The reason for this is that commercial propane is a mixture of several hydrocarbon compounds. The compounds would make it impossible to monitor exhaust gas components accurately because the analyzer is only capable of measuring one compound at any one setting.

The actual results are minimally effected by this change because of the close similarity in chemical structure and heat of combustion values of the compounds.

Propane (C_3H_8) has a net heat of combustion of 19944 btu/lb while propylene (C_3H_6) has a net heat of combustion of 19578 btu/lb. This amounts to a difference of only 366 btu/lb or approximately 2%.

The systems were tested for output characteristics at 10, 20 and 30 psig. These settings correspond to regulator settings of 2.5, 5.8 and 9.

These results are tabulated in Tables 11, 12, 13 & 14.

TABLE 11

Test Results at Regulator Setting of 3.5

Regulator Setting: 3.5

Grams of Fuel Per Hour: 24.50

Fuel Pressure: 10 psi

Fuel Heat Value(BTU/Hr): 1077

Time	Electrical				Hydraulic	
Min.	Volts E_L	Amps I_L	Open Ckt. Volts E_{oc}	Power Watts	Flow Rate Gal/Hr.	Flow Rate Lbs/Hr
0.5	.2	.21				
1.0	.4	.39				
1.5	.58	.57				
2.0	.70	.74				
2.5	.82	.88				
3.0	1.80	.80				
5.0	2.80	1.20				
10.0	3.60	1.7	5.75	6.12	21.6	180.14
15.0	3.60	1.72	5.80	6.19	21.6	180.14
20.0	3.70	1.68	5.80	6.21	21.6	180.14
25.0	3.65	1.68	5.75	6.13	21.8	181.81
30.0	3.65	1.68	5.75	6.13	21.8	181.81

Time	Thermal					
Min.	Temp. in °F	Temp. Out °F	ΔT	BTU/Hr In Fluid	Thermal Eff.	System Eff.
15.0	75.3	78.8	3.5	63 .5	58.5	60.9
20.0	75.8	79.4	3.6	648.5	60.2	62.6
25.0	76.4	80.0	3.6	654.5	60.7	63.2
30.0	77.0	80.5	3.6	654.5	60.7	63.2

TABLE 12

Test Results at Regulator Setting of 6.5

Regulator Setting; 6.5

Grams of Fuel Per Hour: 38.00

Fuel Pressure: 20 PSI

Fuel Heat Value(BTU/Hr): 1670

Time	Electrical				Hydraulic	
Min.	E _L	I _L	E _{oc}	Watts	Gal/Hr.	Lbs/Hr
30.0	3.8	1.8	7.25			
31.0	4.0	1.9				
32.0	4.15	2.0				
33.0	4.30	2.15				
34.0	4.4	2.15	7.50			
35.0	4.45	2.19				
40.0	4.5	2.20	7.6	9.9	26.5	221
45.0	4.5	2.15	7.6	9.7	26.8	223.5
50.0	4.5	2.14	7.6	9.7	26.8	223.5
55.0	4.50	2.15	7.6	9.7	26.8	223.5

Time	Thermal					
Min.	Temp. in °F	Temp. Out °F	Δ T	BTU/Hr In Fluid	Thermal Eff.	System Eff.
40.0	79.1	83.1	4.0	884.1	52.9	55.0
45.0	79.9	84.0	4.1	916.3	54.8	57.0
50.0	80.5	84.5	4.0	894	53.5	55.6
55.0	81.0	85.0	4.0	894	53.5	55.6

TABLE 13

Test Results at Regulator Setting of 9.0

Regulator Setting: 9.0

Grams of Fuel Per Hour: 44.0

Fuel Pressure: 26 PSI

Fuel Heat Value(BTU/Hr): 1934

Time	Electrical				Hydraulic	
Min.	E _L	I _L	E _{oc}	Watts	Gal/Hr.	Lbs/Hr
56.0	4.70	2.25	8.0			
57.0	4.75	2.30				
58.0	4.75	2.30				
59.0	4.80	2.35				
60.0	4.80	2.32	8.2	11.1	28.5	237.7
65.0	4.80	2.35	8.2	11.3	28.8	240.2
70.0	4.80	2.35	8.2	11.3	28.8	240.2

Time	Thermal					
Min.	Temp. in °F	Temp. Out °F	Δ T	BTU/Hr In Fluid	Thermal Eff.	System Eff.
60.0	82.5	86.8	4.3	1022.1	52.8	54.9
65.0	83.5	87.6	4.1	984.8	50.9	52.9
70.0	84.0	88.2	4.2	1008.8	52.1	54.2

TABLE 14

Test Results at Regulator Setting of 9

Regulator Setting: 9

Grams of Fuel Per Hour: 44.0

Fuel Pressure: 26

Fuel Heat Value(BTU/Hr): 1934

Time	Electrical				Hydraulic	
Min.	E _L	I _L	E _{oc}	Watts	Gal/Hr.	Lbs/Hr
0.5	.34	.10				
1.0	.42	.28				
1.5	.50	.40				
2.0	.80	.82				
3.0	2.0	1.3				
4.0	3.75	1.8				
5.0	4.4	2.1				
10.0	4.8	2.5	8.5	11.9	28.5	237.7
15.0	4.9	2.45	8.5	12.0	28.8	240.2
20.0	4.95	2.43	8.5	12.0	29.2	243.5
25.0	5.0	2.4	8.6	12.0	29.2	243.5
30.0	5.0	2.4	8.6	12.0	28.8	240.2

Time	Thermal					
Min.	Temp. in °F	Temp. Out °F	ΔT	BTU/Hr In Fluid	Thermal Eff.	System Eff.
10.0	69.0	73.6	4.6	1093.4	56.5	58.7
15.0	69.2	73.8	4.6	1104.9	57.1	59.4
20.0	70.8	75.3	4.5	1095.7	56.6	58.9
25.0	73.0	77.5	4.5	1095.7	56.6	58.9
30.0	73.4	77.9	4.5	1080.9	55.8	58.0

TABLE 15

EXHAUST GAS CONCENTRATION

<u>Regulator Setting</u>	<u>Fuel Pressure (PSIG)</u>	<u>Carbon Monoxide (CO)</u>	<u>Propane (C₃H₈)</u>
3.5	10	27.1 PPM	4.83 PPM
6.5	20	62.6 PPM	11.82 PPM
9	26	87.47 PPM	6.44 PPM

Figure 50 is a plot of how the voltage and flow rate increase with time at various fuel settings.

Curve A indicates the voltage size as a step function with respect to fuel pressure while Curve B shows the voltage rise and corresponding flow rate at 30 psig in one step.

Table 15 tabulates the exhaust gas results obtained at various fuel settings.

Table 16 tabulates the test results obtained from evaluation of the DC-DC Converter. This data indicates that the unit can be used at the lower fuel settings which was not possible in previous units due to the higher input voltage required.

TABLE 16

<u>Voltage Input</u>	<u>Voltage Output</u>
1.0	3.2
1.5	6.2
2.0	9.0
2.5	11.8
3.0	11.9
4.0	11.9
5.0	11.9
6.0	11.9

This data indicates that a fuel setting of 3 provides sufficient input voltage to the converter to give a 12 VDC output.

6.0 CONCLUSIONS

6.1 Design & R & M Conclusions

Contract N62269-76-C-0289 can be broken down into six distinct stages each having their own conclusion. These stages are listed below together with a summary of work done.

6.1.1 Seat Kit Study

The first four to six weeks of the contract were spent determining the relevant differences among the various RSSK-1A seat kits as manufactured by Scott Aviation, Rocket Jet Division of American Flight Safety and East/West Industries. The results of this study are stated in depth in Section 2.1.

In addition to the differences among RSSK-1A seat kits among manufacturers, two other potential problems exist that could cause potential interchangeability problems. These are:

6.1.1.1 Differences in a Single manufacturer's Seat Kit Due to Tolerances

Lack of detailed internal RSSK sub-component placement specifications allows manufacturers to work to liberal tolerances in the installation of these components. (e.g. oxygen tank, oxygen valves, mounting bracketry, etc.) Because of severe DAPS volume limitations in any seat kit, small variations in RSSK component placement might well prevent an already close fitting DAPS from being installed in a given kit.

Because of the unavailability to date of manufacturer's production drawing packages, ESC has not been able to take into consideration DAPS space restrictions which might result from seat kit component placement tolerance variations.

6.1.1.2 Differences in a Single Manufacturer's Kit Due To Production Run

The Navy purchases Rigid Seat Survival Kits from one or more manufacturers at any given time in large quantities and presumably, on the basis of lowest sealed bid. This "batch" procurement practice results in the manufacturer gearing up for production in order to deliver some number of seat kits, then suspending operations until the next seat kit buy.

Although no hard evidence has been identified to date to prove that seat kits vary from run to run, it is highly probable that such differences do occur. Because of the latitude allowed by the envelope specification, it is possible that the variation between a single manufacturer's production runs is of the same order of magnitude as the variation already observed between manufacturers.

6.1.2 Design Layout

Several weeks were spent generating design layouts so as to determine optimum component location and maximum void volume utilization.

Based on these layouts, it was determined that radical changes would have to be made to the existing design if the RSSK-1A DAPS was to be interchangeable among the three kit manufacturers.

The major conclusion was that the existing combustion chamber design was not suited for packaging in the available space. This mandated that a new combustion chamber be designed.

Other conclusions arrived at from the layout were that the pressure gauge and temperature gauge would have to be deleted. The deletion of these gauges minimally impacted the design primarily due to the fact that regardless of what the gauges indicated, the degree of comfort would ultimately be determined by the user and the comfort level is a very subjective thing varying greatly from individual to individual.

6.1.3 Developmental Testing & System Design

Extensive testing was performed on several prototype combustion chambers that would fit into the available space for the new DAPS design.

Several important facts became evident as a results of this testing. The three major points that affect combustion chamber design are catalytic bed size, thermoelectric thermal contact and heat exchanger design. These points are discussed in more detail below.

6.1.3.1 Catalytic Bed Size

For any given fuel consumption rate there is a

very narrow limit between too much and too little catalyst. The affects of too little catalyst is obviously an excess of unburned fuel in the exhaust with a resulting waste of fuel. The affects of too much catalyst is not as obvious. It was learned from conversations with Matthey Bishop Corporation, the manufacturer of the catalyst, that if too much catalyst is present the air fuel mixture becomes richer and richer with a resulting decrease in available oxygen for combustion.

When this state exists, the products of combustion start to recombine to form methane gas in an extremely endothermic reaction. This reaction absorbs large amounts of heat thereby decreasing the temperature of the hot side. The net effect of this situation is also a decrease in system performance.

It was concluded that the proposed design operated on the extreme edge of having sufficient catalyst to combust the required amount for the required heat.

6.1.3.2 Thermoelectric Module Thermal Contact

In the course of developmental testing it was determined that the power generating ability of the modules is extremely sensitive to surface finish of the mating surfaces and also to contact pressure.

It is important that the maximum amount of module surface area is in contact with the maximum amount area on the hot pin plate and cold heat exchanger sides of the modules.

When there are large areas of poor contact, there results a corresponding drop in power generation which feeds back into system efficiency.

Even when the mating surfaces are perfectly flat and smooth the power output of the modules is extremely sensitive to clamping force. Too little force also results in a drop in power generated.

6.1.3.3 Heat Exchanger Design

The third major conclusion resulting from the combustion chamber test is the degree of affect the design of the heat exchanger has with respect to heat extraction and pick up.

As stated in Section 3.0 of this report, the efficiency of the heat exchanger is dependent upon the heat transfer coefficient and available heat pick up area. Test results indicate that depending upon heat exchanger design, the thermal efficiency can be affected by 8 to 10%.

6.1.4 System Build

Previous systems were difficult to build and test due to the packaging density and the number of flexible tube runs. The new design is much easier to assemble and test. Assembly time required to build the combustion chamber has been reduced by 50% with the incorporation of the new design.

The removal of the temperature and pressure gauge also resulted in a decrease in assembly time due to the reduction in the number of connections that had to be made in the fuel and hydraulic lines.

Another innovation incorporated into this design is the use of preformed hard line fluid lines. These dip brazed fittings enable sharp bends to be made without danger of kinking a line with resultant loss of fluid flow.

The use of soft line fluid runs has been used only in the case of easily accessible runs. These above mentioned design changes have greatly facilitated the assembly of the units.

6.1.5 System Test

The results of the testing indicate that the new design RSSK-1A DAPS is superior in performance to the previous designs. The combustion efficiency has improved from 10% to 15% to a thermal efficiency of 60 to 65%.

This increase is attributed to proper combustion chamber sizing, resulting in more complete combustion, good thermal contact, resulting in more available power, optimized heat exchanger efficiency, resulting in more heat transfer into the water.

6.1.6 Reliability and Maintainability

An extensive R & M effort was performed so as to determine as realistically as possible the reliability and mean time between failures of the DAPS.

The availability of R & M data for mechanical systems proves to be a major problem in determining an absolute reliability for the DAPS.

The manufacturers of the majority of the components used in the RSSK-1A system did not have any reliability data for their products because the majority of them were developed for commercial application. Where no data was available an approximation of the reliability of the component was made based on available data for similar components.

Based on these results, Energy Systems Corporation concludes that the reliability of the DAPS System as currently designed is within an acceptable distance from the optimum goal of a reliability of .976 or 1000 hours mean time between failures.

Recommendations of future actions are found in Section 7.0 of this report.

7.0 RECOMMENDATIONS

7.1 Design

Energy Systems Corporation has developed the DAPS System to an advanced preproduction state.

At this point in time there are two routes that NADC can pursue.

- 1) Design DAPS Systems for each seat kit design as they become qualified for field use.
- 2) Design a Universal DAPS that could possibly be interchangeable among the majority of the RSSK kit designs.

The potential problems likely to be encountered, should option 1 above be selected, are outlined in Section 6.1.1 of this report.

Should this be the selected course of action several controls would have to be implemented to guarantee interchangeability of the DAPS system among the kits manufactured by the various RSSK-1A manufacturing houses.

These controls would require as an absolute minimum rigid control of interior seat kit dimensions as well as component location and orientation be placed on all current and future fabrications. Current specifications only define outside dimensions which affect aircraft interface and allow virtually unlimited leeway with internal component placement.

This procedure would guarantee that the DAPS would be interchangeable among the kits as designed by all manufacturers.

These controls would, however, have to be instituted by the Navy as they are the seat kit user who can dictate seat kit specifications to the manufacturer and strictly enforced if interchangeability is to be a reality.

The second approach, and that preferred by Energy Systems Corporation is the concept of a "Universal DAPS".

Energy Systems Corporation recommends that Naval Air Development Center, Crew Systems Department, initiate a program whereby the feasibility of such a system could be determined.

Recent discoveries and developments by ESC indicate that such a system might be possible. Further DAPS miniaturization appears possible and some new concepts in packaging should they prove satisfactory could allow a great deal of flexibility in RSSK/DAPS installation.

Details of the conceptual "Universal DAPS" design are discussed below.

The DAPS System concept is primarily designed to extend survival time during a search and rescue operation, not to provide comfort for the downed airman.

Energy Systems Corporation has performed extensive theoretical studies of heat loss by a man in an encapsulating life raft to the ambient and the results indicate that a heat production rate of 100 watts is sufficient to compensate the heat loss by a man in the expected range of temperatures (See Appendix E for Calculations).

Based on these calculations, it seems that the existing system is over designed from a thermal output stand point.

Work under the RSSK-1A design contract has indicated that further DAPS miniaturization is possible. These size reductions, coupled with overall DAPS simplification and radical

component packaging concepts, open the door for realistic consideration of a universal DAPS.

It has been demonstrated by ESC that by proper selection of thermoelectric modules and by proper mating surface preparation, that the rated power output (5.5 to 6.5 watts) of the individual module can be obtained. The first feature of a Universal DAPS, then, would be a reduction in the number of thermoelectric modules from two to one.

Use of one module, given that it can be practically implemented, will allow construction of a combustion chamber of approximate dimensions: 1" x 2" by 2". Other features of a reduced size combustion chamber are discussed below;

7.1.1 Reduced Volume of Catalyst

The latest RSSK-1A DAPS combustion chamber contains 15 to 17 grams of Matthey-Bishop 1% platinum catalyst. This amount of catalyst is sufficient to oxidize propane at a rate of 40 grams per hour and results in a thermal output of 900 BTU/Hr. (264 thermal watts). The 15 grams of catalyst is easily contained within the above mentioned chamber volume.

If the DAPS thermal output requirement could be reduced, say to 150 or even 100 thermal watts, further reduction in catalyst volume, thus combustion chamber volume, could be made. Appendix C addresses this problem and derives the DAPS thermal output required to maintain the interior of the encapsulating liferaft at 60°F.

7.1.2 Optimized Heat Exchanger Design

ESC tests have shown that DAPS heat exchanger efficiency is very sensitive to changes in heat transfer area and heat transfer coefficient (a function of Reynolds Number). An optimum heat exchanger configuration for the minimum size combustion chamber would be designed analytically, then proven experimentally.

7.1.3 Optimized DAPS Electrical Network

The reduction in number of modules from two to one presents some electrical constraints not seen in current model DAPS. First, a single module system exhibits an output impedance one-half that observed in two module systems. In order to draw maximum power from the single module, a DC motor with approximately

one-half the motor resistance must be selected. Similarly, the motor voltage available (approximately 4.0 VDC in current DAPS) is reduced to approximately 2.5 VDC. Obviously a new motor must be found for the Universal DAPS.

The second and more obvious constraint is that of one-half the available power from only one thermoelectric module. Proper module selection will allow a ceiling power availability of 6.5 watts. Careful attention must, therefore, be paid to power budget allocations to the various DAPS sub-components.

Optimizing the DAPS electrical network is a complex exercise, often impossible with standard components. First, the motor must exhibit an input impedance (at operating speed and temperature) which matches as closely as possible the thermoelectric module output impedance at its operating temperature. Generally, the motor impedance of standard off-the-shelf motors is not as low (typically less than one ohm) as is required by the thermoelectric circuit. Secondly, the motor operating speed must be at the point of maximum motorefficiency, as well as at the point of maximum pump efficiency. Selection of a positive displacement pump which yields the proper output (pressure and flow) at a torque and speed input compatible with the motor has proven difficult in the past. In addition to input/output matching, the DAPS pump must be of certain dimensions, be driven by a zero leakage magnetic coupling, and exhibit high pumping efficiencies at the corresponding motor speed. To date, selection of the ideal pump from commercially available products has resulted in few alternatives.

Design of the Universal DAPS will represent a systems engineering effort which will take into consideration, and possibly modify, overall DAPS heat delivery requirements. Working backwards from the heat output requirement, the optimum heat exchanger design will be effected to give maximum heat delivery at a flow rate consistent with reduced power constraints. Flow and pressure considerations and the thermoelectric module characteristics will then dictate motor selection.

7.1.4 Improved Pump

Although technically, the pump is part of the electrical system discussed in Paragraph 4 and one of the largest single consumers of power as discussed in Paragraph 5, it warrants separate consideration because of its importance to the successful design of the Universal DAPS. The problem to date has been one of

finding a commercial pump which will pump the required DAPS flow at DAPS pressure drops yet still match up operationally with the rest of the thermoelectric/motor network. In particular, the existing pump experiences very high torque losses at the speeds at which it is driven by the existing motor. Two possible solutions exist, both of which would be pursued by ESC under a Universal DAPS program.

A. Custom design and fabricate the proper pump for DAPS application. This approach would also include custom modification of existing commercial pumps to suit other DAPS requirements. This approach appears to be the most attractive, since it would allow ESC to assure maximum efficiency at the required design point. In addition, ESC could tailor the size of the pump to Universal DAPS specifications.

B. A gear reduction could be used to run the pump at a slower speed, thereby cutting down considerably the speed dependent torque losses now experienced. The gear train losses would be more than compensated for by increased pump efficiency, but the gearing mechanism would require more space and add to DAPS weight.

7.1.5 Power Sharing

As has been pointed out in previous Paragraphs, several engineering approaches to designing a DAPS which will perform to specification using only one module (6.5 watts) have been discussed. Each approach offers, in itself, a viable solution to the Universal DAPS design problem. There is, however, one more approach which warrants discussion and which points out once again the many engineering approaches available in successful DAPS design.

The hydraulic pump and the DC-DC converter are the only two DAPS components consuming electrical power. It is conceivable, and practical, that these two components could share the limited electrical power available in a Universal DAPS. A downed airman in an emergency situation needs regulated 12 VDC power and he needs heat to warm his body - but not necessarily at the same time. The price to be paid in designing such a DAPS is, of course, increased system complexity and decreased system reliability (due to the complexity and added number of parts).

A power sharing arrangement might be designed to allow the DC-DC converter to draw all the power it requires (say for a PRC 90 radio) at the expense of the pump. As the pump slowed down, the temperature of the thermoelectric modules and the heat exchangers would rise. When the heat exchanger temperature exceeded a safe level, a temperature actuated switch would return power to the pump allowing excess heat to be carried away to the tubulated garment. As the temperature fell to acceptable levels, maximum power would be returned to the DC-DC converter, thus to the radio. The required switching would take place electronically, with all necessary components being solid state.

The most radical change from current generation DAPS would be the removal of the fuel pressure regulator. The DAPS will be designed such that a single fixed rate of heated water will be supplied to the airman's tubulated suit. An in-depth analysis will be first performed to determine just what this heat delivery rate should be. Connecting the fuel umbilical to the fuel tank will automatically start fuel flow to the combustion chamber. The airman will then press the ignition button and the DAPS will operate on its own. If too much heat is being delivered, the airman has the option of disconnecting the fuel line from the tank.

The resulting benefits to be realized with this approach are many:

- Cost Reduction
- Size Reduction
- Ease of Storing in Seat Kit
- Simplicity of Operation
- Seat Kit Interchangeability

Based on these advantages Energy Systems Corporation strongly recommends that NADC fund a R & D contract to determine the feasibility of the universal DAPS concept.

7.2 Reliability and Maintainability

The problems listed in Section 4.2.2.3 have led Energy Systems Corporation to recommend a follow-on Reliability Program geared specifically towards obtaining the reliability data required to confidently predict the RSSK-1A DAPS reliability. The major effort during this program would be in the area of Reliability Development Testing and Reliability demonstration. These two tasks are outlined below:

7.2.1 Reliability Development Testing

Plans and procedures for reliability development testing have been established and would be implemented during this program. The purpose of this testing is three fold: (1) to estimate the achieved reliability and to provide feedback of data as a basis for making reliability improvements, (2) to confirm the adequacy of the individual components, and (3) to identify additional failure modes and failure rates.

Those components that would be tested during this contract include: (1) complete DAPS units, (2) pump/motor assemblies (3) combustion chamber, (4) fuel tanks and (5) piezoelectric igniters. The sample size for testing has yet to be determined.

Tests, and their basic formats, that would be performed during this program include:

1. Operating Temperature Test

This test would be performed to determine whether or not the unit (or component) will operate satisfactorily over the temperature range specified in the contract. The basic format of this test would be that of test procedure 4.1.2 and 4.2.1 of MIL-E-5272C (environmental testing, aeronautical and associated equipment, general specification for).

2. Temperature Cycling Test

This test would be performed for the purpose of determining the effects of temperature cycling on the operation of the unit (or component). The basic format would be that of test procedure 5.2.3.1 of MIL-STD-781B (reliability tests: exponential distribution).

3. Temperature Storage

The objective of this test would be to determine whether or not the storage temperature range has a harmful effect on the unit (or component).

4. Vibration Test

The objective of this test would be to determine whether or not the unit will operate satisfactorily after being subjected to the vibration spectrum of the aircraft. The basic format of this test would be that of test procedure 4.7.10.1 of MIL-S-81018A (Survival Kit Container, Aircraft Seat with Oxygen; General Specification for).

5. Shock Test

This test would be performed to determine whether or not the unit will survive and operate satisfactorily after being ejected from the aircraft. The basic format of this test would be test procedure 4.7.5.4 of MIL-S-81018A.

6. Life Test

The purpose of this test would be to obtain additional information on the operating characteristics, the life, and the failure rate of each of the major components in the DAPS System.

This reliability testing would offer a partial solution to the problems listed in Section 4.2.2.3 of this report. Since these tests would be used for reliability evaluation and not reliability demonstration, they should be performed by qualified in-house personnel.

7.2.2 Reliability Demonstration Test Support

The actual reliability demonstration should be conducted by NADC or by an impartial outside agency chosen by NADC. However, it is proposed that Energy Systems Corporation support this Reliability Demonstration as follows.

The Program Manager would develop plans and procedures for the demonstration test and would include the ground rules and criteria for deciding whether the results of any particular test be classified as a success or failure.

Energy Systems Corporation would provide detailed test plans and procedures for the testing and would supply on-site testing, evaluation, and analysis support as required by the Reliability Demonstration Test agency.

APPENDIX A

CALCULATION OF INITIAL FAILURE RATES
FOR THE RSSK-1A DAPS BASED ON AN
OVERALL SUCCESS PROBABILITY OF .976

APPENDIX A

CALCULATION OF INITIAL FAILURE RATES FOR THE RSSK-1A DAPS BASED ON AN OVERALL SUCCESS PROBABILITY OF .976

Assume:

$\Delta t = 30$ hours (24 hours in-raft operation plus 6 hours operation during testing)

$$P(\Delta t) = e^{-\Delta t \lambda_T}$$

$$.976 = e^{(-30)(\lambda_T)}$$

$$\ln(.976) = \ln\left(e^{(-30)(\lambda_T)}\right)$$

$$-.0243 = -30 \lambda_T$$

$$\lambda_T = 81 \times 10^{-5}$$

Let:

$\lambda_1 =$ the failure rate of the external fuel components

$\lambda_2 =$ the failure rate of the DAPS components

$P_1 =$ the success probability of the external fuel sub-system

$P_2 =$ the success probability of the DAPS sub-system

$$\lambda_T = \lambda_1 + \lambda_2$$

$$\text{Assume: } \lambda_1 = 15 \times 10^{-5}$$

$$\lambda_2 = 66 \times 10^{-5}$$

$$P_1(\Delta t) = e^{-\Delta t \lambda_1}$$

$$P_1(30) = e^{(-30)(15 \times 10^{-5})}$$

$$P_1(30) = .9955$$

$$P_2(\Delta t) = e^{-\Delta t \lambda_2}$$

$$P_2(30) = e^{(-30)(66 \times 10^{-5})}$$

$$P_2(30) = .980$$

EXTERNAL FUEL SUB-SYSTEM

$$P_1 = .9955$$

$$\lambda_1 = 15 \times 10^{-5}$$

Let: λ_3 = the failure rate of the fuel tank

λ_4 = the failure rate of the fuel line

P_3 = the success prob. of the fuel tank

P_4 = success prob. of the fuel line

$$\lambda_1 = \lambda_3 + \lambda_4$$

$$\text{Assume: } \lambda_3 = 10 \times 10^{-5}$$

$$\lambda_4 = 5 \times 10^{-5}$$

$$P_3(\Delta t) = e^{-\Delta t \lambda_3}$$

$$P_3(30) = e^{(-30)(10 \times 10^{-5})}$$

$$P_3(30) = .997$$

$$P_4(\Delta t) = e^{-\Delta t \lambda_4}$$

$$P_4(30) = e^{(-30)(5 \times 10^{-5})}$$

$$P_4(30) = .9985$$

DAPS SUB-SYSTEM

$$P_2 = .980$$

$$\lambda_2 = 72 \times 10^{-5}$$

Let: λ_5 = the failure rate of the internal fuel assembly

λ_6 = the failure rate of the combustion chamber assembly

λ_7 = the failure rate of the fluid assembly

λ_8 = the failure rate of the electrical assembly

P_5 = success probability of internal fuel

P_6 = success probability of combustion chamber

P_7 = success probability of fluid assembly

P_8 = success probability of electrical assembly

$$\lambda_2 = \lambda_5 + \lambda_6 + \lambda_7 + \lambda_8 = 72 \times 10^{-5}$$

Assume: $\lambda_5 = 5 \times 10^{-5}$

$$\lambda_6 = 20 \times 10^{-5}$$

$$P_5(\Delta t) = e^{-\Delta t \lambda_5}$$

$$P_5(30) = e^{(-30)(5 \times 10^{-5})}$$

$$P_5(30) = .9985$$

$$\lambda_7 = 28 \times 10^{-5}$$

$$\lambda_8 = 19 \times 10^{-5}$$

$$P_6(\Delta t) = e^{-\Delta t \lambda_6}$$

$$P_6(30) = e^{(-30)(20 \times 10^{-5})}$$

$$P_6(30) = .994$$

$$P_7(\Delta t) = e^{-\Delta t \lambda_7}$$

$$P_7(30) = e^{(-30)(28 \times 10^{-5})}$$

$$P_7(30) = .9916$$

$$P_8(\Delta t) = e^{-\Delta t \lambda_8}$$

$$P_8(30) = e^{(-30)(19 \times 10^{-5})}$$

$$P_8(30) = .9943$$

INTERNAL FUEL ASSEMBLY

$$P_5 = .9985$$

$$\lambda_5 = 5 \times 10^{-5}$$

Let: λ_9 = the failure rate of the pressure regulator

λ_{10} = the failure rate of the fuel tubing

P_9 = the success probability of the pressure regulator

P_{10} = the success probability of the fuel tubing

$$\lambda_5 = \lambda_9 + \lambda_{10}$$

Assume: $\lambda_9 = 3 \times 10^{-5}$

$$\lambda_{10} = 2 \times 10^{-5}$$

$$P_9(\Delta t) = e^{-\Delta t \lambda_9}$$

$$P_9(30) = e^{(-30)(3 \times 10^{-5})}$$

$$P_9(30) = .9991$$

$$P_{10}(\Delta t) = e^{-\Delta t \lambda_{10}}$$

$$P_{10}(30) = e^{(-30)(2 \times 10^{-5})}$$

$$P_{10}(30) = .9994$$

COMBUSTION CHAMBER ASSEMBLY

$$P_6 = .994$$

$$\lambda_6 = 20 \times 10^{-5}$$

Let: λ_{11} = the failure rate of the thermoelectrics

λ_{12} = the failure rate of the piezoelectric

P_{11} = the success probability of the thermoelectrics

P_{12} = the success probability of the piezoelectric

$$\lambda_6 = \lambda_{11} + \lambda_{12}$$

Assume: $\lambda_{11} = 10 \times 10^{-5}$
 $\lambda_{12} = 10 \times 10^{-5}$

$$P_{11}(\Delta t) = e^{-\Delta t \lambda_{11}}$$

$$P_{11}(30) = e^{(-30)(10 \times 10^{-5})}$$

$$P_{11}(30) = .997$$

$$P_{12}(\Delta t) = e^{-\Delta t \lambda_{12}}$$

$$P_{12}(30) = e^{(-30)(10 \times 10^{-5})}$$

$$P_{12}(30) = .997$$

FLUID ASSEMBLY

$$P_7 = .9916$$

$$\lambda_7 = 28 \times 10^{-5}$$

Let: λ_{13} = the failure rate of the pump

λ_{14} = the failure rate of the fluid lines

λ_{15} = the failure rate of the fluid connector

P_{13} = the success probability of the pump

P_{14} = the success probability of the fluid lines

P_{15} = the success probability of the fluid connector

$$\lambda_7 = \lambda_{13} + \lambda_{14} + \lambda_{15}$$

Assume: $\lambda_{13} = 8 \times 10^{-5}$

$\lambda_{14} = 2 \times 10^{-5}$

$\lambda_{15} = 18 \times 10^{-5}$

$P_{13}(\Delta t) = e^{-\Delta t \lambda_{13}}$

$P_{13}(30) = e^{(-30)(8 \times 10^{-5})}$

$P_{13}(30) = .9976$

$P_{14}(\Delta t) = e^{-\Delta t \lambda_{14}}$

$P_{14}(30) = e^{(-30)(2 \times 10^{-5})}$

$P_{14}(30) = .9994$

$P_{15}(\Delta t) = e^{-\Delta t \lambda_{15}}$

$P_{15}(30) = e^{(-30)(18 \times 10^{-5})}$

$P_{15}(30) = .9946$

ELECTRICAL ASSEMBLY

$P_8 = .9958$

$\lambda_8 = 14 \times 10^{-5}$

Let:

λ_{16} = the failure rate of the D.C. - D.C. converter

λ_{17} = the failure rate of the motor

λ_{18} = the failure rate of the 12 V.D.C. connector

P_{16} = the success probability of the D.C.-D.C. converter

P_{17} = the success probability of the motor

P_{18} = the success probability of the 12 V.D.C. connector

$$\lambda_8 = \lambda_{16} + \lambda_{17} + \lambda_{18}$$

Assume: $\lambda_{16} = 3 \times 10^{-5}$

$\lambda_{17} = 8 \times 10^{-5}$

$\lambda_{18} = 3 \times 10^{-5}$

$P_{16}(\Delta t) = e^{-\Delta t \lambda_{16}}$

$P_{16}(30) = e^{(-30)(3 \times 10^{-5})}$

$P_{16}(30) = .9991$

$P_{17}(\Delta t) = e^{-\Delta t \lambda_{17}}$

$P_{17}(30) = e^{(-30)(8 \times 10^{-5})}$

$P_{17}(30) = .9976$

$P_{18}(\Delta t) = e^{-\Delta t \lambda_{18}}$

$P_{18}(30) = e^{(-30)(3 \times 10^{-5})}$

$P_{18}(30) = .9991$

APPENDIX B

CALCULATION OF PREDICTED
INDIVIDUAL COMPONENT FAILURE RATES

APPENDIX B

CALCULATION OF PREDICTED INDIVIDUAL COMPONENT FAILURE RATES

MIL-HDBK-217B (2.8.5-1)

D. C. MOTOR

$$\lambda_b = Ae^x \quad \text{where } x = \left(\frac{T + 273}{N_T} \right)^G$$

T = operating hot spot temp. in °C

= ambient temperature + 50°C

T = 75°C

Assume the rated insulation hot-spot temperature = 105°C

$$\therefore A = 7.20 \times 10^{-4}$$

$$N_T = 352$$

$$G = 14.0$$

$$x = \left(\frac{T + 273}{N_T} \right)^G = \left(\frac{75 + 273}{352} \right)^{14}$$

$$x = .852$$

$$\lambda_b = Ae^x = (7.20 \times 10^{-4}) (e^{.852})$$

$$\lambda_b = 1.68 \times 10^{-3}$$

From Table 2.8.1-2

$$\pi_F = 24$$

$$\lambda_E = \lambda_b \pi_F = (1.68 \times 10^{-3}) (24)$$

$$\lambda_E = 4.032 \times 10^{-2}$$

From Figure 2.8.1-3 The MTTF = 4000 hours

Operational time = 30 hours

Operating at 125% of hours rated

$$\frac{T_{op}}{MTTF} = \frac{30}{4000} = .0075$$

Inserting this value into Figure 2.8.1-5 yields a wear-out percent of population of .03.

$$\lambda_w = \frac{P_{pop}(10)^4}{T_{op}} = \frac{.03 \times 10^4}{30} = 10 \text{ failures}/10^6 \text{ hours}$$

$$\lambda_E + \lambda_w = 10.04 \text{ failures}/10^6 \text{ hours}$$

$$\lambda_p = (\lambda_E + \lambda_w) \pi_E$$

$$\lambda_p = (10.04) (2.5)$$

$$\lambda_p = 25.1 \text{ failures}/10^6 \text{ hours}$$

$$P(\Delta t) = e^{-\Delta t \lambda_p}$$

$$P(30) = e^{(-30)(25.1 \times 10^{-6})}$$

$$P(30) = .99924$$

Definitions:

λ_b = base failure rate

π_F = motor family and quality factor

λ_E = electrical failure rate

T_{op} = operating time

P_{pop} = % of motor mechanical failures during operating period, T_{op} .

λ_W = mechanical failure rate

π_E = environmental factor

D.C. - D.C. CONVERTER

PARTS COUNT REL. PREDICTION
INFOR. SOURCE: (MIL-HDBK-217B)

$$\lambda_{EQUIP} = \sum_{i=1}^{i=n} N_i (\lambda_G \pi_Q)_i$$

Where: λ_{EQUIP} = total equipment failure rate (failures/ 10^6 hours)

λ_G = generic failure rate for the i^{th} generic part (failures/ 10^6 hours).

π_Q = quality factor for the i^{th} generic part

n = number of different generic part categories

N_i = quantity of i^{th} generic part

PART	# of Parts per Converter	π_Q	λ_G
REGULATOR	1	5.0	1.12×10^{-6}
RESISTOR	2	0.1	$.018 \times 10^{-6}$
CAPACITOR	2	0.1	$.26 \times 10^{-6}$
DIODE	2	1.0	1.1×10^{-6}
TRANSFORMER	1	1.0	$.12 \times 10^{-6}$
TRANSISTOR	2	1.0	1.6×10^{-6}

$$\lambda_{\text{EQUIP}} = \left[(1)(1.12 \times 10^{-6})(5) \right] + \left[(2)(.018 \times 10^{-6})(.1) \right] + \left[(2)(.26 \times 10^{-6})(.1) \right] \\ + \left[(2)(1.1 \times 10^{-6})(1) \right] + \left[(1)(.12 \times 10^{-6})(1) \right] + \left[(2)(1.6 \times 10^{-6})(1.0) \right]$$

$$\lambda_{\text{EQUIP}} = 1.11756 \times 10^{-5}$$

$$P(\Delta t) = e^{(-\Delta t)(\lambda_{\text{EQUIP}})} = e^{(-30)(1.11756 \times 10^{-5})} = .9997$$

12 V.D.C. ELECTRICAL CONNECTOR

Information Source: MIL-HDBK-217B (2.11-1)

Definitions:

λ_p = the connector failure rate

λ_b = base failure rate

π_E = environmental adjustment factor

π_p = failure rate modifier

N = number of active pins

λ_{cyc} = cycling failure rate

A = constant

T_o = constant

N_T = constant

G = constant

P = constant

T = operating temperature ($^{\circ}\text{C}$)

i = amperes per contact

$$\lambda_p = \lambda_b (\pi_E \times \pi_p) + N\lambda_{\text{cyc}} \text{ (failures/} 10^6 \text{ hours)}$$

Insert Material: Neoprene (Type D)

$$\lambda_b = Ae^x$$

$$\text{Where } x = \left(\frac{T + 273}{N_T} \right) G + \left(\frac{T + 273}{T_o} \right) P$$

From Table 2.11-1 (MIL-HDBK-217B)

$$A = 12.3$$

$$T_o = 358$$

$$N_T = -1528.8$$

$$G = -1$$

$$P = 4.72$$

$$T = \text{operating temperature } (^{\circ}\text{C})$$

$$= \text{ambient temperature} + \text{temp. rise (Table 2.11-4)}$$

$$\text{maximum ambient temperature} = 25^{\circ}\text{C}$$

$$\text{Temperature rise} = .64 (i)^{1.85}$$

$$= .64 (.050)^{1.85}$$

$$= .0025^{\circ}\text{C (negligible)}$$

$$\begin{aligned} x &= \left(\frac{T + 273}{N_T} \right) G + \left(\frac{T + 273}{T_o} \right) P \\ &= \left(\frac{25 + 273}{-1528.8} \right) (-1) + \left(\frac{25 + 273}{358} \right) 4.72 \end{aligned}$$

$$x = -4.7095$$

$$\begin{aligned} \lambda_b &= Ae^x \\ &= 12.3e^{-4.7095} \end{aligned}$$

$$\lambda_b = .1108$$

$$\begin{aligned}
N &= 4 \text{ pins} \\
\pi_E &= 10.0 \text{ (Table 2.11-6 Assume } A_u \text{ environment)} \\
\pi_p &= 1.72 \text{ (Table 2.11-7)} \\
\lambda_{cyc} &= .0011 \text{ (Table 2.11-8) Assume } 10 \text{ cycles}/10^3 \text{ hours)} \\
\lambda_p &= b (\pi_E \times \pi_p) + N \lambda_{cyc} \text{ (failures}/10^6 \text{ hours)} \\
&= (.1108)(10 \times 1.72) + (4) (.0011) \\
\lambda_p &= 1.9104 \text{ Failures}/10^6 \text{ hours} \\
P(\Delta t) &= e^{-\Delta t \lambda_p} = e^{(-30)(1.9104 \times 10^{-6})} = .99994
\end{aligned}$$

THERMOELECTRICS

Source of Information:

Nuclear Systems, Inc.

Instrument Division

82 couples/module

164 elements/module

328 solder joints/module

Using an average failure rate of 5×10^{-8} for each solder joint (from NSI Instrument Division) of a thermoelectric cooling module, the failure rate of the module can be calculated.

$$\lambda_p = (\pi_E)(5.0 \text{ failures}/10^8 \text{ hours/solder joint}) \\
(328 \text{ solder joints})$$

$$\lambda_p = (10)(5 \times 10^{-8})(328)$$

$$\lambda_p = 1.64 \times 10^{-4} / \text{module}$$

$$P(\Delta t) = e^{-\Delta t \lambda_p}$$

$$P(30) = e^{(-30)(1.64 \times 10^{-4})}$$

$$P(30) = .995 \text{ (per module)}$$

The RSSK-1A DAPS has two modules in series. Therefore:

$$P_{\text{overall}}(\Delta t) = .995 \times .995 = .990$$

FLUID CONNECTORS

Assume:

(1) No vibration effects (manufacturers data)

(2) 1 failure per 10,000 connectors

$$\lambda_T = 1 \times 10^{-4}$$

$$P(\Delta t) = e^{-\Delta t \lambda_T}$$

$$P(30) = e^{(-30)(1 \times 10^{-4})}$$

$$P(30) = .997$$

PRESSURE REGULATOR

λ_T = part failure rate

λ_b = base failure rate

π_E = environmental adjustment factor

π_Q = quality adjustment factor

Works in excess of 100 million cycles (manufacturers data)

Assume:

$$\Delta c = 30 \text{ cycles}$$

$$\pi_E = 10 \text{ (from Reliability Design Handbook, IIT Research Institute)}$$

$$\pi_Q = 150 \text{ (from Reliability Design Handbook, IIT Research Institute)}$$

$$\lambda_b = 1 \times 10^{-8}$$

$$\lambda_T = (\lambda_b) (\lambda_E) (\pi_Q)$$

$$\lambda_T = (\lambda_b) (10) (150)$$

$$\lambda_T = 1500 \lambda_b$$

$$\lambda_T = 15 \times 10^{-6}$$

$$P(\Delta c) = e^{-\Delta c \lambda_T}$$

$$P(30) = e^{(-30)(15 \times 10^{-6})}$$

$$P(30) = .99955$$

CONNECTIONS

Approximate number of connections per RSSK-1A DAPS:

- 1 - weld
- 17 - solder
- 7 - pipe
- 12 - dip braze
- 14 - hose clamps
- 51 - total connections

Assume:

(1) The average failure for each of the above is 5.0×10^{-8} . This value is taken from NSI data on solder connections for thermoelectric modules.

Therefore:

$$\lambda_T = (51 \text{ connections/unit}) (5 \times 10^{-8} \text{ failures/connection})$$

$$\lambda_T = 2.55 \times 10^{-6} \text{ failures/unit}$$

$$P(\Delta t) = e^{-\Delta t \lambda_T}$$

$$P(30) = e^{(-30)(2.55 \times 10^{-6})}$$

$$P(30) = .99992$$

PIEZOELECTRIC

Assume:

(1) 1 failure per 10,000 piezoelectrics

$$\lambda_T = 1 \times 10^{-4}$$

$$P(\Delta t) = e^{-\Delta t \lambda_T}$$

$$P(30) = e^{(-30)(1 \times 10^{-4})}$$

$$P(30) = .997$$

APPENDIX C

THERMAL REQUIREMENTS FOR COLD WATER
AND LIFE RAFT EXPOSURES

APPENDIX C

THERMAL REQUIREMENTS FOR COLD WATER AND LIFE RAFT EXPOSURES

This appendix is included as back-up information for the recommendation that a universal DAPS is feasible. As previously stated calculations indicate, a thermal input of 100 watts should be adequate to balance thermal heat losses of a man exposed to 20°F ambient air temperatures.

The following analysis is based upon the paper published in "Aerospace Medicine" by John F. Hall Jr. (1)

Following are the assumptions and definition of terms used in the calculations.

It is assumed that the airman enters the life raft within five(5) minutes after immersion in 32°F water.

Insulation Values Estimates

- Ig = Net effective insulation value of the body clothing worn. Insulation value of the dry anti-exposure suite (CWV-21/p) = 1.2 clo(2). The wetting reduced the clothing insulation by 25% to 0.9 clo.
- I raft = Insulation value of the wet raft. Insulation value of the dry life raft, insulated canopy type (LRU-6/p) = 1.0 clo. The wetting reduces the raft insulation value by 30%, to 0.7 clo.
- Ia, raft = Insulation value of the air inside the raft. The effective insulation value of the raft air is 0.5 clo.

Life Raft Heat Transfer Calculations

- Ts = Mean skin temperature, °C.
- Ta = Ambient Air Temperature, °C.
- Sa = Body Surface area (1.8 m²)

$$\dot{m} = \text{Metabolic heat production, Kcal}/\dot{m}^2/\text{hr.}$$

Assuming $\dot{m} = 75 \text{ Kcal}/\dot{m}^2/\text{hr}$, of this 25% is lost by evaporation. Therefore, net metabolic heat lost by radiation and convection (dry heat);

$$\begin{aligned} &= 75 \times 0.75 \times 1.8 \\ &= 100 \text{ Kcal/hr.} \end{aligned}$$

$$-\dot{Q} = \text{Heat loss through clothing and life raft, Kcal/hr.}$$

$$-\dot{Q} = \frac{5.55 (T_s - T_a) SA}{I_g + (I_{\text{raft}} + I_{a, \text{raft}})} \text{ K cal/hr}$$

$$\text{for, } T_a = -6.7^\circ\text{C } (20^\circ\text{F})$$

$$T_s = 32^\circ\text{C } (89.6^\circ\text{F})$$

$$SA = 1.8 \text{ m}^2$$

$$I_g = 0.9 \text{ clo}$$

$$I_{\text{raft}} = 0.7 \text{ clo}$$

$$I_{a, \text{raft}} = 0.5 \text{ clo}$$

$$\dot{Q} = \frac{-5.55 (32 + 6.7) \times 1.8}{0.9 + (0.7 + 0.5)}$$

$$= -184 \text{ Kcal/hr}$$

Therefore, net body heat loss (without DAPS heating),

$$= \dot{Q} + \dot{m} \text{ (dry)}$$

$$= -184 + 100$$

$$= -84 \text{ Kcal/hr } (= .98 \text{ watts})$$

This means that approximately 84 Kcal/hr (98 watts) of heat must be provided to the man-raft ambient to maintain the airman's body temperature constant. The heat requirement will be slightly more if the body is allowed to cool within safe tolerance limits. The 84 Kcal/hr. heat delivery from the DAPS to the raft will provide indefinite tolerance at 20°F to the man in the raft without any cold exposure.

(1) Hall, John F., Jr., "Prediction of Tolerance in Cold Water and Life Raft Exposures", Aerospace Medicine, 43(3) 281-286, 1972.

(2) Definition of Clo: Clo is a unit of thermal insulation of the clothing system and the overlying still air. One clo insulation will result in 5.55 Kcal per hour of dry heat transfer (convection plus radiation) per unit of temperature gradient ($^{\circ}\text{C}$) from one meter square of surface area $\frac{1^{\circ}\text{C}}{\text{K cal/M}^2/\text{hr}} = 5.55 \text{ clo}$

APPENDIX D

RSSK-1A DAPS OPERATING INSTRUCTIONS

APPENDIX D

RSSK-1A DAPS OPERATING INSTRUCTIONS

The following procedure is recommended to deploy and operate the DAPS.

- 1) Remove the DAPS heater/fuel coil assembly from the seat kit by unlatching catches located at positions A, B, C & D (Figure 1).
- 2) Connect fluid umbilical on DAPS to mating connection of suit.
- 3) Remove exhaust port cover
- 4) Admit fuel to DAPS by connecting fuel umbilical on fuel coil to mating connection on DAPS.
- 5) Admit fuel to the combustion chamber in DAPS by adjusting fuel regulator to a setting of 8.
- 6) Aim exhaust port away from clothing and raft.
- 7) Press ignition button to start fuel burning.
- 8) Check exhaust port for flame.
- 9) If no flame and heat visible repeat step 7 until ignition occurs.
- 10) System will start pumping fluid through tubulated garment within two minutes.
- 11) Allow system to reach equilibrium, approximately 15 minutes and set at desired thermal requirement. A higher fuel setting will result in a greater thermal input to the man with corresponding decrease in fuel duration. A decal showing approximate fuel duration vs regulator setting is provided to indicate expected fuel durations.
- 12) To operate auxiliary equipment from the 12V outlet, connect input jack on equipment to connector on DAPS. It is recommended that auxilliary equipment be used only ~~between~~ fuel settings of 4 and 7.

- 13) To secure the DAPS, turn regulator knob to zero setting, disconnect fuel umbilical and allow system to coast to a stop (approximately 5 minutes); disconnect fluid umbilical from suit. ---- Warning: under no circumstances should system be operated with fluid connectors unattached to a suitable thermal sink. Operating DAPS with no or inadequate flow will result in damage to the DAPS and possibly the operator.

APPENDIX E

MAINTENANCE AND REPAIR

APPENDIX E

MAINTENANCE AND REPAIR

Following is a list and description of basic maintenance items required on the RSSK-1A DAPS.

1. Replenishing Tubulated Suit and Power Source Fluid

Over a period of time and with repeated use, some loss of fluid and inclusion of air will occur in the system. The amount of spillage, for the Air lock connectors is negligible with rapid connection. However, with a slow or fumbling engagement, a fair amount could be realized. Air inclusion could be as little as .0033 cubic inches per connection. The DAPS will operate satisfactorily with a limited amount of air in the fluid lines.

INSPECTION: Connect the tubulated suit to the DAPS. Observe the suit fluid lines near the connector for air. If the air bubble is more than one inch long in either tube, the suit and DAPS should be refilled with a 50 percent ethylene glycol and 50 percent water solution. An extra connector will be required for replenishing the fluid in the DAPS.

Manufacturer: Air-Lock, Inc.
Gulf Street
Milford, Connecticut 06460

Part Number: 9575-01

The DAPS and the tubulated suit can be filled or replenished using the extra connector and a pump. The pumping rate should not exceed .75 gallons per minute.

2. It is recommended that the DAPS and the tubulated suit be flushed with a freshly mixed antifreeze solution once a year to avoid scale build-up.

3. The igniter electrode in the exhaust port should be cleaned periodically with abrasive paper or cloth.

Table E-1 gives the expected replacement schedule for the major components of the RSSK-1A DAPS System.

Following is a list of the most common failure modes, the possible causes, and the repair action to be followed to correct each failure (Table E-2). All repair work should be done by a skilled technician familiar with the system, and any major repairs that are required should be performed by ESC personnel only.

	REQUIRED ($\times 10^{-6}$)	PREDICTED ($\times 10^{-6}$)	ACTUAL ($\times 10^{-6}$)
FUEL TANK	100	100	
PRESSURE REGULATOR	30	15	
FUEL TUBING	50	50	
PIEZOELEC- TRIC	100	100	
THERMO- ELECTRIC	100	328	
PUMP	80	80	
FLUID LINES	20	20	
FLUID CONNECTOR	180	100	
MOTOR	80	25.1	
12 VDC CONNECTOR	30	1.9	
D.C.-D.C. CONVERTER	30	11.2	
CONNECTIONS (solder, dip, brazed, weld, pipe, clamps)	2.6	2.6	

RSSK-1A FAILURE RATE DATA

Table E-1

TABLE E-2

<u>SYMPTOM</u>	<u>POSSIBLE CAUSE</u>	<u>REPAIR ACTION</u>
(1) Cannot connect fuel supply to unit.	(A) Damaged fuel connector	(A) Replace Fuel connector
(2) Unit fails to ignite.	(A) Insufficient fuel supply	(A) Replace fuel cylinder
	(B) Clogged orifice	(B) Remove and either clean or replace orifice
	(C) Spark gap too great	(C) Readjust ground
	(D) Spark shorting back to duct wall	(D) Clean electrode and ground
	(E) Spark shorting at the piezoelectric	(E) Replace piezoelectric
(3) Combustion not sustained	(A) Insufficient fuel supply	(A) Replace fuel cylinder
(4) No pumping of fluid	(A) Excessive amount of air in system	(A) Replenish fluid
	(B) Broken or disconnected electrical lead	(B) Repair or reconnect
	(C) Crimped or collapsed fluid lines	(C) Replace tubing
	(D) Broken thermoelectric module	(D) Replace module

<u>Symptom</u>	<u>Possible Cause</u>	<u>Repair Action</u>
(5) Unit starts but then overheats	(A) Leak in fluid system	(A) Check all fluid lines and connections. Replace bad section of tubing or repair connection
	(B) Fuel flow rate too high	(B) Reduce the fuel setting
(6) No 12 VDC output	(A) Broken or disconnected electrical lead	(A) Repair or reconnect
	(B) Broken connecting pin	(B) Replace the electrical connector

CREW SYSTEMS DEPARTMENT
DISTRIBUTION LIST

DDC, Alexandria, Va. -----	12
National Library of Medicine, Bethesda, Md. -----	1
Bureau of Medicine and Surgery (Code 71) -----	3
Bureau of Medicine and Surgery (Code 713)-----	1
Bureau of Medicine and Surgery (Code 7113) -----	1
CNO (OP-098E), Pentagon -----	1
Naval Aerospace Medical Research Lab. (Code L1), Pensacola -----	1
Naval Aerospace Medical Research Lab. (Physiology), Pensacola -----	1
Naval Training Equipment Center (N-2), Orlando -----	2
NMRI (Tech. Ref. Library), Bethesda -----	1
Naval Submarine Med. Center (Library), Groton -----	1
NAVAIRSYSCOM (AIR-531) -----	1
NAVAIRSYSCOM (AIR-954) -----	2
NAVAIRSYSCOM (AIR-5311G) -----	1
NAVAIRSYSCOM (AIR-5315) -----	2
Navy Med. Neuropsychiatric Res. Unit, San Diego -----	1
Naval Safety Center, Norfolk -----	1
Naval Air Test Center, Patuxent River -----	1
ONR (Code 107), Arlington -----	1
FAA (AC-100), Oklahoma City -----	1
FAA (AC-101.1), Oklahoma City -----	1
Dept. Transportation Library (FAA), Washington, D.C. -----	2
6570 AMRL/DAL Library, Wright-Patterson AFB -----	1
HQ, USAF/RDPS, Washington, D. C. -----	1
USAF SAM (SUL-4), Brooks AFB, Texas -----	1
USAF SAM/RAW, Brooks AFB, Texas -----	1
Air University Library, Maxwell AFB, Alabama -----	1
HQ, TAC, SGS, Langley AFB, Virginia -----	1
Aerospace Pathology Branch, Washington, D.C. -----	1
Edgewood Arsenal (SMUEA-TS-L) Aberdeen Proving Ground, Md. -----	1
USA Natick Labs. (Tech. Library), Natick, Mass. -----	1
ITPR Lab., U. S. ARI (Dr. Dusek), Arlington, Virginia -----	1
NASA-Lewis Research Center (Library), Cleveland -----	2
NASA-Johnson Space Center (E.L. Hays), Houston -----	1
Science and Tech. Div., Library of Congress -----	1
National Institutes of Health (Library), Bethesda -----	1
National Research Council (Med. Records) -----	1
U.S. Army Aeromedical Research Lab., Fort Rucker -----	1
NAMRL Detachment, New Orleans -----	1
HQ, USAF/SGPA, Washington, D.C. -----	1
COMOPTEVFOR, Norfolk -----	2
HQ, Naval Material Command -----	1

DISTRIBUTION LIST (Cont'd)

American Institutes for Research, Pittsburgh -----	1
Aviation Medicine Research Lab., Columbus -----	1
Biological Abstracts, Philadelphia -----	1
University of California, Davis -----	1
Calspan Corp. (Library), Buffalo -----	1
Countway Library of Medicine, Boston -----	1
Drexel University (Biomedical Engrg.), Philadelphia -----	1
University of Illinois, Chicago -----	1
Indiana University, Indianapolis -----	1
Library of College of Physicians of Philadelphia -----	1
Lovelace Foundation, Albuquerque -----	1
Ohio State University, Columbus -----	1
University of Pennsylvania, Philadelphia -----	1
John B. Pierce Foundation Laboratory, New Haven -----	1
Presbyterian-Univ. of Pa. Medical Center, Philadelphia -----	1
University of Southern California, Los Angeles -----	1
Temple University Hospital (Dr. Kern), Philadelphia -----	1
Wayne State University, Detroit -----	1
Institute of Marine Biomedical Research, Wilmington, N.C. -----	2

David Clark Co., Worcester, Mass. -----	1
Convair Aerospace Div., San Diego -----	1
General Electric Co., Philadelphia -----	1
Grumman Aerospace Corp., Bethpage, N.Y. -----	1
Hageman Consulting Services, Fort Worth -----	1
Lockheed-California, Burbank -----	1
Rockwell International, Los Angeles -----	1
Fairchild Republic Co., Farmingdale, N.Y. -----	1
Vought Systems Div., LTV Aerospace, Dallas -----	2
Webb Associates, Yellow Springs, Ohio -----	1

Dr. Carl C. Clark, Baltimore -----	1
Capt. Herbert Shepler, Brimerton, Wa. -----	1